

**Studies on Poly (Lactic Acid)/Chitosan based Bioresorbable  
composites for Orthopaedic Applications**

*Thesis submitted to  
Indian Institute of Technology Guwahati  
for the award of the degree*

*of*

**Doctor of Philosophy**

*by*

**Devleena Bose**

**(Roll Number: 186107004)**

*Under the supervision of*

**Prof. Vimal Katiyar**



**Department of Chemical Engineering  
Indian Institute of Technology, Guwahati  
Guwahati 781039, Assam, India.**

**October, 2025**

© 2025, Devleena Bose. All rights reserved.





*Dedicated to...*

*my husband, Pratik Nag*



## DECLARATION

I declare that

- a. the work contained in this thesis is original and has been done by me under the guidance of my supervisors.
- b. the work has not been submitted to any other Institute for any degree or diploma.
- c. I have followed the guidelines provided by the Institute in preparing the thesis.
- d. I have conformed to the norms and guidelines given in the Ethical Code of conduct of the Institute.
- e. whenever I have used materials (data, theoretical analysis, figures, and text) from other sources, I have given due credit to them by citing them in the text of the thesis and giving their details in the references. Further, I have taken permission from the copyright owners of the sources, whenever necessary

*Devleena Bose*

**Devleena Bose**



## CERTIFICATE OF APPROVAL

Date: \_\_\_\_\_

Certified that the thesis entitled '**Studies on Poly (Lactic Acid)/Chitosan based Bioresorbable composites for Orthopaedic Application**' submitted by **Devleena Bose** to the **Indian Institute of Technology Guwahati** is a record of an original research work carried out by him under my supervision and guidance. The thesis has fulfilled all requirements as per the regulations of the institute and, in my opinion, has reached the standard needed for submission. The findings embodied in this thesis have not been submitted to any other University or Institute for the award of any degree or diploma

**Signature:**

**Prof. Vimal Katiyar**  
Department of Chemical Engineering  
Indian Institute of Technology Guwahati  
Guwahati-781039, Assam, India



## Acknowledgement

By the immense grace and blessing of the Almighty, I take this opportunity to express my heartfelt gratitude to my supervisor, Prof. Vimal Katiyar. His belief in me, along with his guidance and encouragement throughout my PhD journey, has been invaluable. His consistent instructions, positive outlook, and enthusiasm made this experience enriching and manageable. I am thankful for his support and availability for work-related discussions, which helped me navigate this research journey.

I would also like to acknowledge my Doctoral Committee: Prof. Utpal Bora from the Department of Bioscience and Bioengineering, Dr Chandan Das from the Department of Chemical Engineering, and Dr Poonam Kumari from the Department of Mechanical Engineering for their insightful observations and suggestions at various stages of my research study. I am thankful to SERB, FICCI, and ORTHOTECH for awarding me the Industrial Prime Minister Research Fellowship (PMRF) during my doctoral studies in 2020. I extend my gratitude to Mr. Sushant Banerjee, CEO and founder of Orthotech India Pvt. Ltd., for being an active mentor and sharing his valuable experience. I sincerely thank Mrs. Suneeta Banerjee, Managing Director of Orthotech, for her constant encouragement and constructive feedback.

I acknowledge the use of sophisticated facilities at the Central Instrument Facility and CSP, IIT Guwahati. Furthermore, I would like to express my sincere gratitude to the heads and authorities of the Department of Chemical Engineering and my Institute for their cooperation and support. Many thanks to all the technical staff in my department and CSP for their assistance. I especially extend my heartfelt thanks to my seniors, friends, Dr. Siddharth Bhasney and Dr. Gourhari from my lab, for their meaningful suggestions regarding my research. I am grateful to all my lab members for their cooperation and team spirit.

To my husband, Dr. Pratik Nag, I am profoundly indebted for your endless patience, motivation, and encouragement, which have made this journey possible. Your unwavering motivation and guidance have been a beacon of light throughout my academic and personal growth. It is truly difficult to express the extent of efforts you have contributed.

To my beloved mom, Mrs. Gitanjali Bose, and dad, Mr. Gautam Bose, I owe everything to your unconditional love, support, and the values you instilled in me. Your constant encouragement during challenging times and belief in my potential has been my greatest source of strength, teaching me through countless discussions about work ethics and life lessons. Love to my little sister, Ms. Anusua, for her compassion and affection.

I express my heartfelt love to my mother-in-law, Mrs Pratima Nag, and father-in-law, Mr Dilip Kumar Nag, for supporting all my decisions and ensuring I perform my best. Last, but certainly not least, I am sincerely grateful to everyone I came across and those who contributed to my well-being during this journey.

Devleena Bose



## Abstract

The ageing global population, coupled with an increasing number of trauma cases such as accidents and sports injuries, has led to a higher incidence of bone fractures. These fractures require immediate medical attention, often in the form of orthopaedic surgery that involves implanting external or internal fixation devices. The choice of internal fixation devices, such as bone plates, screws, and pins, depends on the severity of the injury and the location of the fracture.

While conventional metallic fixation implants provide stable initial post-operative support for fractured bones, allowing for early mobilization, they come with certain drawbacks. These include the dissolution of metallic ions, which can accumulate in local lymph nodes and other organs, the stress shielding phenomenon, and the generation of artefacts on computed tomography (CT) scans. Consequently, patients often require secondary surgery to remove the metallic implants after the fracture has healed, resulting in a more invasive procedure that increases the overall socio-economic burden on patients.

An alternative solution is to replace conventional fixation devices with bioresorbable polymer systems, whose properties can be customized to match those of natural bone. Once implanted, these bioresorbable implants break down into harmless by-products that are eventually eliminated from the body, thereby allowing the host tissue to replace them. This approach eliminates the need for revision surgeries and addresses the limitations associated with traditional implants.

The current study found that adding modified chitosan (MCS) and hydroxyapatite (HAp) to a Polylactic acid (PLA) matrix significantly enhances the load-bearing capacity and bioactivity of the implants. Various analyses, including surface morphology, differential scanning calorimetry, contact angle measurements, thermogravimetric analysis, Fourier transform infrared spectroscopy, and mechanical strength testing, were conducted to examine the characteristics of the prepared bio-composite.

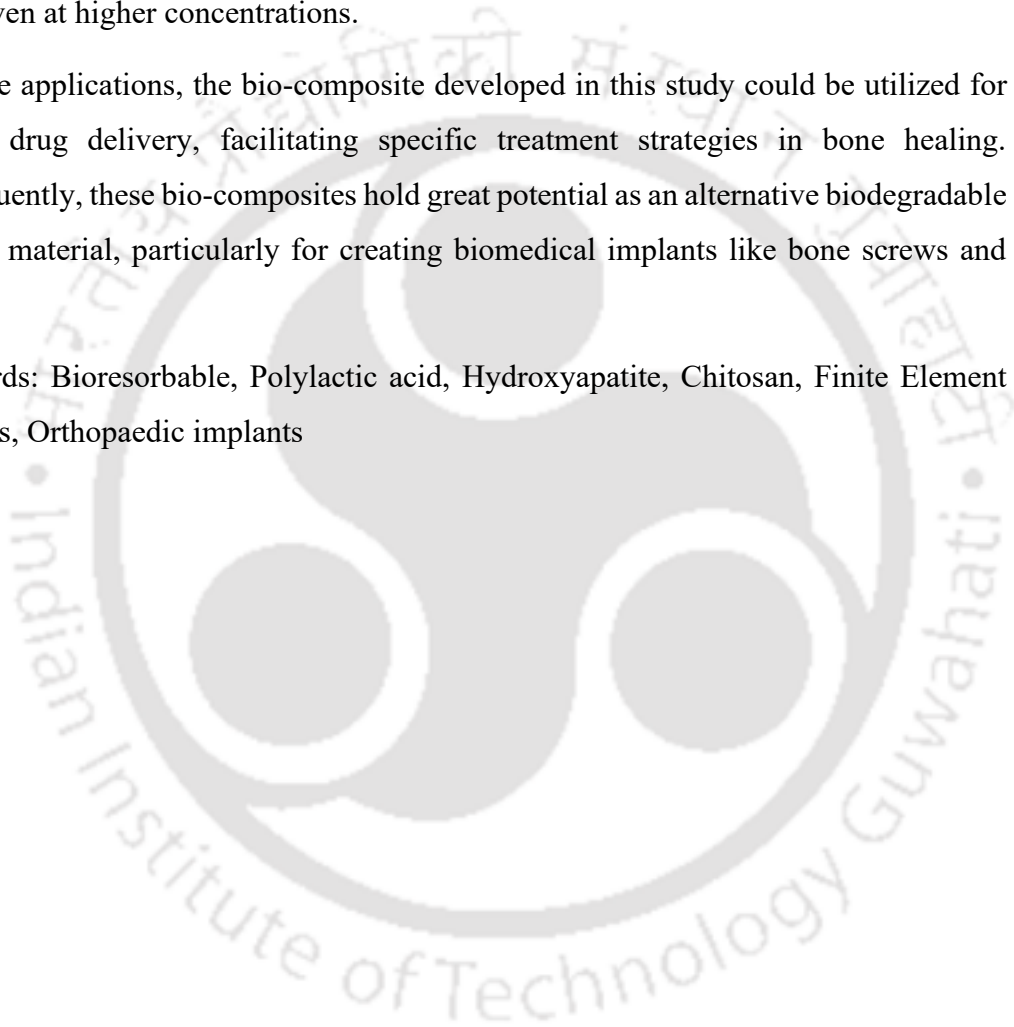
The interaction between nHAp, MCS, and PLA made the synthesized bio-composites superior in terms of chemical properties and mechano-thermal stability compared to neat PLA. Contact angle studies demonstrated improved surface wettability, indicating

that the bio-composites are suitable for cell proliferation. Additionally, the incorporation of nHAp increased Young's modulus without causing phase separation.

Moreover, in silico studies using Finite Element (FE) analysis were employed to assess the suitability of the PLA-based composite as an implant material for low load-bearing fracture fixation devices. For high load-bearing fracture sites, the fabricated bio-composite was applied as a coating over conventional metallic implants. Cytotoxicity studies confirmed the nontoxic nature of the bio-composite on mouse fibroblast cell lines, even at higher concentrations.

In future applications, the bio-composite developed in this study could be utilized for in situ drug delivery, facilitating specific treatment strategies in bone healing. Consequently, these bio-composites hold great potential as an alternative biodegradable implant material, particularly for creating biomedical implants like bone screws and plates.

Keywords: Bioresorbable, Polylactic acid, Hydroxyapatite, Chitosan, Finite Element Analysis, Orthopaedic implants



## Contents

Title page	i
Declaration	v
Certificate of approval	vii
Acknowledgements	ix
Abstract	xi
Contents	xiii
List of symbols and abbreviations	xv
List of figures	xviii
List of tables	xx
<b>Chapter 1: Introduction and literature review</b>	<b>1</b>
1.1 Introduction	1
1.2 Global and Indian scenario of the orthopaedic devices market	3
1.3 Material properties of bone tissue	4
1.4 Bone fracture healing	6
1.5 Types of Implant Material	7
1.5.1 Bio-metals	7
1.5.2 Types of Metallic orthopaedic Fixation Devices	9
1.5.3 Problems with metallic internal fixation devices	10
1.5.4 Alternate solution to metallic fixation devices	11
1.6 Bioresorbable implants	12
1.6.1 Advantages of bioresorbable devices	15
1.6.2 Challenges associated with bioresorbable polymers and IFDs	17
1.7 Desirable osteo-fixation devices	17
1.8 Finite Element (FE) studies	18
1.9 Literature Survey	19
1.10 Research Gap	26
1.10.1 Objectives	28
1.11 Overview of the thesis	29
<b>Chapter 2: Materials and Methodology</b>	<b>31</b>
2.1 Introduction	31
2.2 Materials	31
2.3 Methodology	32
2.2.1 Purification of commercial-grade PLA	32
2.2.2 Synthesis of modified Chitosan (MCS) by condensation polymerization	33
2.2.3 Processing of PLA/MCS/nHAp bio-composites by melt-blending	34

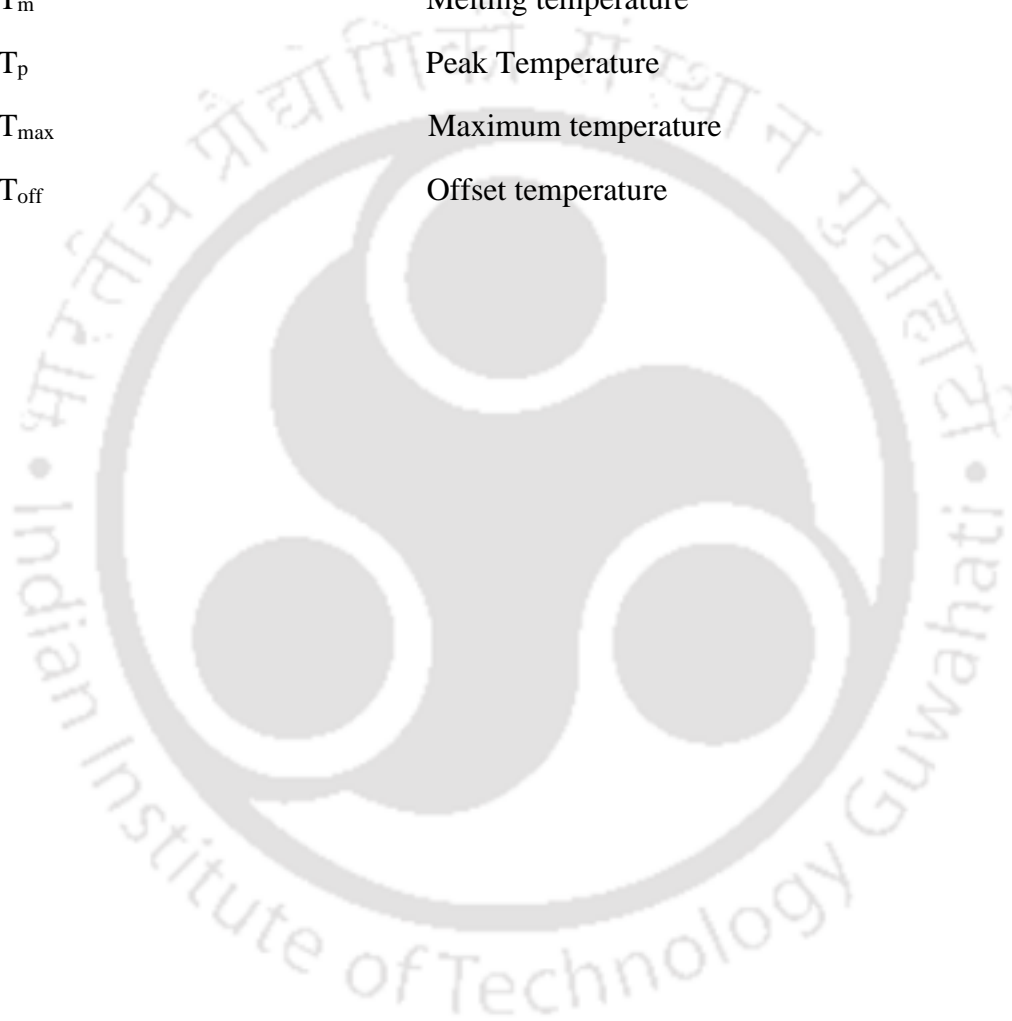
2.2.4 Analytical instrumentation and Characterization of PLA/MCS/nHAp bio-composites	35
2.2.5 FE model generation of the mandibular bone and distal tibia implanted construct	39
<b>Chapter 3: Fabrication of nano-hydroxyapatite and chitosan-reinforced polylactic acid bio-composite for bioresorbable internal fixation device</b>	<b>45</b>
3.1 Introduction	45
3.2 Results and Discussion	47
3.2.1 Mechanical tests	47
3.2.2 Fourier transform infrared analysis	48
3.2.3 Thermogravimetric analysis	49
3.2.4 Differential scanning calorimetry analysis	51
3.2.5 Contact angle study	52
3.2.6 Surface morphology	53
3.3 Summary of findings	55
<b>Chapter 4: A finite element study to predict the viability of PLA-based composite implants for mandibular joint fracture</b>	<b>57</b>
4.1 Introduction	57
4.3 Results and Discussion	59
4.5 Summary of findings	65
<b>Chapter 5: <i>in vitro</i> cytotoxicity study and <i>in silico</i> analysis of the PLA/nHAp/MCS bio-composite as a coating material for high load-bearing implants</b>	<b>67</b>
5.1 Introduction	71
5.3 Results and Discussion	70
5.5 Summary of the findings	75
<b>Chapter 6: Conclusions</b>	<b>77</b>
6.1 Introduction	77
6.2 Future Scope	81
<b>References</b>	<b>83</b>
<b>About the author</b>	<b>103</b>

## List of symbols and abbreviations

Most of the notations and abbreviations are defined as they may appear in the thesis.

### Notations

$T_g$	Glass transition temperature
$T_o$	Onset degradation temperature
$T_{cc}$	Cold crystallization temperature
$T_m$	Melting temperature
$T_p$	Peak Temperature
$T_{max}$	Maximum temperature
$T_{off}$	Offset temperature



## Abbreviations

CAD	Computer-Aided Design
CAGR	Compound Annual Growth Rate
CT	Computed Tomography
FE	Finite Element
Fig.	Figure
ASTM	American society for testing and materials
Ti	Titanium
ATR	Attenuated total reflectance
CS	Chitosan
MCS	Modified chitosan
RBF	Round bottom flask
RH	Relative humidity
OLLA	Oligomer of Lactic acid
CS-g-OLLA	Chitosan-grafted oligomeric L-lactic acid
FDA	Food and Drug Administration
FESEM	Field emission scanning electron microscopy
FTIR	Fourier transform infrared spectroscopy
TGA	Thermogravimetric analysis
UTM	Universal Testing Machine
E	Young's modulus
DSC	Differential scanning calorimetry
EDX	Energy dispersive X-ray spectroscopy
PLA	Polylactic acid
$M_w$	Weight average molecular weight
$M_n$	Number average molecular weight
PLGA	Polylactic-co-glycolic acid
LA	Lactic acid
nHAp	nano-Hydroxyapatite

PCL	Polycaprolactone
PGA	Polyglycolic acid
PLA/nHAp	polylactic acid/nanohydroxyapatite
PLA/nHAp/MCS	polylactic acid/nanohydroxyapatite/modified chitosan
MPa	Mega Pascal
GPa	Giga Pascal
TS	Tensile strength
YM	Youngs Modulus





## List of Figures

<b>Figure no.</b>		<b>Page no.</b>
1.1	Stress-strain curve for Cortical bone (Villette et al.,2018)	5
1.2	Stress-strain curve for cancellous bone (Villette et al.,2018)	5
1.3	Examples of conservative methods: Cast and Splint (Google).	6
1.4	Examples of non-conservative methods: Plates and Screws	6
1.5	Stages of secondary bone healing	7
1.6	Flowchart depicting the overview of the research statement	28
1.7	Flowchart depicting the overall goal of the thesis objective-wise	29
2.1	Purification of PLA	32
2.2	Synthesis of modified chitosan (MCS)	33
2.3	Processing of PLA/MCS/nHAp bio-composite by melt-blending	35
2.4	Functioning layout diagram of the extrusion cum injection molding	36
2.5	Mechanical strength analysis of the specimen under UTM.	37
2.6	CT data of human cranio-maxillo facial part with extracted mandibular joint (lower right corner)	40
2.9	3D CAD model: (a) Implant (b) Tibia extracted from CT dataset	43
3.1	Mechanical testing (a) Young's modulus (b) Tensile strength and elongation of the prepared samples	47
3.2	FTIR spectra of the neat PLA and the prepared bio-composites.	49
3.3	Plots of (a) TGA and (b) DTG of the prepared samples	50
3.4	DSC plot of PLA, PLA/nHAp, PLA/nHAp/6 wt%MCS and PLA/nHAp//9%MCS.	52
3.5	Contact angle analysis of the prepared samples.	53
3.6	FESEM images of (a) nHAp (b) modified chitosan (MCS) (c) neat PLA (d) PLA/nHAp (e) PLA/nHAp/MCS	54
3.7	EDX analysis of (a) neat PLA (b) nHAp (c) MCS (d) PLA/nHAp/MCS	55
4.1	Mechanical testing (a) Young's modulus (b) Tensile strength and elongation of the fabricated samples	59

<b>4.2</b>	Predicted von Mises stress distribution in hairline mandibular fracture considered under biting load condition: (a) PLA+HAp+MCS composite plate, (b) Ti alloy plate.	60
<b>4.3</b>	Predicted von Mises stress distribution in mandibular fracture having gap ~1 mm considered under the biting load conditions: (a) PLA+HAp+MCS composite plate, (b) Ti alloy plate.	61
<b>4.4</b>	Predicted von Mises stress distribution in mandibular fracture having gap ~ 1mm considered under the biting load and occlusal loading conditions: (a) PLA+HAp+MCS composite plate, (b) Ti alloy plate.	62
<b>4.5</b>	Predicted displacement plots in mandibular fracture having gap ~1mm considered under the biting load condition: (a) PLA+HAp+MCS composite plate, (b) Ti alloy plate.	62
<b>4.6</b>	Predicted displacement plots in mandibular fracture having gap ~1mm considered under the biting load and occlusal loading condition: (a) PLA+HAp+MCS, (b) Ti alloy plate.	64
<b>4.7</b>	Displacement plot of PLA composite and Ti alloy based mandibular construct: comparison under biting force with different combination of plate and screw material.	65
<b>5.1</b>	FE model of the tibia and implant.	70
<b>5.2</b>	von Mises stress distribution of the implant: (a) PLA+HAp+MCS coated Ti alloy implant, (b) Ti alloy implant.	70
<b>5.3</b>	Von Mises stress distribution of the tibia: (a) PLA+HAp+MCS coated Ti alloy implant, (b) Ti alloy implant.	71
<b>5.4</b>	Von Mises stress distribution of the implanted tibia: (a) PLA+HAp+MCS coated Ti alloy implant, (b) Ti alloy implant.	72
<b>5.5</b>	displacement plot of the implanted tibia: (a) PLA+HAp+MCS coated Ti alloy implant; (b) Ti alloy implant.	73
<b>5.6</b>	in vitro– 24 hrs, 48 hrs, and 72 hrs cytotoxicity of test product in terms of percentage cell viability against Mouse fibroblast (L929) cell line by MTT assay.	73
<b>5.7</b>	Microscopic observations of cells after 72 hrs treatment with test product.	74
<b>6.1</b>	Schematic illustration of the work done in the present thesis.	78
<b>6.2</b>	Fabricated screw from PLA-based bio-composite as per ASTM standards by extrusion cum injection molding.	79

## List of tables

<b>Table no.</b>		<b>Page no.</b>
1.1	The presence of elements in Bone and HAp (Langer and Vacanti, 2003).	2
1.2	Material properties of some implant materials (Nakano, 2019; Liang et al., 2023).	8
1.3	Properties of various polymers (Daniels et al., 2019).	13
2.1	Parameters of the injection cum molding process.	34
2.2	Specifications corresponding to the plate and screw. (All measurements are in mm.)	40
2.3	Material property data (based on ASTM 308 <sup>#</sup> , Torres et al., 2015*).	41
3.1	DSC Thermogram analysis	51



# Chapter 1

## Introduction and Review of Literature

### 1.1. Introduction

Bone fractures are becoming more common, and the related mortality rate is comparatively high. The problem with this type of fracture is that it causes immense pain whenever there is stress at the fracture site, and re-joining the shattered bone is likely the best course of treatment. It requires immediate medical attention in the form of orthopaedic surgery, generally involving the implantation of internal fixation devices (IFDs), e.g., bone plates, screws, staples, pins, etc. The fixation device should possess sufficient mechanical strength and stability to support the alignment of the broken bone fragments and enable early mobilisation of the fractured site. Though conventional orthopaedic metallic implants have been extremely successful in restoring mobility, reducing pain, and improving the quality of life in millions of individuals each year, the incidence of re-surgery, surgical site infections and long-term bone remodelling remain major challenges with the traditional orthopaedic metallic implants. Treatment focuses on developing patient-specific implants with the required mechanical qualities to enable early functional therapy and rehabilitation. Bioresorbable polymeric internal fixation devices, the properties of which lie almost in the range of our natural bone properties, offer several distinct advantages over traditional devices. Once implanted in the body, they break down into harmless by-products, eventually eliminated from the body and replaced by host tissue. Thus, the need for a second surgical procedure to remove them can be averted. The healing process may continue for any time between 4-6 months [Onche et al., 2011], and treatment is based on the attempts to develop patient-specific implants with requisite mechanical properties, which will allow early functional therapy and rehabilitation.

The skeletal system has a rigid structure that supports and protects soft tissues. The bone's principal role is to withstand a load. From an engineering perspective, bone is an isotropic, non-homogeneous, and viscoelastic material. In dry weight, bone is

composed of roughly 65% inorganic minerals, mostly impure hydroxyapatite (HAp) ( $\text{Ca}_{10}(\text{PO}_4)_6(\text{OH})_2$ ), which provides resistance to compressive stresses, and 35% organic constituents, which include bone cells, fluids, and the organic bone matrix, which is composed of 90% type collagen and 10% non-collagen proteins shown in Table 1.1.

**Table 1.1:** The presence of elements in bone and HAp (Langer and Vacanti, 2003).

Elements	Bone	HAp
Ca (wt. %)	36.6	39.6
P (wt.%)	17.1	18.5
CO <sub>2</sub> (wt.%)	4.8	--
Na (wt.%)	1.0	--
K (wt.%)	0.07	--
Mg (wt.%)	0.6	--
Sr (wt.%)	0.05	--
F (wt.%)	0.1	--
Zn (ppm)	39	--
Ca/P ratio	1.65	1.67

Macroscopically, bone is classified into two main types based on density: cortical and cancellous. Cortical bone, making up about 80% of bone mass, is denser with a porosity of 3-4%. In contrast, cancellous bone, which consists of a mesh of trabeculae and has a porosity of 70-80%, is significantly weaker, with a modulus and strength around 20 times lower than cortical bone. Each type has specific structures: long bones (e.g., femur), short bones (e.g., wrist), and flat bones (e.g., skull), with significant variability in their cortical and cancellous composition. For instance, the ulna is 92% cortical, while a typical vertebra is 62% cortical and 38% cancellous. Long bones can be divided into three sections: the diaphysis (main shaft of cortical bone), epiphysis (expanded ends with articular cartilage), and metaphysis (transition area). Cancellous bone is mostly present within the last two sections.

Microscopically, bone is further classified into woven and lamellar types. Woven bone is immature, found in fetuses, young individuals, and during fracture healing, while lamellar bone is more organized and grows more slowly. The periosteum and endosteum are connective tissues covering the outer and inner surfaces of bone, providing nourishment and housing nerves, with the endosteum also lining the medullary cavity.

Bone is a complex tissue that features three essential types of cells: osteoblasts, osteoclasts, and osteocytes, each playing a vital role in bone remodelling. Osteoblasts, generated in the periosteum and stromal tissue of bone marrow, are critical for bone formation. As they create new bone tissue, some become trapped within the mineralized matrix and develop into osteocytes. Osteoclasts, derived from bone marrow, are responsible for bone resorption; they break down bone tissue using acids that dissolve minerals and enzymes that degrade collagen. This process is crucial as it releases vital minerals and other important molecules from the bone matrix into the bloodstream, supporting overall health. Osteocytes, the final cell type, are essentially matured osteoblasts residing within the bone matrix, maintaining the bone's integrity and function. Understanding these cells' roles underscores our skeletal system's dynamic and essential nature.

## **1.2 Global and Indian scenario of the orthopaedic devices market**

The global orthopaedic device market size was USD 53.44 billion in 2019 and is forecasted to reach USD 68.51 billion by 2027, exhibiting a CAGR of 6.6% during the period [Fortune Business Insight, 2020]. The growing prevalence of bone degenerative disorders such as osteoporosis and rheumatoid arthritis and sports accidents leading to bone injuries will spur the demand for trauma fixation devices in the future years. Moreover, the adoption of innovation in implant technology and advancement in healthcare facilities are also driving factors to boost the growth of the global market during the forecast period. However, device complications or strict regulatory reforms can impede the growth of the market. The global internal trauma fixation devices market can be segmented based on the type of fracture, application, product, end-user and geography in the below-mentioned. Artificial joints and fixation devices are the two major segments in the orthopaedic market that are estimated to be around Rs.2400 crores in the Indian Market, and it will grow at around 20% every year for the next decade to reach Rs.16000 crores by 2030 [Orthopedic Devices Market – At a Turning Point, 2017]. Compared to knee or hip joint replacement, external and internal fixation devices such as plates, screws, and intramedullary nails are far cheaper, which makes it a preferred technology when clinically feasible. The Indian orthopaedic devices market is worth around \$375 million or Rs. 2,400 crores, of which knee and hip joints constitute alone a staggering 54% and is followed by the trauma fixation market, which includes internal and external fixation devices. North America has been dominating the

Orthopaedic Device Market. It is expected to maintain its dominance throughout this period due to the increasing awareness of minimally invasive procedures for orthopaedic surgeries [Global Medical Devices Packaging Market: Growth, Trends and Forecast (2020-2025)]. The Asia-Pacific market is anticipated to see significant growth owing to increasing medical tourism due to the availability of cost-efficient and advanced healthcare treatment options compared to the other geographical regions [Global Market Insights Inc]. In 2014, the USA accounted for over 50% of India's imports, followed by the European Union, accounting for 26.6%, led by Ireland (16.3%), mainly due to the manufacturing activities of United States multinationals in Europe [MediPoint: Trauma Fixation - Global Analysis and Market Forecasts]. A few of the major foreign industry competitors featured in the global trauma fixation devices market are Wright Medical Group N.V., Smith & Nephew, Johnson & Johnson (DePuy Synthes), Integra Life Sciences, Stryker Corporation and Zimmer Biomet Holdings Inc., among the other industry players. Major Indian players profiled in this segment are Atlas Surgical, Narang Medical, Apothecaries Sundries Manufacturing Co. (ASCO) and Invicta Meditek Ltd [Trauma Fixation Devices Market Global Industry Analysis]. The industry participants emphasize on mergers & acquisitions as well as novel product developments to strengthen their position in the market and gain larger revenue share. Similarly, latest trend of bioresorbable implant market is gaining momentum due to result of technological advancement. Bioresorbable plates, pins, and screw implants are widely used for fracture fixation in orthopaedic surgeries and trauma care. Hence, operations to remove the synthetic material are not required. These bioresorbable products should be corrosion-resistant and absorb in the body. They should not be mutagenic and accumulate into toxic products. The bioabsorbable implants Market has been analysed across regions of North America, Latin America, Europe, East Asia, South Asia, Oceania, and Middle East & Africa (MEA).

### **1.3. Material properties of bone tissue**

In general, bone exhibits anisotropic elastic modulus in different anatomic directions. For example, the elastic modulus in the longitudinal direction of a long bone (17.4 GPa for human bone and 20 GPa for bovine bone) is more significant than in the transverse direction (9.6 GPa for human bone and 11.7 GPa for bovine bone). An orthotropic or transversely isotropic constitutive relation describes cortical bone properties fairly well [Zysset et al., 1999]. Cancellous bone is a complex material with significant

heterogeneity. Its elastic and strength properties vary across anatomic sites, with ageing and diseases. Cancellous bone is classified from an engineering material perspective as a composite, anisotropic, open porous cellular solid like many biological materials. It displays visco-elastic behaviour, as well as damage susceptibility during cyclic loading. It has been established, theoretically and experimentally, that Young's modulus of cancellous bone was strongly dependent on the bone's apparent density [Gibson, 1985].

i) Cortical Bone: An Elastic modulus in the range of 17 GPa was found in the initial

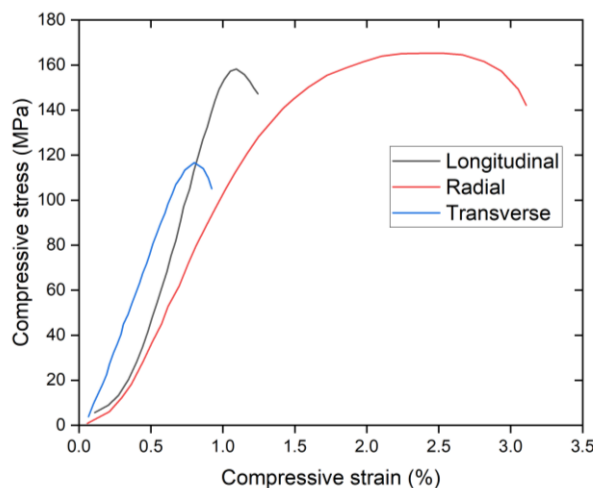


**Fig. 1.1:** Stress-strain curve for Cortical bone (Villette et al., 2018).

linearly elastic region. In the intermediate region, the bone exhibits nonlinear elastoplastic behaviour. This region is characterised by bone yielding with yield strength value reported to be around 110 MPa. The final region exhibits linear plastic behaviour with a strain hardening modulus of 0.9 GPa. The bone was found to have fractured when the tensile stress was 128 MPa and the

corresponding tensile strain was 0.026. The elastic moduli and strength values of a bone specimen depends on the strain rate, indicative of the viscoelastic property of the bone.

ii) Cancellous Bone: The stress-strain curve of cancellous bone has three distinct phases of behaviour.

Phase 1: Behaviour is linear elastic as the cell walls bend or compress axially.

Phase 2: Eventually, at high enough loads, the cells begin to collapse by elastic buckling, plastic yielding or brittle fracture of the cell walls. This second phase of collapse progresses at a roughly

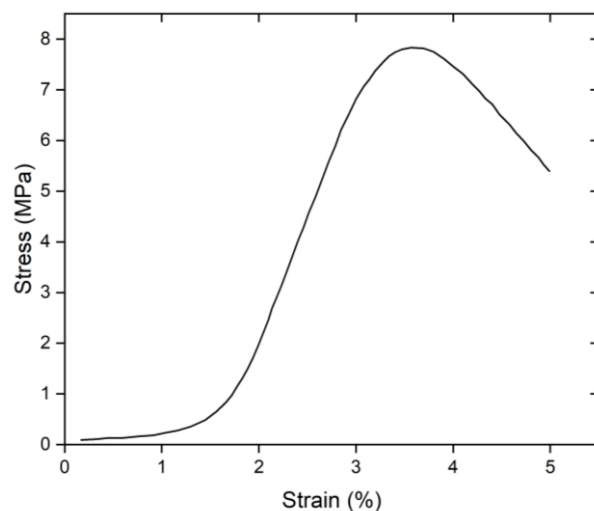


**Fig. 1.2:** Stress-strain curve for Cancellous bone (Villette et al., 2018).

constant load until the cell walls meet and touch.

Phase 3: Once this happens the resistance to load increases, giving rise to a final increasingly steep portion of the stress-strain curve.

#### 1.4. Bone fracture healing

The biology of fracture healing is a complex biological process that depends on specific regenerative patterns and involves changes in the expression of several thousand genes. Fracture healing is the biology of repair at the fracture site that proceeds through a series of stages successfully. Bone healing conditions can be achieved either by conservative or non-conservative methods.

**Conservative Method:** This treatment of fracture involves repositioning the bone fragments, wound closure (if necessary)

and application of a cast or a splint to hold the bone in place. Immobilization facilitates the joining of the fragments along with the healing process. It requires early callus formation and gradual transformation of the primitive tissue to bone. Early mobilization should be achieved as early as possible to prevent stiffening of the joints. Example: Cast, splint, traction etc.

**Non-conservative Method:** The fracture site in these healing methods must be held more securely providing more stability. This may result in more rapid healing and repair processes can even skip some of the early stages.

Example: Plate, screws, Intra medullary (IM) rod and nails etc.



**Fig. 1.3:** Examples of conservative methods: Cast (top) and Splint [Google].



**Fig. 1.4:** Examples of non-conservative methods: Plates and Screws, (Source: [www.indiamart.com](http://www.indiamart.com)).

Bone healing takes place relatively either by primary or secondary bone healing.

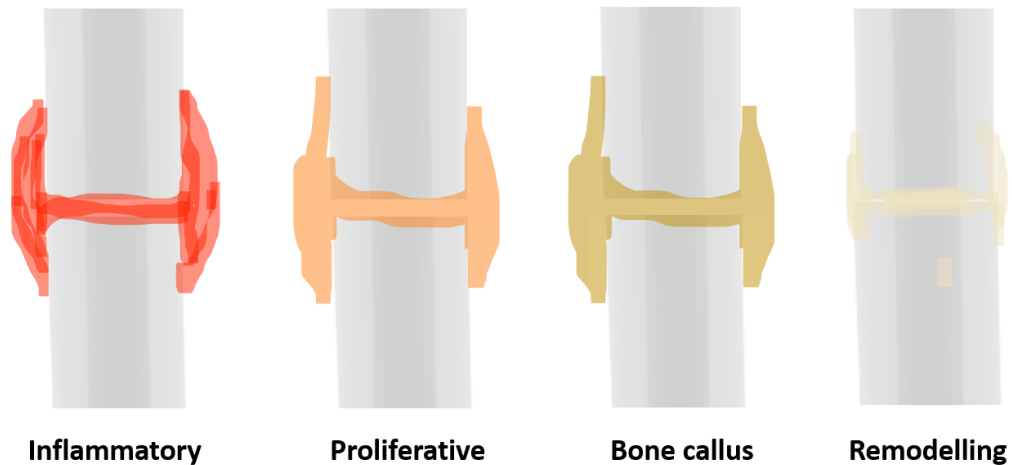


**Fig. 1.5:** Stages of secondary bone healing.

- a) **Primary Bone Healing:** Primary bone healing involves a direct attempt by the cortex to re-establish itself after interruption without forming a fracture callus. It is, however, a rarity that all the edges conform exactly, and hence this type of healing is less seen.
- b) **Secondary Bone Healing:** Secondary bone healing involves the classical stages of injury, haemorrhage, inflammation, primary soft callus formation, callus mineralization and callus remodelling.

### **1.5. Types of Implant Material**

Implant materials play a crucial role in the fixation process. The use of biomaterials for internal fixation devices is one of the important factors to be considered for its performance. An ideal implant material should be chemically inert, biocompatible, corrosion-resistant, wear-resistant, high-strength, and cost-effective. A variety of metals, polymers, and ceramics fall under this category.

#### **1.5.1. Bio-metals**

Bio-metals are inorganic metallic biomaterials that are neither bioactive nor biodegradable. Common examples of bio-metals include stainless steel, cobalt alloys, and titanium alloys, widely used in orthopaedics. The first metallic materials successfully utilized in orthopaedic applications during the twentieth century were stainless steel and cobalt-chrome-based alloys. Stainless steel is favoured for its mechanical strength, affordability, versatility in shaping, and durability, making it a reliable choice for various medical applications. Specifically, stainless steel AISI 316L

(ASTM F138 20) is commonly used in temporary implant devices such as fracture plates, screws, and hip nails [Özbek et al., 2002]. Following stainless steel, cobalt-chromium alloys emerged as an option for surgical implants due to their high resistance to corrosion, fatigue, and wear, although they are relatively heavy. The ASTM recommends four types of cobalt-chromium (Co- Cr) alloys for surgical implant applications including cast Co-Cr-Mo alloy (F75), wrought Co- Cr-W-Ni alloy (F90), wrought Co-Ni-Cr-Mo alloy (F562) and wrought Co-Ni-Cr-Mo-W-Fe alloy (F563) are recommended by the ASTM. However, some varieties of cobalt alloys are toxic to human in vitro studies.

Titanium (Ti) and its alloys were introduced in the 1940s. It was observed that, in addition to being lightweight, they possess excellent osteointegration properties, which reduce the risks of loosening and failure in medical applications. Alloys such as ASTM F67 and the Ti-6Al-4V ELI alloy (ASTM F136) are commonly used in biomedical applications. Recently, new titanium alloys have been developed that do not contain harmful elements [Nomura et al., 2010]. The mechanical properties of an implant, including elastic modulus (stiffness), tensile strength, flexural modulus, and percentage elongation, play significant roles in bone fracture healing. Elastic modulus measures the strain in response to a given tensile or compressive stress, while tensile strength indicates the maximum stress the material can withstand before breaking. The percentage elongation assesses the ductility of the material before a fracture occurs. Inadequate stiffness at the repair site can promote motion, which supports bone healing. However, eliminating micromotion can hinder the healing process and cause stress-

**Table 1.2:** Mechanical properties of some implant materials (Nakano, 2019; Liang et al., 2023).

<b>Materials</b>	<b>Elastic Modulus (GPa)</b>	<b>Tensile strength (MPa)</b>
<b>Al<sub>2</sub>O<sub>3</sub></b>	350	1000 to 10,000
<b>SS316</b>	210	600-1000
<b>Ti6Al4V</b>	120	900
<b>Co-Cr alloy</b>	210	1085
<b>Ti</b>	100	620
<b>Bio-glass</b>	35	42
<b>Zirconia</b>	220	820
<b>HA</b>	95	50

shielding [Nag and Chanda, 2021]. It was also observed that some inflammation reactions near the surrounding tissues caused by corrosion and ion leaching occur, leading to the removal of the implants through surgery. The mechanical properties of some implant materials and tissue are listed in Table 1.2. Among several other metals studied for implant applications, magnesium attracted the most significant interest in the field of bio-degradable metallic materials [Vojtěch et al., 2011]. The application of degradable magnesium alloys in orthopaedic applications has shown mechanical properties more similar to bone properties that can be achieved by selected magnesium alloys as compared to titanium and steel. In addition, it could be favourable in terms of reducing bone degradation and stress shielding. Magnesium-based screws have been used in bone healing clinical trials without notable side effects reported by patients [Gu et al., 2009]. Magnesium alloys have higher strength and ductility than organic polymers and are thus preferential for load-bearing applications. However, corrosion rates obtained for magnesium alloys were reported to differ by four orders of magnitude between *in vitro* and *in vivo* conditions [Ma et al., 2014]. Corrosion results in hydrogen gas accumulation in the tissue; accumulating solid corrosion products may exert pressure on non-yielding bony tissue, leading to premature implant failure, which is one of the major drawbacks of magnesium-based implants. Studies on Mg-Zn alloys highlight their mechanical properties, which can be adjusted according to requirements but still remain to be established as high strength with respect to titanium or stainless steel. Studies also acknowledge that zinc alloy degradation products have no adverse effects and are biocompatible. Application of carbon fibres as biomaterials of first generation has also been studied in total hip replacement and internal fixation, but the concern lies over the release of debris into the surrounding tissues, evoking an adverse cellular response, which is undesirable [Brandwood et al., 1992].

### **1.5.2 Types of Metallic orthopaedic Fixation Devices**

Repairing harmed or ailing musculoskeletal tissues is a noteworthy clinical issue and fixation devices are used to support the alignment of bone fragments during the healing process. Fixatory implants can be either internal or external. External fixation (EF) device is a simple, quick and safe procedure to stabilize fractures in poly traumatised patients. Internal fixation devices (IFDs) have enough mechanical strength and allow early mobilization of the injured part (MDMP Index). The selection of internal fixation

devices depends on the sites of bone fracture. The conventional metallic internal fixation devices that are extensively used can be classified as:

**Cortical screw:** The cortical screw features dense spiral threads running over its surface with an aggressive pitch, lower thread depth and larger core diameter, allowing them to engage well in cortical bone, primarily in the diaphysis region. It transforms torsional stresses into compression. The screw threads carve their way through the bone upon insertion, allowing cortical screws to be self-tapping. The basic function of a screw is to disperse and distribute mechanical load in load-bearing applications [Felfel et al., 2013].

**Cancellous screw:** Long bone fractures are typically repaired using cancellous screws, which serve to secure the cancellous bone. These screws are most commonly used in the metaphysis of long bones, where cancellous bone is prevalent. Unlike cortical screws, cancellous screws have threads that are more widely spaced, deeper and have smaller core diameter [Ricci et al., 2010]. Since cancellous bone is significantly less dense than cortical bone, cancellous screws are often employed in low or non-load-bearing applications primarily by drilling method.

**Bone plates:** A bone plate is fixed to the screws which secure the plate and orient the bone, aiding in the healing process. It is also known as orthopaedic bone plates and is used to secure shattered bones with screws. It is available in a variety of configurations, including dynamic compression plate (DCP) and least contact dynamic compression plate. Bone plates can be left in situ after healing or removed, depending on the type of fracture cases [Ratner et al., 2004].

**Steinmann pins:** These are frequently used to keep together fragments of bone that are too tiny to be repaired with screws. They are commonly used alongside other types of internal fixation, although they can also be used alone to heal fractures in non-load bearing situation like torn ligament or cartilage of limbs [Pietrzak et al., 2002]. Steinmann Pins are typically constructed from implant-grade stainless steel. Steinmann pins are comparable to K-wires, except they have bigger diameters. These pins commonly feature trocar, chisel, or spherical ends with a partially threaded or smooth outer diameter.

### **1.5.3 Problems with metallic internal fixation devices**

Traditional metallic fixation device provides reliable and stable initial post-operative restoration of the fractured bones allowing early mobilization but the main disadvantage associated with them is the need of secondary surgical removal of the hardware after the reunion of the fractured bone which may sometimes lead to bone re-fracture. Very stiff metallic materials may cause osteoporosis beneath the implants because of stress shielding and may lead to bone fracture at the implant site. Stress shielding occurs when two or more components with different moduli from one mechanical system. The component with higher modulus bears most of the load and protects the other component [Nag et al., 2022]. On the other hand, if flexible implants with inadequate strength are used, it may result in non-union of the fracture and thus causing pain. Therefore, trade-off should be reached between strength and stiffness. Ideally, as the fracture heals, the stiffness of the fixation device should decrease as the bone strength increases. While relatively rare, corrosion of metallic implants is not a negligible concern. Also, metallic implants interfere with post-operative CT scans, MRI images or radiography [Onche et al., 2020; Son et al., 2012].

#### **1.5.4 Alternate solution to metallic fixation devices**

The second generation of biomaterials appeared in the 1960s, introduced by [Kulkarni et al., 1971], with the development of bioactive materials' ability to interact with the biological environment to enhance the biological response and the tissue/surface bonding. Bioactivity refers to any interaction or effect that materials exert on cells with the aim of leading or activating them to specific responses and behaviours. None of the metallic materials used in orthopaedics is bioactive per se. However, two approaches can be considered to obtain bioactive metals. The first one consists of coating the surface of the implant with a bioactive ceramic HAp. The second one is to chemically modify the surface of the material to obtain the deposition of a bioactive ceramic in vivo or to induce proteins and cell adhesion and other tissue/material interactions. Ceramics have good compatibility and corrosion resistance, but limitations like low toughness, brittleness, low mechanical reliability, and high density restrict their use in high load-bearing applications.

The second alternative solution could be application of bioabsorbable polymeric IFDs, which properties lies almost in the range of our natural bone properties. The application of biomaterials such as bioresorbable polymeric materials in the medical device industry has experienced rapid growth in recent decades and can be considered

as a substitute for metallic fixations in orthopaedics and trauma. The development of resorbable biomaterials displayed a controlled chemical breakdown and the resorption of the polymer chains.

### **1.6 Bioresorbable implants**

The term 'bioresorbable' can be defined as materials or devices that, after implantation in the body, serve their intended purpose and gradually get degraded in the body into harmless products. Moreover, it gets eliminated from the body without any physical intervention, leaving no sign of injury or repair. The first use of bioresorbable orthopaedic devices dates back to the early 1960s. The implant material, along with the properties of bone, must also be biocompatible to promote host cell adhesion, which is important to prevent bacterial adhesion on the exposed host tissue surface. Self-degrading implant materials with bone-like mechanical parameters minimized stress-shielding, and suitable degradation characteristics could reduce long-term side effects associated with conventional permanent implant materials [Brown and Farrar, 2008]. The proposed materials must meet the physical and chemical demands of clinical applications. The physical demands include high strength, appropriate initial modulus and controlled degradation rate. During the early healing stages, high strength to resist mechanical stresses and must be able to carry external and physiological loads. The appropriate modulus indicates that the material must not be too stiff or too flexible for the special purpose for which it is intended. The loss of strength and modulus in vivo must be in coordination with the increase of strength and modulus of healing tissues. The medical demands are linked to the biocompatibility of the materials and non-toxicity of the degradation products [Weiler et al., 2000]. Biodegradable polymers of synthetic and natural origin such as polyglycolide (PGA), polylactide (PLA), polydioxanone (PDS), poly(3-caprolactone) (PCL), polyhydroxybutyrate (PHB), polyorthoester, chitosan, poly (2-hydroxyethyl- methacrylate) (PHEMA), hyaluronic acid and other hydrogels were extensively studied during this period (Table 1.3). In the last decades, these materials have been used as promising candidates in many orthopaedic applications like substitution, repair of bone fractures (including ligament fixation), cartilage, meniscus and intervertebral disc as sutures, rods, screws, pins and plates. Rapid degradation is an undesirable phenomenon in medical implant applications and can be avoided through proper choice of materials and design [Brown and Farrar, 2008]. Therefore, the general criteria of selecting polymer for use in bio-

resorbable internal fixation devices should be based on tailoring its mechanical properties and its degradation time to the need of application. The widely used synthetic biopolymers along with their excellent properties and the challenges associated with it

**Table 1.3:** Properties of various polymers (Daniels et al., 2019).

Polymers	Melting temperature (°C)	Glass transition temperature (°C)	Modulus (GPa)	Elongation (%)	Degradation time (months)
DLPLA	Amorphous	55-60	1.9	3-10	12 to 16
PGA	220-230	35-45	6-7		6-12
PLA	150-162	45-60	0.35-3.5		Several years
PLLA	170-200	55-65	2.7-4.14	5-10	>24
P-DL-LA	Amorphous	50-60	1-3.45		12-16
PCL	59-64	-60-(-65)	0.2-0.4	300-500	>24
PDO	N/A	-10-0	1.5	N/A	6 to 12
PGA-TMC	N/A	N/A	2.4	N/A	6 to 12
85/15 DLPLG	Amorphous	50-55	2.0	3-10	5 to 6
75/25 DLPLG	Amorphous	50-55	2.0	3-10	4 to 5
65/35 DLPLG	Amorphous	45-50	2.0	3-10	3 to 4
50/50 DLPLG	Amorphous	45-50	2.0	3-10	1 to 2
PLGA (50/50)	Amorphous	50-55	1.4-2.8	--	3-6
PLGA (85/15)	Amorphous	50-55	1.4-2.8	--	3-6
PLGA (90/10)	Amorphous	50-55	--	--	<3
PHB	168-182	5-15	3.5-4	5-8	
PPF	30-50	-60	--	--	>24

have been discussed in this section. The best-known biodegradable polymers approved by the FDA (Food and Drug Administration) and mostly used for resorbable implantable devices are polylactide (PLA), polyglycolide (PGA), their copolymers and also polycaprolactone (PCL) and polydioxanone (PDO or PDS) among others [Middleton. & Tipton, 2000].

Polyglycolic acid (PGA) is a hard, tough crystalline polymer of high molecular weight (20,000 to 145,000) with high melting points (220-230°C) and a glass transition temperature of 34-40° C. It has a tensile strength of 57 MPa and a tensile modulus of

6-7 GPa. The mechanical strength of the PGA is found to increase when spun into fibre due to the preferred high molecular orientation of the fibre [Ashammakhi and Rokkanen, 1997]. Self-reinforced PGA (SR-PGA) shows the strength properties of stainless surgical steel (330 MPa [Suuronen et al., 2000]). PGA lose its mechanical properties in the body within 6 weeks and get resorbed in less than one year. PGA undergoes degradation in a two-stage process where first scission of ester bonds take place due to penetration of water in the amorphous region followed by hydrolytic attack in the crystalline domains [Holland et al., 1987].

Poly(lactic acid) (PLA) on the other hand is a semi-crystalline polymer, which has two enantiomeric isomers, designated as D and L, or as a racemic mixture, designated as DL [Suuronen et al., 1999]. It is the L form (PLLA) and DL form (PDLLA) forms of PLA that are used in medical applications. L-PLA is semi-crystalline in nature and PDLLA is the copolymer of L-Lactic acid and D-Lactic acid which is more amorphous, thus making it more suitable for homogenous dispersion of drug in the polymer matrix [Jain et al., 2000]. Poly-DL-lactic acid has no detectable glass transition temperature ( $T_g$ ) and has a melting point ( $T_m$ ) of about 60°C. Poly-L-lactic acid has a  $T_m$  of about 174-184°C with a  $T_g$  of 57°C [Serlo et al., 2002]. PLLA has good mechanical properties with a bending strength of 240 MPa and a degradation time of up to 5-7 years. The degradation rate of PDLLA can be varied by altering the percentage composition of the D and L components [Suuronen et al., 1999]. P(D,L)LA undergoes degradation in two stages. First, the scission of the random hydrolytic chain of the ester bonds occurs along with linear loss in molecular weight. The second stage generally starts at an average molecular weight of 15,000. This phase also marks weight loss and total loss of tensile strength, accompanied by an increase in chain breakdown [Holland et al., 1987].

The next most widely used set of materials is probably polylactide copolymerized with polyglycolide (PGLA), which is substantially amorphous and retains 70% of its initial strength up to 8 weeks, degrading within 1 year [Suuronen et al., 1999]. Copolymerisation slows the rate of PGA degradation, but the rate of PLA degradation increases. The degradation range of PLA-PGA copolymers varies depending on their compositional ratios. This copolymer exhibits a glassy nature due to its  $T_g$  being above the physiological temperature of 37°C. The degree of crystallinity and the  $T_m$  of the polymers are directly related to the molecular weight of the polymer [Jain et al., 2000].

The significant mechanical strength due to their rigid chain structure gives them an added advantage as drug delivery devices. PGLA undergoes hydrolytic degradation with random chain scission and loss of molecular weight which is dependent on its physical properties like molecular weight, degree of crystallinity and glass transition temperature.

PCL is partially crystalline, with a melting point of 59-64° C and a glass transition temperature of 60°C. It has a tensile strength of 16 MPa and a tensile modulus of 0.4 GPa. PCL is highly hydrophobic with a comparatively longer degradation time [Henkel, 2013]. Due to low melting temperatures, PCL is easily processed by conventional melting techniques and can be filled with stiffer materials (particles of fibres) for better mechanical properties.

Differences in the degree of crystallinity among different materials have a pronounced effect on mechanical properties and degradation rate. Generally, compared to amorphous polymers, semi-crystalline polymers have higher strength and stiffness and are, therefore, suitable for load-bearing applications. Amorphous polymers tend to degrade faster with respect to semi-crystalline polymers with the same chemistry. PLLA and PGA have a regular structure and are able to crystallise compared to PDLLA and PGLA, which are amorphous. Another factor affecting degradation rate is the hydrophilicity, for e.g.: hydrophilic PGA degrades significantly faster than the more hydrophobic PLA and PCL. PCL is highly hydrophobic and has a longer degradation time than PLA, which makes it suitable for applications where a longer degradation time is required. Therefore, all the properties must be considered to fabricate a device with the material of interest.

It is desirable that an ideal material must retain its strength typically 8-12 weeks during tissue healing and then controllably lose mass so as to allow growth of new tissue and replacement of the polymer. Rate of degradation and mechanical properties can be tailored by use of additives or fillers and use of co-polymers. However, polymer undergoing bulk degradation tend to degrade via loss of molecular weight followed by strength loss. Table 1.3 shows the properties of various bioabsorbable polymers suitable materials for applications as orthopedic fixations along with their properties [Rezwan et al., 2006; Durucan et al., 2001].

### **1.6.1 Advantages of bioresorbable devices**

They offer a number of distinct advantages over traditional devices. Once implanted in the body, they break down into harmless by-products, eliminated from the body and get replaced by host tissue. Thus, the need of a secondary surgical procedure to remove them can be averted. The possibility of stress-shielding associated with long term use of metallic implants can be eliminated due to low stiffness of bioresorbable implants compared to bone and also avoid complications like corrosion, stress-shielding, release of metal ions. In addition to that, bioresorbable devices are radiolucent and hence do not interfere with current imaging techniques e.g. CT or MRI and post-operative radiotherapy. They are also being used for delivering bioactive agents and have the ability to transfer the load to healing bone and soft tissues.

### **1.6.2 Challenges associated with bioresorbable polymers and IFDs**

The complications arising from these devices that have hampered its general acceptance clinically are mentioned below.

- i) **Rate of degradation:** As discussed earlier in the previous section about the advantages of using bioresorbable polymers to date, the challenges associated with them also need to be identified. Sometimes, materials with required strength have less resorption time, causing early degradation of the implant and eventually leading to implant failure. Tailoring of the degradation rate needs to be done to match the healing process of tissues [Klee and Höcker., 2000].
- ii) **Foreign body reaction:** One of the major drawbacks is the complications arising from the adverse host response invoked inside the body due to the degradation products when it exceeds the clearance capacity of the body [Enislidis et al., 1998]. It has been observed that the clinical complications are mostly associated with the homopolymers as opposed to the co-polymers and the adverse reactions are in the form of inflammation, fistulas and tenderness. It is desirable that a bioresorbable material used for construction must have more amorphous region compared to crystalline as amorphous state can be degraded easily and is safe for in vivo implantation.
- iii) **Mechanical strength:** Development of high strength modulus materials for high load bearing applications with an optimum degradation profile still remains one of the key challenges. Biodegradable fixation implants are typically made thicker and wider than the corresponding metal implants in order to achieve sufficient fixation stability.

The various inorganic fillers are available such as hydroxyapatite, silk nano-fibres, MgO, SiO<sub>2</sub> and additive active fillers like silver, zinc, copper etc. for antimicrobial properties [Brown and Farrar, 2008], which could be used in various combination of loading in order to optimize the stability of the fixation devices in all aspects. Fabrication of perfect IFDs can also be achieved by the combination of different polymer systems or by orientation of polymer chains. Moreover, the degradation behaviour is also not similar with that of the metallic implants as the properties of polymer-based materials varies with temperature, conditions and surrounding environments.

iv) **Multifunctionality:** Fabrication of a drug-eluting bioresorbable implant can be challenging as incorporation of additives in the polymer matrix may compromise with the mechanical strength is more vulnerable to denaturation and lack of controlled release.

v) **Infection Susceptibility:** Implant-related infections due to the formation of bacterial biofilms remain one of the leading reasons for implant failure from osteomyelitis, resulting in high socio-economic loss. The incidence of infection ranges from 0.2 to 2 %, depending on various factors like surgical procedure, microorganism's and host's type, type of fracture, type of implant, and antibacterial prophylaxis.

### **1.7 Desirable osteo-fixation devices**

The current study will concentrate on developing novel devices to serve three different functions, namely, osteo-fixation, osteo-conduction and infection prophylaxis.

**Osteo-fixation:** Bioresorbable fixation devices eliminate stress-shielding as they decompose gradually and transfer the load to the healing tissue, and also, the secondary operation for removal of the device is not needed, which reduces the total cost compared to metallic devices. The development of high-strength modulus materials for high load-bearing applications with an optimum degradation profile still remains one of the key challenges. Biodegradable fixation implants are typically made thicker and wider than the corresponding metal implants or by using a polymer with a high molecular weight in order to achieve sufficient fixation stability. Various other approaches involve the incorporation of fillers and fibres such as hydroxyapatite, chitosan, silk, carbon and glass fibres and oriented chains to reinforce the matrix of the device. However, the degree of reinforcement depends on the adhesion promoters that can be used which normally possess toxic effects. However, self-reinforced (SR) technology based on

reinforcing elements with the same chemical composition as that of matrix helps in manufacturing implants of ultra-high strength. Self-reinforced resorbable composites fulfil the physical demands of secure fixation materials and devices because they have a ductile deformation mode, high initial strength, appropriate elastic modulus and they lose their strength gradually and are totally absorbable [Rokkanen et al., 1990]. Incorporation of antimicrobial agents to bioresorbable materials can impair their mechanical strength that has been confirmed by the in-vitro immersion tests of antibiotic containing screws where the shear strength decreased to half within six weeks. However, promising results can be seen in SR high strength with drug-eluting characteristics developed by Ashammakhi et al. (2005) in cranio- maxillofacial surgery (CMF).

**Osteo-conduction:** An osteoconductive agent is added to promote early healing by the growth of bone tissue with gradual degradation of the implant. Arbind et al. in their work have used hydroxyapatite in PLA-Hap composites that acted as a bioactive material. BG has been shown to be a promising bone substitute material in experimental bone defects. Bioactive Glass (BG) are silicate glasses containing sodium, calcium, and phosphate as the main components [Turunen et al., 1994]. BG was first introduced by Hench et al. in 1971. BGs are osteoconductive and have bone bonding characteristic. BG are useful in the treatment of fresh bone defects adjacent to dental implants. It acts as a filler in bone defects [Heikkilä et al., 1995]. PLGA is found to possess osteoconductive properties, permitting gradual replacement of the implant by bone. Loading this polymer with osteogenic cells may also confer osteoinductive properties. Ruuttila et al. showed that SR-PLA 70 plates coated with BG are capable of inducing a proliferative response of human primary osteoblasts and appear to support the development of mature osteoblast phenotype (Ruuttila et al., 2006).

### **1.8 Finite Element (FE) studies**

FE Analysis has been extensively used in the design and evaluation of fixation plates and screws to overcome the most drawback of the current fixation devices: fatigue failure of the device and stress shielding of the bone. A 3-D analysis is necessary to take into account the complex geometry of the plate system and predict stress distribution in the bone. FE is a numerical approach that provides approximate solutions to differential equations that form a boundary value problem. FE based technique was established in the 1960s, but was introduced in bone research in the 1970s. To allow

the analysis of complex geometries, boundary conditions and material properties the overall structure is arranged as a set of discrete problems. The geometric representation consists in a mesh of element connected at nodal points, whose displacements are calculated from applied boundary conditions and mapped into local strains and stresses of the whole structure. Finite-Element (FE) analysis is a numerical method commonly utilised in designing and evaluating fixation plates and screws to address fatigue failure and bone stress shielding issues. A 3D analysis is required to account for the complex geometry of the plate-screw system and to anticipate stress distribution in the bone. The role of FE lies in generating approximate solutions to differential equations that form a boundary value issue. The FE-based technique was developed in the 1960s but was first used in bone research in the 1970s. To allow for the analysis of complex geometries, boundary conditions, and material properties, the overall structure is organised as a collection of discrete problems. The geometric representation is made up of a mesh of elements connected at nodal points, with displacements derived from applied boundary conditions and mapped into local strains and stresses of the entire structure.

The effect of stress shielding was investigated using a 3D, quarter-symmetric FE model based on a canine femoral diaphysis plated with a polymer or metal design [Ferguson, 1996]. FE can be used to investigate the underlying mechanics of various biological tissues, such as how these structures will behave to varying loading situations or limitations. Bone remodelling is extensively researched using FE analysis. When bone tissue is loaded, its mechanical environment changes and the tissue responds by producing local mechanical stimuli. These prediction algorithms are frequently implemented in a feedback loop, in which the model's attributes are updated with each iteration. In practice, the trustworthiness of the numerical modelling technique can only be determined by comparing the results to experimental data acquired under identical conditions [Hefzy and Singh, 1997]. When the experimental validations cannot be done, any source of error calls for proper address using multiple meshes and multiple exploratory runs. Bernakiewicz. et al. (2002) concluded in their study that by using an FE model it is possible to carry out predictions without a direct experimental validation of the model. The FE model aids in understanding the mechanical behaviour of orthopaedic devices and can provide extra information about particular patients to assist the orthopaedic surgeon in decision-making before surgery.

## 1.9 Literature Review

Lin et al. (1992) studied the ciprofloxacin concentrations in bone released from PLA implants in rabbits and its efficacy in the treatment of induced osteomyelitis. Implants demonstrated therapeutic local concentration and low systemic levels over an eight-week interval. Using the chronic osteomyelitis rabbit model, a comparative series demonstrated the therapeutic efficacy of antibiotic-PLA in the treatment of chronic osteomyelitis. Overbeck et al. (1995) tested the penetration depth of ciprofloxacin into bone cortex and marrow from ciprofloxacin-releasing PGA implants in rabbits. After four weeks of implantation, bactericidal levels were measured up to a penetration depth of nearly 10 mm. The study showed a significantly greater penetration of ciprofloxacin into bone than has been reported for gentamycin cement beads. Koort et al. (2005) has shown that ciprofloxacin and bio glass containing PDLLA 50/50 implants are efficient in the treatment of localized osteomyelitis due to *Staphylococcus aureus*.

Andreopoulos et al. (1996) measured in vitro antibiotic concentrations released from PLA implants. Release was controlled by the drug diffusion and the matrix degradation, the latter being the most critical factor. The obtained concentration levels were above MIC against the major causative bacteria of osteomyelitis. Nie et al. (1998) tested ofloxacin-releasing P(D/L)LGA implants to treat induced *Pseudomonas aeruginosa* osteomyelitis in rabbits. Implants were suitable vehicles for the delivery of high local concentrations of ofloxacin. These concentrations resulted in eradication of the bacterial pathogen in this rabbit model. Veiranto et al. (2002) studied in vitro self-reinforced ciprofloxacin-releasing P(D/L)LLA 70/30 screws. The screws gradually released ciprofloxacin and at the same time had sufficient mechanical strength at least 12 weeks at the level, which ensures their fixation properties. Wang et al. (2004) investigated cefazolin- and gentamicin-releasing PLGA 50/50 implants for a long-term drug release in vitro. The results suggested that the bioresorbable beads released high concentrations of antibiotic (well above minimum inhibitory concentration) in vitro for the period of time needed to treat bone infection, i.e. 2-4 weeks. This would enable their use as the first line choice for patients with osteomyelitis and various infections as well as for the prophylaxis of these infections.

Lucke et al. (2005) compared PDLLA coated, uncoated and Gentamicin PDLLA-coated K-wires in the treatment of induced osteomyelitis in rat tibias. Half of the animals also received a single shot of gentamicin 30 min prior to surgery. Implant-

related osteomyelitis could be prevented by prophylaxis of systemically applied gentamycin in 15% of animals. Onset of infection could be prevented in 90 % of animals treated with gentamicin-coated K-wires, and in 80 % of the animals that were treated with a combination of local and systemic application. The local application from PDLA-coated implants might support systemic prophylaxis in preventing implant-associated osteomyelitis. Makinen et al. (2005) explored a bioabsorbable ciprofloxacin-containing bone screw (Ab- PLGA) to prevent biomaterial-related infection due to *S. aureus* in a rabbit model and demonstrated that cultures of all Ab-PLGA screws contaminated with *S.aureus* before implantation were negative in follow-up. The shear strength of the implant confirmed from in- vitro immersion testing was decreased to half within 6 weeks due to incorporation of antimicrobial agent which have restricted the widespread of clinical application of these implants. The study confirmed the in vivo efficacy of bioresorbable antibiotic containing bone screws in the prevention of biomaterial-related infection.

Ashammakhi et al. (2005) have used bioabsorbable polymers (PLGA 80/20 or PLDLA 70/30) as the matrix and ciprofloxacin (CF) as antibiotic to develop the implant. Initial shear strengths of the studied ciprofloxacin releasing screws were 152 MPa (P/L/DL)LA) and 172 MPa (PLGA). Studied screws retained their mechanical properties for least 12 weeks (P(L/DL)LA) and 9 weeks (PLGA) in vitro. CF was found to be released after 44 weeks (P/L/DL)LA) and 23 weeks (PLGA) in vitro and significantly inhibited *S. epidermidis* growth. Niemelä et al. (2006) compared ciprofloxacin-PLGA, PLGA and titanium screws in preventing bacterial attachment and biofilm formation in vitro. Ciprofloxacin-PLGA implants were superior. After 21 days incubation in *S. epidermidis* suspension, no biofilm was observed on 93-100% of PLGA ciprofloxacin implants and on 74-93% of titanium implants (Niemelä et al. 2006). In the same study PLGA-ciprofloxacin implants showed clear bacterial growth inhibition on agar plates, while titanium and plain PLGA implants did not show any inhibition.

Shi et al. (2016) in their work incorporated gentamicin into silk-based screws which not only retained the impressive mechanical features and biocompatibility of PSS but also exhibited high and durable antimicrobial activity against *S. aureus* and *E. coli* in vitro. The antibacterial activity remained high even after 4 weeks of immersion in protease solution. These GSS provide both impressive material properties and

antibacterial activity and have great potential for use in orthopaedic implants to reduce the incidence of second surgeries. Tappa et al. (2019) in their work fabricated gentamicin (GS) and methotrexate (MTX) loaded PLA implants. There was a significant reduction in mechanical strength of the PLA constructs with the addition of drug-containing compounds. Extruded control PLA prints had a mean flexural strength of 78 MPa. Samples printed with GS and MTX showed a 14.4% and 17.1% decrease in strength, respectively. However, GS-impregnated implants demonstrated bacterial inhibition in plate cultures and similarly, MTX-impregnated implants demonstrated a cytotoxic effect in osteosarcoma assays.

Yang et al. (2016) thoroughly investigated the growth, *in vitro* biodegradation, and cytocompatibility of nHAp coatings on biodegradable magnesium alloys. Magnesium alloys are undeniably promising materials for orthopaedic applications due to their degradable nature; however, their rapid degradation rates pose significant challenges for sustained use. The implementation of HAp coatings on magnesium substrates not only enhances cytocompatibility but also makes them highly suitable for orthopaedic applications. The coating process carried out through a straightforward hydrothermal deposition method, effectively improves corrosion resistance and significantly reduces the rapid degradation of magnesium-based implants. Inzana, Schwarz, Kates, and Awad (2016) described a biomaterials-based strategy for treating implants associated with osteomyelitis, a chronic bone infection. Treatment of these infections frequently necessitates a mix of antibiotics delivered systemically and locally at the afflicted spot via a biomaterial spacer. Poly (methyl methacrylate) (PMMA) is widely regarded as the gold standard for this application; however, it has several drawbacks, including problems with antibiotic release, incompatibility with various antimicrobial agents, and the need for follow-up surgeries until surgical reconstruction of the lost bone is possible. Antimicrobial coatings for implants are critical and must be developed within the context of biomaterials. Future experimental designs should prioritise the use of animal models when assessing biomaterial delivery technologies.

Lebre et al. (2017) studied how the shape and size of HAp particles influence inflammatory responses after implantation. This study demonstrates a link between the physical properties of HAp particles and immunological responses. The researchers discovered that the size and morphology of HAp particles have considerably impact the production of inflammatory cytokines, both *in vitro* and *in vivo*. Smaller, needle-shaped

HAp particles generated a longer inflammatory response than spherical-shaped nanoparticles and bigger spherical HAp particles. This study shows that smaller HAp particles could be useful tools for encouraging successful tissue remodelling, regulating immune cell responses, and sending information to adjacent tissues. Chen et al. (2017) investigated the mechanical characteristics and biocompatibility of porous titanium scaffolds used in bone tissue engineering, to facilitate bone regeneration and repair. These scaffolds were constructed utilizing a powder metallurgy method, with magnesium powders serving as the space to facilitate holding material. The scaffolds had porosity levels of up to 50 per cent. Their linked structure encourages tissue growth in the surrounding areas. Disegi et al. (2000) tested the degradation of resorbable 70:30 poly (L/DL-lactide) craniofacial bone implants in vitro. The fixings were placed in rigid polyurethane foam and subjected to a phosphate buffer solution for eight weeks. The test block was found to be suitable for conducting the mechanical test. After 4- and 8-week immersion periods, the pull-out strengths of 1.5 mm resorbable screws were found to be no different than those of unexposed control samples, although screw shear strengths were lowered.

G. Huang et al. (2018) investigated PLA nanocomposites and PDL-grafted nHAp via stereo-complexation which show better interfacial adhesion for bone repair and regeneration. This strategy resulted in increased tensile strength and other mechanical properties, making it a potential method for creating material composites for load-bearing bone restoration applications. G. Huang et al. (2018) discussed PLA nanocomposites and PDL-grafted nHAp, demonstrating improved interfacial adhesion for bone repair and regeneration through stereo-complexation. This approach enhanced tensile strength and other mechanical properties, ultimately providing a promising method for developing material composites suitable for load-bearing bone repair applications. C.E. Wen et al. (2001) demonstrated the fabrication of porous titanium (Ti) and magnesium (Mg) foams for bone substitutes utilising a powder metallurgical technique. The foams displayed an open cellular structure, with pore diameters ranging from 200 to 500  $\mu\text{m}$  and porosities of roughly 78% for Ti foam and 50% for Mg foam. The compressive strengths for Ti foam were 35 MPa and 2.33 MPa for Mg foam, respectively, while cancellous bone strengths typically vary between 3 to 20 MPa. Young's modulus was 5.3 GPa for Ti foam and 0.35 GPa for Mg foam, which were identical to natural bone values. Prati, Kim, & Matthewson (2017) conducted a study

on the fatigue behaviour of absorbable sutures in a controlled environment, focusing on the time to fracture. They measured fatigue as a function of the applied load. At high applied loads, a shift in the failure mechanism was observed; failures became brittle and were primarily influenced by the applied stress. In contrast, at lower loads, the failures were more ductile and were further affected by the test environment.

Ozan, Lin, Li, & Wen, (2017) described Ti-Ta-Zr-Nb (TTZN) alloys with extremely high strength for orthopaedic implant applications. TTZN has been combined utilising the electron alloy design method. The microstructure, mechanical properties, and cytocompatibility of TTZN alloys were investigated. The modulus of resilience ranged from 6.21 to 9.37 MJ/m<sup>3</sup>, allowing for the creation of implants with great flexibility, which would be favourable to the reduced stress shielding phenomenon. Excellent compatibility with cell adhesion was eventually identified and, therefore, presented as a suitable material for usage in orthopaedic implants. Jaiswal et al., (2017) examined properties of the biodegradable composite Mg-3Zn-HA for use in orthopaedic fixture attachments, comprising mechanical, corrosion, and biocompatibility. They found that the elastic modulus was similar to that of cortical bone, and magnesium ions, after leaching, did not affect the cell tissues. Hydroxyapatite (HAp) was prepared using wet precipitation techniques, which successfully achieved the desired corrosion resistance and adjustable mechanical characteristics by incorporating HAp into the Mg-Zn matrix. Kulkova et al., (2017) described novel approaches to creating bioactive surfaces for these composites. Bioactive glass granules encapsulated in the resin were exposed through surface etching using an excimer laser. They examined two different kinds of bioactive surfaces: HAp granules and bioactive glass. In comparison to HAp, it was found that the bioactive glass exhibits greater cell adhesion in cell culture. Cell attachment was more successful because of the surface roughness, which was between 100 and 300  $\mu\text{m}$ .

Lebre et al., (2017) investigated the effect of HAp particle shape and size on inflammatory responses after implantation. This study demonstrates a connection between the immune responses and the physical characteristics of HAp particles. The size and shape of the HAp particle were found to affect the *in vivo* and *in vitro* production of inflammatory cytokines. Compared to spherical-shaped nanoparticles and larger-sized spherical HAp particles, smaller needle-shaped HAp particles produced a more prolonged inflammatory response. This suggested that these could be

useful tools for promoting successful tissue remodelling and modulating the immune cell response and signals to surrounding tissues. Tajbakhsh and Hajiali (2017) conducted a thorough investigation into the synthesis and characteristics of biocomposites built from polylactic acid (PLA) and ceramics for bone tissue engineering. They pointed out that PLA has certain drawbacks, such as decreased mechanical strength and restricted cell attachment because of its hydrophobic properties. However, due to its bioactive qualities, the addition of hydroxyapatite (HAp) greatly increases mechanical strength and improves cell adhesion.

Wang et al. (2014) examined nanostructured calcium phosphate biomaterials and stem cells in bone tissue engineering. Effective orthopaedic healing materials, they emphasised, fill up bone defects and serve as scaffolds that control cell behaviour utilising topographical, mechanical, and chemical cues. These nanostructured biomaterials encourage cell adhesion, proliferation, differentiation, and spreading, all of which improve bone repair. The study concluded that these biomaterials, which resemble real bone, have advantages over conventional materials, including higher surface-to-volume ratios, better wettability, and superior mechanical properties.

Felfel et al. (2011) investigated the degradation, flexural, compressive, and shear properties of totally bioresorbable composite rods. These composite rods were made by compression moulding at 100 °C, with phosphate glass fibre reinforcing polylactic acid (PLA) with an acceptable fibre volume proportion. Degradation tests were carried out in phosphate-buffered saline (PBS). The mechanical properties of the rods were assessed before and following the deterioration trials. Mechanical characteristics reduced following immersion in PBS due to the plasticising influence of water within the composite and fibre breakdown. Following degradation, the composite rods developed porous structures, identified as the primary cause of the decrease in mechanical characteristics and mass. A study conducted by Böstman and Pihlajamäki in 2000 focused on cost analysis regarding savings achieved through the use of absorbable polyester pins and screws for the internal fixation of small fragment fractures. This cost analysis included both medical care expenses and the costs associated with lost work time. The research examined 994 fracture patients treated with absorbable internal fixation devices, alongside 1,173 patients who underwent surgery using conventional metallic devices. The types of fractures analyzed included uni- and trimalleolar fractures of the ankle, olecranon fractures, and metacarpal

fractures. The study found that the breakeven point for costs was reached at a removal rate of 19% for metacarpal fractures, 21% for unimalleolar fractures, 46% for olecranon fractures, and 54% for trimalleolar fractures.

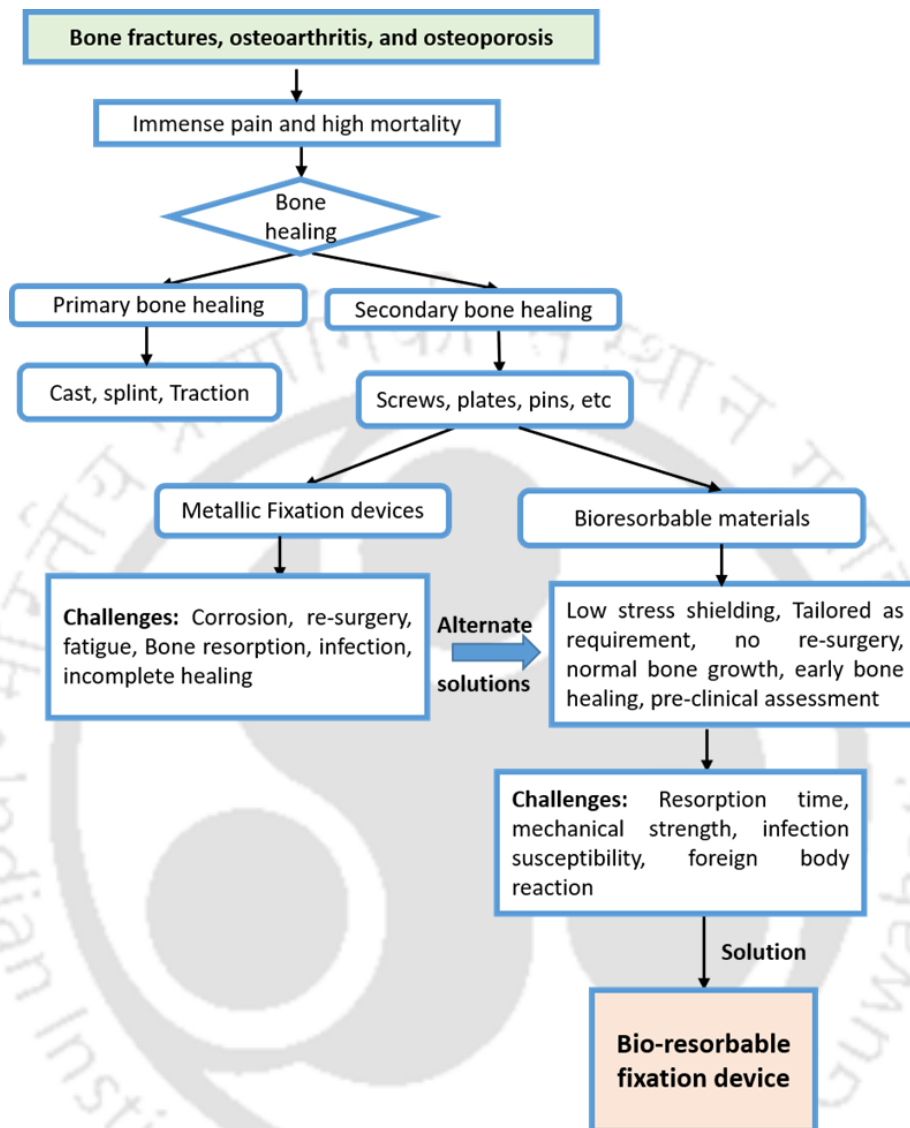
### **1.10 Research Gap**

There is limited literature on fabricating bioabsorbable fracture fixation materials using nanoparticle technology or additive polymers that meet standard dimensions. Furthermore, the fabrication of bioabsorbable internal fixation devices using injection moulding has not received much attention. Complications may arise from the non-biocompatibility of the breakdown products rather than the implants themselves, as well as from their long-term in vivo performance. One potential solution is the use of polymer-ceramic composite systems. Adding bioactive ceramic fillers, such as hydroxyapatite, tricalcium phosphate, or other calcium salts, to a bioresorbable polymer can enhance osteoconductivity, promote bone regeneration, and help buffer the acidic breakdown products, thus reducing the likelihood of an immune response in the body. PLA and its copolymers have been widely used in various fracture fixation devices. Additionally, composites made from PLA as the matrix and bioactive fillers like silk fibres and glass fibres can improve mechanical effectiveness and performance.

Although the literature indicates the fabrication of PLA/HAp composites with a modulus similar to that of cortical bone, controlling their resorption rates remains a challenge. Moreover, a detailed investigation into the fabrication of drug-eluting, load-bearing bioresorbable fixation devices made from PLA/nHAp composites has not yet been fully confirmed by available research. Further research is needed to validate the efficacy of in vitro hydrolytic degradation and to characterize mechanical properties according to ASTM standards. This work is crucial to meeting the requirements for bioabsorbable internal fixation devices (IFDs) for various age groups and remains a priority for future investigation.

Extensive research is needed to validate the efficacy of in vitro hydrolytic degradation and to characterize the mechanical properties according to ASTM standards. This is essential for developing bioabsorbable internal fixation devices (IFDs) suitable for various age groups. Future investigations should include in vivo studies of these internal fixation devices to observe their behavioural response when exposed to living organisms. Additionally, incorporating various functional nanofillers

into the existing matrix and reinforcement is vital for fabricating effective internal fixation devices.



Though several works have reported using PLA and its composites as a biodegradable non-load bearing implant material, the strength, morphology, and other physicochemical properties are still a matter of concern [Russias et al., 2006; Kontakis et al., 2007]. While the clinical outcome of the different implants made of bio-degradable material is still debatable, there is hardly any consensus on their viability as internal fracture fixation device. However, no study has combined PLA, modified chitosan (MCS) and HAp for biomedical applications and as an alternative to the metallic fixation device for non-load bearing applications. Also, there is no clear biomechanical parameter based on which a comparative stability assessment of these extramedullary implants can be made. Moreover, various authors have previously

employed FE analysis to assess the performance of metallic plates fracture fixation, there is no detailed FE study on PLA-based fractured plates in low load-bearing body regions [Tarashi et al., 2016; Peng et al., 2015; Lovald et al., 2006; Haneef et al., 2019; Ilavarasi et al., 2011; Vajgel et al., 2013]. Most of the FE analysis work on polymeric implants are based on simplistic assumptions or data carried from other reported experiments [Ilavarasi et al., 2011; Vajgel et al., 2013; Narra et al., 2014; Wang et al., 2016]. There is also a lack of rigorous preclinical assessment that considers the osteotomies' physiological loading conditions. With recent advances in computation biomechanics and synthesis of biomaterials, FE analysis can be employed once the material is fabricated to successfully assess the performance of different implant materials and evaluate the efficacy of various implantation techniques.

### 1.11 Objectives

The following objectives were set for the research work:

- **Objective 1:** Fabrication of nano-hydroxyapatite and chitosan-reinforced PLA bio-composite and its subsequent thermo-mechano-analysis as bioabsorbable internal fixation devices.
- **Objective 2:** *in silico* biomechanical analysis of the formulated PLA-based composite as an implant material for low load-bearing fracture fixation devices.
- **Objective 3:** *in vitro* cytotoxicity study and *in silico* analysis of the formulated PLA-based composite as a coating material on the surfaces of high load-bearing metallic implants.

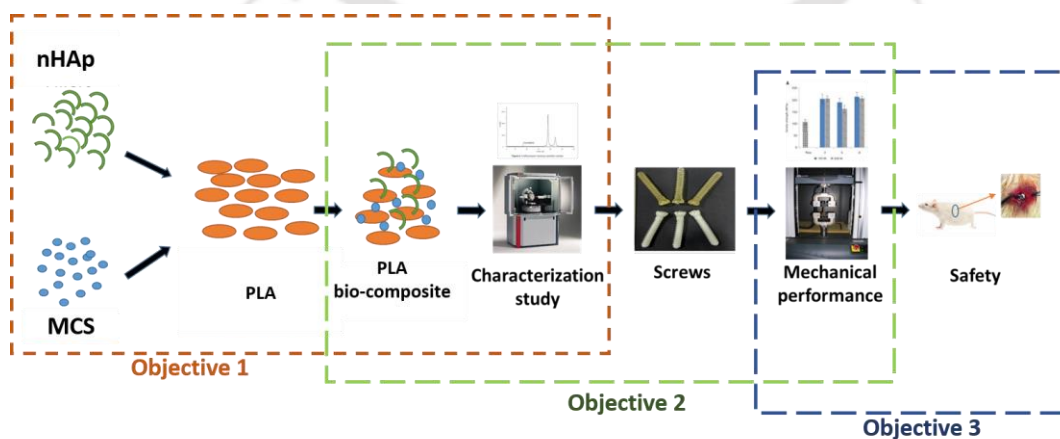


**Fig. 1.7:** Flow chart depicting the overall goal of the thesis objective-wise.

### 1.12 Overview of the thesis

Overall, the work has been conceived in 6 chapters. Chapter 1 provides a comprehensive review of the literature and current state of the art related to the field related to the various polymeric based bio-composite implants and their viability as a fracture fixation device using FE analysis. Further the research gaps were discussed and the objective for the present study was outlined. Chapter 2 explains the techniques related to the synthesis of polymers, the chemicals used for various experiments, and the methodologies employed in the *in silico* studies. Chapter 3 deals with the fabrication of nano-hydroxyapatite (nHAp) and modified chitosan (MCS) reinforced polylactic acid (PLA) bio composite for bioresorbable internal fixation device. The chapter in detail discusses the synthesis technique of the bio-composite and the associated characterisation. In Chapter 4, the mechanical strength of the bio-composites was measured and the concentration that would deliver the highest strength was identified. Moreover, PLA based bio-composite were biomechanically evaluated through *in silico* study using FE analysis to check its viability for mandibular joint fracture. The aim of Chapter 5 was to test the fabricated bio-composites for their *in vitro* cytotoxicity activity by MTT assay on mouse fibroblast (L929) cell line and further predict its performance as a coating material over the metallic implants for high load bearing bone fracture. Chapter 6 summarises the salient findings of the present work.



## Chapter 2

### Materials and Methodology

#### 2.1 Introduction

It has often been observed that the bioabsorbable polymeric materials used as IFDs do not adequately support the load-bearing capacity and degrade too early, which can hinder bone fracture healing. PLA is a bio-based, aliphatic polyester used in various applications, including food packaging, bone defects, wound healing, tissue engineering and others. At the same time, its processing techniques take into consideration the most important factors, such as mechanical properties, sustainability during processing, and performance stability. However, incorporating various fillers such as HAp, CS, silver, and copper to improve properties such as load bearing capacities, bioactivity, and antimicrobial and anti-inflammatory effects can also accelerate new bone tissue regeneration, increase cell adhesion, and boost bioactivity.

This chapter describes the use of PLA and various chemicals as per protocols for the experiments performed in the present research work. MCS and nHAp are selected as filler materials to be introduced into the PLA matrix. The synthesis of modified chitosan, conversion of PLA from commercial grade to pure grade, and fabrication of composites, followed by distinct physicochemical and thermo-mechanic characterisation studies are elaborately discussed. The chapter further deals with the techniques for extracting patient-specific bone models from CT data, mesh generation, and the development of FE models.

#### 2.2 Materials

Commercial grade PLA (2003D, D-lactic acid: 1.4%, L-lactic acid: 98.6%, granules form, density of 1.24 g/cm<sup>3</sup>, melt flow index: 0.73g/min at 210°C, Mw/Mn = 1.8) with number average molecular weight (Mn) of ~150,000 Da and weight average (Mw) of ~2,00,000 Da respectively was supplied by Natureworks®, USA was used in this investigation. The commercial nHAp (size of ~200 nm) is procured from Sigma

Aldrich, India and is utilised as a filler in this research work. Commercial medium molecular-weight chitosan ( $M_w = 240$  to  $280$  kDa, degree of deacetylation  $\sim 80\%$ ) was received from Sigma-Aldrich, India. L-lactic acid (LA, 20% assay) aqueous solution procured from Purac, India. Whatman filter paper (grade 1) was used to extract the MCS. Chloroform (analytical grade, Assay min. 99%, density at  $20^\circ\text{C}$ :  $1.474$ - $1.480$  g/ml) was procured from SRL Chemicals, India. Finar Chemicals, India, supplied methanol. HPLC-grade chloroform was procured from Merck, India. Acetone ( $\sim 99\%$ , density at  $20^\circ\text{C}$ :  $0.791$ - $0.793$ g/ml) was procured from Fisher Scientific, India. All the materials without PLA were being used as received without further purification. Millipore water (Metrohm, ELIX 3) was used as a solvent in contact angle analysis.

## 2.2. Methodology

### 2.2.1. Purification of commercial-grade PLA

As reported in the literature, the commercial PLA (2003D) granules were purified by a precipitation method. The purification of the commercial PLA into a medical-grade PLA has been carried out to make it suitable for medical applications. At room temperature, 50 g of PLA granules was dissolved in 250 mL chloroform and precipitated in 1000 mL methanol. Then, it was dried in a hot air oven at  $55^\circ\text{C}$  for 24 h. The obtained fibrous PLA was converted to powder form at 24000 rpm with a disintegrator (Make: Huanghua, Model: FW100) (Fig. 2.1).

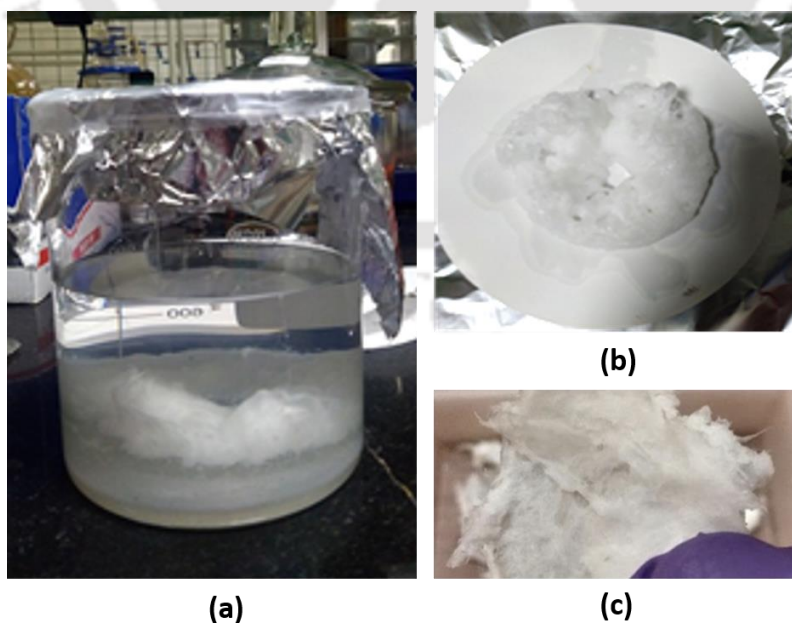


**Fig. 2.1:** Purification of PLA: (a) PLA precipitation in methanol, (b) extracted fibrous PLA, (c) dried PLA flakes.

### 2.2.2. Synthesis of modified Chitosan (MCS) by condensation polymerization

Firstly, the lactic acid (LA) and chitosan were mixed manually in 5:1 (wt/wt %) proportion in a glass beaker based on the performed preliminary investigation. The mixture was kept undisturbed for 12 hours to facilitate the proper soaking of LA into chitosan and enhance its reaction performance [Pal et al.,2015]. A two-neck round-bottom flask (RBF) was placed in the microwave, equipped with a mechanical stirrer

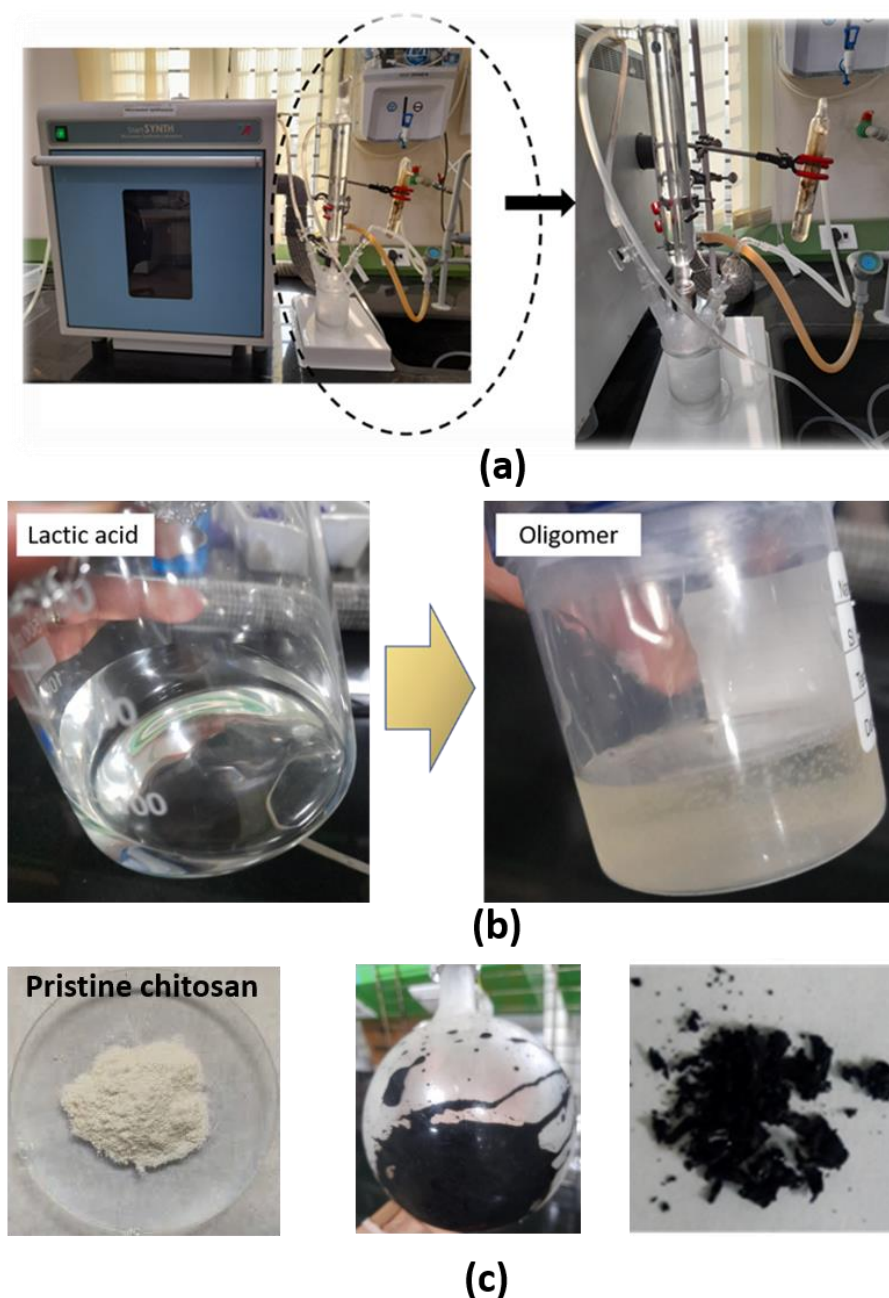


**Fig. 2.2:** Synthesis of modified chitosan (MCS): (a) microwave-assisted setup, (b) conversion of lactic acid to oligomer, (c) resulted modified chitosan post polymerisation.

and a condenser. The soaked mixture was then charged into a two-neck flask with a magnetic bead, and the temperature was increased to 120 °C from room temperature under nitrogen flow. The reaction was exposed to an inert atmosphere for 1 hour to remove the condensate water and lactide. The condensation polymerisation reaction was performed to prepare the OLLA-g-CH master batch in the microwave at 110 °C for 30 min at 240 W under “convection cum microwave” mode. The employed microwave-assisted condensation polymerisation reaction mechanism finally resulted in a viscous blackish-brown residue. The copolymer was further vacuum-filtered and dried to get the desired product (Fig 2.2).

### 2.2.3. Processing of PLA/MCS/nHAp bio-composites by melt-blending

PLA granules, nHAp and MCS were dried at 40°C in a vacuum oven for 12 hours to eliminate the residual moisture content. The MCS was subsequently dissolved in acetone, followed by vacuum filtration using filter paper of pore size ~450µm to discard the undissolved content. Thereafter, the vacuum-dried PLA flakes, nHAp and dried MCS powder were mixed manually and introduced to the hopper where the bio-composites were fabricated with the help of a twin-screw extruder (Haake, Minilab II, Thermo Fischer Scientific). A processing temperature of 180 °C and screw speed of ~ 100 rpm were considered in this investigation to extrude the biopolymer [Prasad et al.,2017]. Neat PLA and PLA/MCS/nHAp bio-composite were received in the form of long strips of dimension~5x0.5 (width x thickness) as products. The dumbbell shape was also fabricated as per ISO527-1BA using an injection molding machine (Haake, Minijet Pro, Thermo Fischer Scientific) at 190°C and a feeding pressure of 50 bar. The mold temperature was maintained at 90°C. The prepared samples were stored in

**Table 2.1:** Parameters of the extrusion cum injection molding process

Processing temperature	180°C
Residence time	1 min
Twin screw speed (rpm)	70
Compressed air pressure	50 bars
Extrusion die (strip with 5 mm)	Flat type

desiccators for further analysis. Figure 2.3 explains the scheme of the process utilised for PLA/Hap composites. Table 2.1 shows the parameters followed during the extrusion process. The media used during the extrusion process is compressed air of pressure in the range of 50-100 bar. Figure 2.4 shows the functioning of the equipment for extrusion cum injection molding process.

The measured quantity of PLA, nHAp, and MCS were loaded in the twin screw extruder through the hopper. The rotation of each screw in the opposite direction enables the proper mixture of material. A residence time of 1 minute was maintained during the operation for thorough melt-mixing. Thus, the biocomposite composition is taken as (i) neat medical grade PLA, (ii) PLA + 15wt% nHAp, (iii) PLA + 15wt%

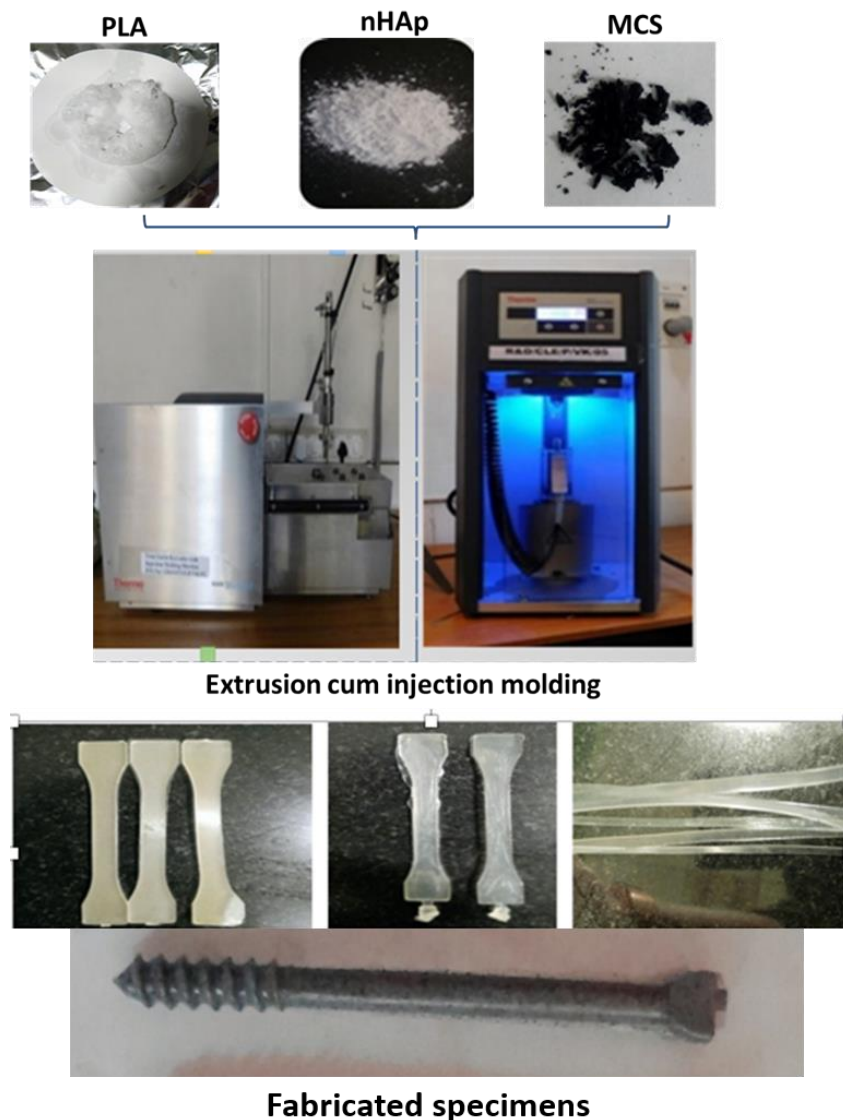


**Fig. 2.3:** Processing of PLA/MCS/nHAp bio-composites by melt-blending using extrusion cum injection molding technique.

nHAp + 6 wt% MCS, and (iv) PLA + 15wt% nHAp + 9 wt% MCS was extruded in the form of long strips with the dimensions of  $\sim 5 \times 5$  mm. The prepared samples were

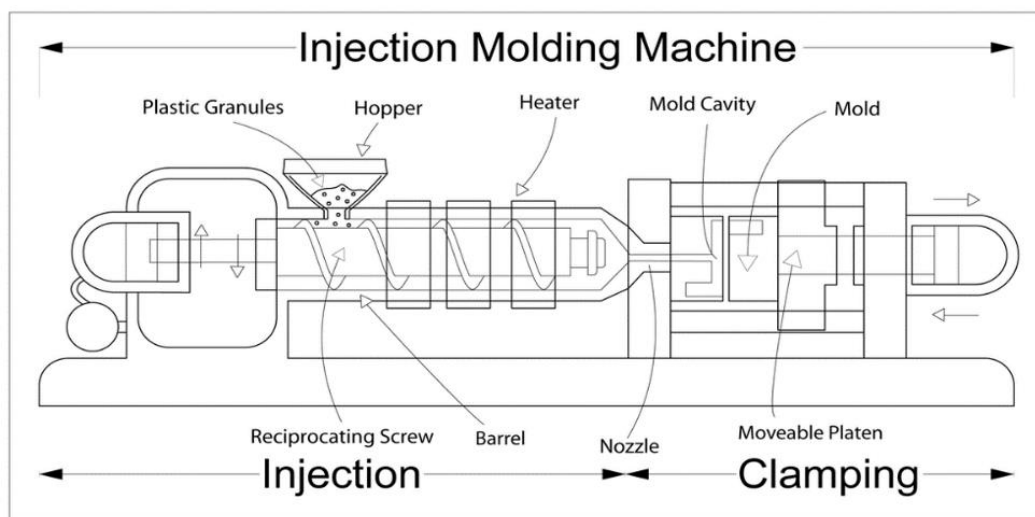


**Fig. 2.4:** Functioning layout diagram of the extrusion cum injection molder (Google).

stored in desiccators for further analysis.

#### 2.2.4 Analytical instrumentation and Characterization of PLA/MCS/nHAp bio-composites

The extruded PLA/MCS/nHAp bio-composites were characterized through various analytical studies like X-ray diffraction studies (XRD), Thermal studies through differential scanning calorimeter (DSC) and thermal gravimetric analysis (TGA), functional group identification through Fourier transform infrared spectroscopy (FTIR) and mechanical testing through a universal tensile testing machine (UTM). Surface wettability measurement through contact angle measurement. The surface morphological studies were done through a field emission scanning electron microscope (FESEM). The total sizes of batches were selected as Neat PLA, 15% nHAp, 20% nHAp, 6% MCS and 9% MCS weight (Wt.)

##### 2.2.4.1 Mechanical properties

Evaluation of the mechanical properties is one of the critical parameters in fabricating a particular biocompatible composite for the design of a biomedical device. The assessment of its ability to withstand mechanical load in fulfilment of a specific function is required in biomedical applications. The prepared PLA composite with the mentioned composition was blended in a twin-screw extruder cum injection moulding. The maximum torque set during the mixing process was 100 Nm at 70 rpm for 1 min

and then extruded. The extruded mixture was then moulded in a microinjection moulding set-up as per ISO 527-2-1BA shape and was characterised by their mechanical properties such as tensile strength, tensile modulus, % elongation, and fractured surface morphology. The test was carried out by a load cell 5kN in a controlled environment (25 °C and 78% RH) and at a cross-head speed of 1 mm/min—accordance with ASTM D638. The name of the instrument utilised for this purpose is the universal testing machine (Kalpak Instruments, India). Three specimens in each combination of samples were considered, and the average obtained in each case is reported along with the standard deviation.

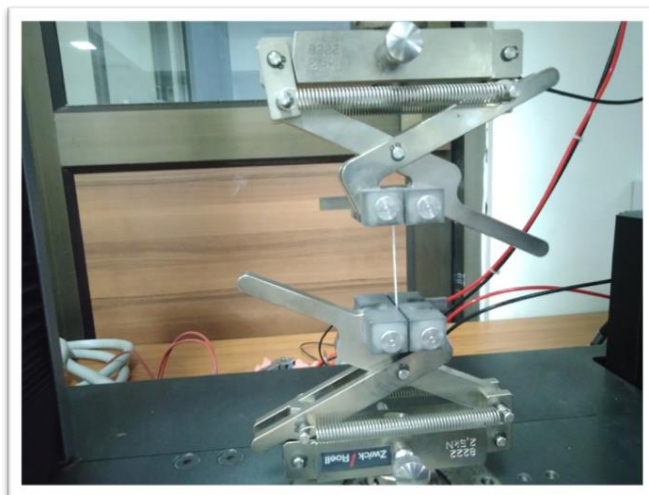


**Fig. 2.5:** Mechanical strength analysis of the specimen under UTM.

#### **2.2.4.2 Fourier transform infrared (FTIR) spectroscopy**

The FTIR spectra of the samples were obtained from attenuated total reflection (ATR) mode in the Frontier FTIR spectrometer (PerkinElmer, USA) at room temperature. The prepared samples were analysed, and the spectra were recorded in the range of 2500 to 500  $\text{cm}^{-1}$ . The various functional groups in the prepared samples were confirmed by analysing the spectra.

#### **2.2.4.3 Thermogravimetric analysis (TGA)**

Thermogravimetric analysis of the prepared samples (~6–7 mg) was performed with the thermogravimetric analyser (TGA-4000, PerkinElmer, USA) to examine the thermal stability and thermal degradation temperature of the samples. The samples were inserted in the alumina crucible of the analyser, and the temperature was increased from 30 to 700 °C with a heating rate of 10 °C/min. Throughout the analysis, an inert atmosphere inside the crucible chamber was maintained using nitrogen gas with a flow rate of 60 mL/min.

#### **2.2.4.4 Differential scanning calorimetry (DSC)**

Different thermal states such as glass transition temperature, cold crystallisation temperature and melting temperature of the prepared melt extruded PLA/MCS/nHAP composite strips were investigated using a DSC (Make: NETZCH, Model: Phoenix 204) in the temperature range of 30 to 200°C, at a scanning rate of 10°C/min under N<sub>2</sub> gas with a flow rate of 60ml/min and by the application of two heating and one cooling cycles. Two thermal cycles were applied, in which the first cycle was done from 30 to 200°C at 10°C/min, followed by isotherm condition maintained at 200°C for 2 min and further a cooling cycle was performed from 200 to 30°C with the same scan rate. The isothermal condition was maintained at 180°C for 2 minutes after the first cycle was completed. The second cycle was repeated as that of the first one to eliminate the thermal history. The first heating was applied to remove the bounded moisture from the composite strips. Further, to ensure the complete crystallization, the sample was cooled down to 30°C at 10°C/min and the temperature was maintained for 1 hour at isothermal condition. Before the analysis, the instrument was calibrated with Indium standards using a platinum-based crucible. The curves plotted from the obtained data by the second cycles recorded the melting temperature, crystallisation temperature, and glass transition temperature of the samples.

#### **2.2.4.5 Contact angle analysis**

Static water contact angle measurements evaluate the wetting behaviour of the surfaces. Contact angle measurement (Make: KRUSS; Model: DSA25E) was performed with the prepared biopolymer samples to study the hydrophobicity and hydrophilicity properties. The sessile drop method investigation was conducted at room temperature. The prepared samples were kept on the glass slide and fixed in the sample holder. A calibrated quantity of water droplet (1 mL) was dropped on the surface of the specimen. The continuous video was recorded for 60 seconds, and the angle was measured at an interval of 10s. Thus, six readings were noted for each sample, and the average was considered for investigation. The wettability property also provides information about cell and bacterial adhesion.

#### **2.2.4.6 Surface morphology**

The prepared samples were characterised with a field emission scanning electron microscope (FESEM) (Zeiss, Germany, Model Sigma) at an accelerating voltage of 2–3 kV. The specimens were mounted on aluminum stubs followed by gold sputtering to make them conductive before subjecting them to analysis. To verify the dispersion of

nHAp along with the oligomeric grafted chitosan, EDX analysis was performed with an accelerating voltage of 20 kV. The presence of elements can be detected by mapping the X-rays generated from the desired elements.

#### **2.2.4.7 X-ray diffractometer**

XRD analysis was analyzed by an X-ray diffractometer (D8 Advance, Bruker, Germany) equipped with a goniometer and Ni-filtered Cu-K $\alpha$  radiation ( $\lambda = 1.54 \text{ \AA}$ ). The operating conditions of diverging and receiving slits were at 40 kV and 40 mA. The relative intensity was recorded in  $2\theta$  range of  $10^\circ$  to  $50^\circ$  with a continuous increment and scan speed of  $0.05^\circ/\text{sec}$  and two sec/step, respectively. All the samples were annealed at  $60^\circ\text{C}$  for 2 h before the analysis. The p and PLA/nHAp bio-composites. The characteristics peak of highest intensity for nHAp was obtained at  $2\theta$  of  $31^\circ$  corresponding to 211 planes. In the case of PLA/nHAp, the sharp crystallization peak at  $2\theta = 16.2^\circ$  is observed from (2, 0, 0) reflection for PLA. The crystallographic analysis of the PLA shows sharp crystalline peaks at  $16.2^\circ$  (2, 0, 0) which correspond to  $\alpha$  crystalline form of the PLA.

#### **2.2.4.8 Determination of cell cytotoxicity by MTT Assay**

The cell culture monolayer was trypsinized and the cell count was adjusted to 100,000 cells/mL using MEM containing 10% FBS. To each well of the 96-well microtitre plate, 0.1 mL of the diluted cell suspension was added. After 24 h, when a partial monolayer was formed, the supernatant was flicked off, the monolayer was washed once with DPBS and different test concentrations were added in triplicates to microtitre plates. The untreated cells were maintained as cell control for comparison. The plates were then incubated at  $37^\circ\text{C}$  for different time intervals (24h, 48h & 72h) in 5% CO<sub>2</sub> atmosphere, and microscopic examination was carried out and observations were noted. After specific time intervals (24h, 48h & 72h), the test solutions in the wells were discarded, and 100  $\mu\text{L}$  of MTT diluted with DPBS was added to each well. The plates were incubated for 3 h at  $37^\circ\text{C}$  in a 5% CO<sub>2</sub> atmosphere. The supernatant was removed, 100  $\mu\text{L}$  of DMSO was added and the plates were gently shaken to solubilise the formed formazan. The absorbance was measured using a microplate reader at a wavelength of 570 nm.

#### **2.2.5 FE model generation of the mandibular bone and distal tibia implanted construct**

The 3D FE models corresponding to the mandibular joint was created from CT scan dataset using medical image processing program Simpleware™ (Synopsys Inc., Mountain view, USA) (Fig. 2.6). The CT scans (512 x 512 resolution, 120 kVp, 1.0 mm slice thickness and 0.64 mm layer spacing) was obtained from an open-source repository [Wallner and Egger, 2018]. The CAD model of the plates and screws was generated using the NURBS modelling environment of Rhinoceros (Fig. 2.7). The fixatory implants were made thicker based on previous research work (Table 2.2) [Altai et al., 2016; Narra et al., 2014]. A non-uniform transverse fracture gap was simulated in the mandibular bone of size~1mm [Wang et al., 2016]. The plates and screws were then virtually implanted with the mandibular joint. The 3D models were then imported into Ansys ICEM CFD v15.0 (ANSYS Inc., PA, USA) to generate volumetric meshing comprising of 10-noded tetrahedral elements. Thereafter, the volumetric mesh was imported to Ansys Mechanical v15.0 (ANSYS Inc., PA, USA) for computational analysis. Mesh convergence analysis was used with three different sizes of mesh of 1mm, 2mm and 3 mm. Increasing the mesh size from 1 mm (fine mesh) to 2mm (medium mesh), varied the peak von Mises stress by ~0.2% whereas the change was almost ~8% from medium sized mesh to coarse sized mesh (3mm). Therefore, the medium sized mesh was considered sufficiently accurate [Nag and Chanda, 2021]. Two different fracture model were analysed: one with hairline fracture in the mandibular joint and the other with varied fracture gap~1mm. An open-source software

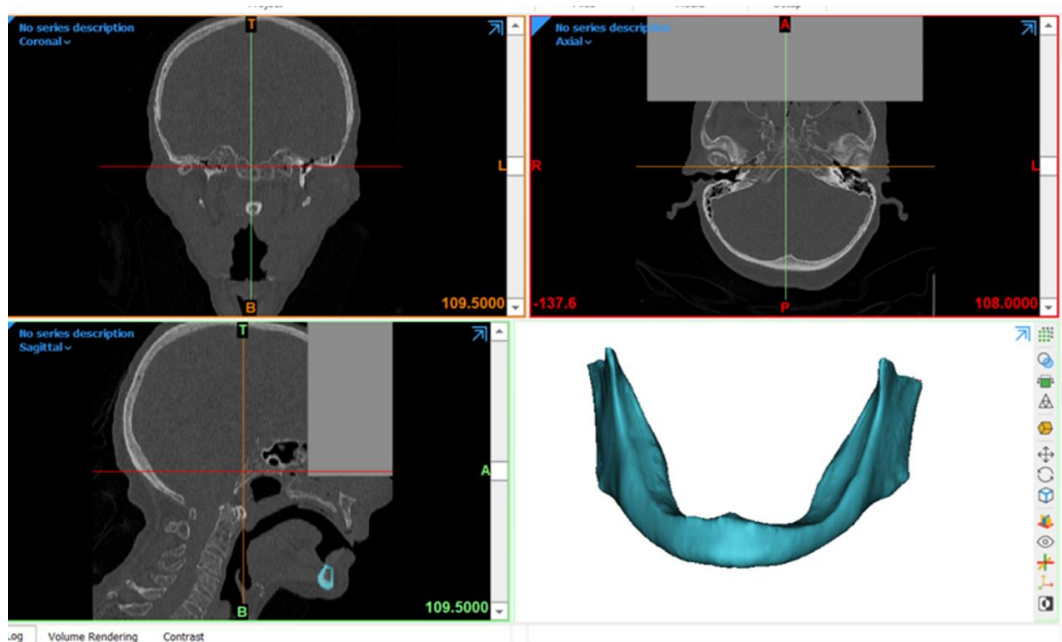


**Fig. 2.6:** CT data of human cranio-maxilla facial part with extracted mandibular joint (lower right corner).

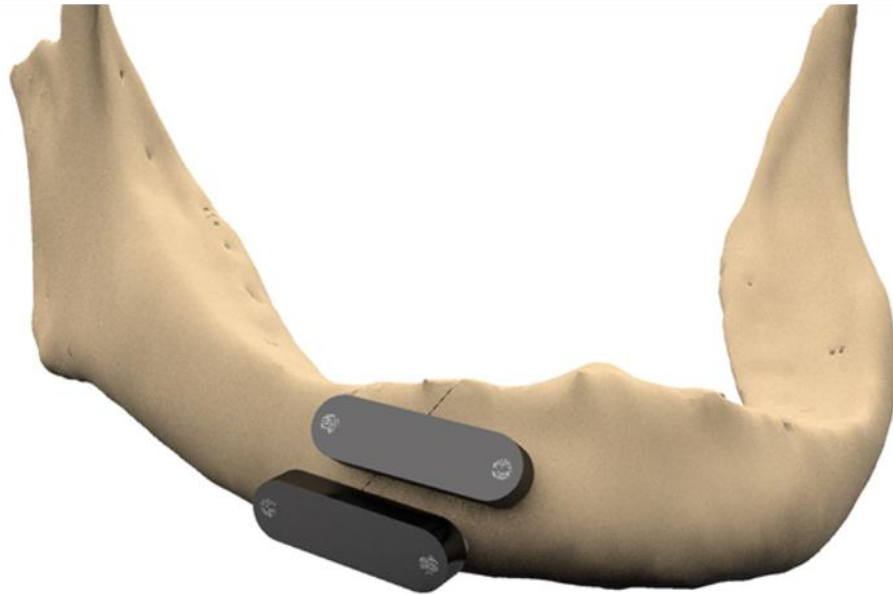


**Fig. 2.7:** CAD model: plates are fixed to the mandibular joint with 1 mm fracture gap.

BONEMAT was used to calculate the average modulus of the bone. Linear elastic, isotropic and homogeneous material property were considered for both the bone and implants (Table 2.3). The material for the implant was considered as Ti and PLA based composites. The modulus of the PLA based composite was measured from the mechanical testing experiment mentioned in section 2.2.4.1. Poisson’s ration of the bone and Ti implant was considered as 0.3, whereas for PLA based composite it was 0.36 [Torres et al., 2015]. Every interface of the FE models has been considered as bonded under all conditions.

**Table 2.2:** Specifications corresponding to the plate and screw. All dimensions are in mm.

Plate thickness	Diameter of Screws		Length of Screws	
	head	shaft	head	shaft
3.0	1.5	2.0	3.0	7.0

**Table 2.3:** Material property data (based on ASTM 308<sup>#</sup>, Torres et al., 2015\*).

Material	Young’s modulus (MPa)	Poisson’s ratio
Cancellous	155*	0.3
Cortical	13,700	0.3
Plate & screw (Titanium)	113,000 <sup>#</sup>	0.3
Plate & screw (PLA/nHAp/MCS)	1,000	0.36*

Various literature has reported the normal bite force applied by human incisor teeth in between 100N and 600N [Cansiz et al., 2015; Arbag et al., 2008]. A load of 100 N was considered as bite force to the mandibular bone in the downward direction and occlusal load of 132 N was considered on the lower first molar of both the sides (Fig. 2.8) [Harada et al., 2000]. The mandibular lower edge was constrained at all six DOF's and the acetabulum part was constrained to all the three translatory DOF's whereas the upside boundary was constrained to translation in the X axis and rotation wrt. Y and Z axis [Wang et al., 2016; Haneef et al., 2019].

The 3D FE model corresponding to the tibia was created from the CT scan dataset of ta cacinoma patient using the medical image processing program D2P (3D SYSTEM, South Carolina, USA). The FE model of the DT-NBA, however, was generated based on the shape of the distal tibia of the patient using Geomagic Freeform (3D SYSTEM, South Carolina, USA (Fig. 2.9 a)). A coating layer of 1 mm thickness of the PLA/HAp/MCS bio-composite was considered between the bone and implant. The virtual implantation of the DT-NBA to the tibia was also carried out in the Freeform modelling environment (Fig. 2.9 b). The 3D models were then imported into Ansys ICEM CFD

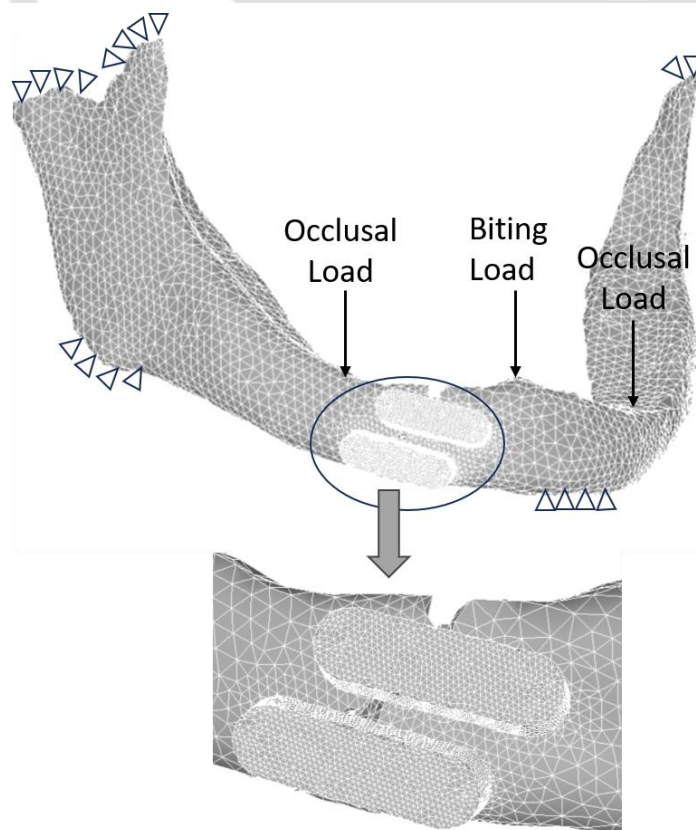


**Fig. 2.8:** 3D FE model of the implanted mandibular bone subjected to different loading and constraints.

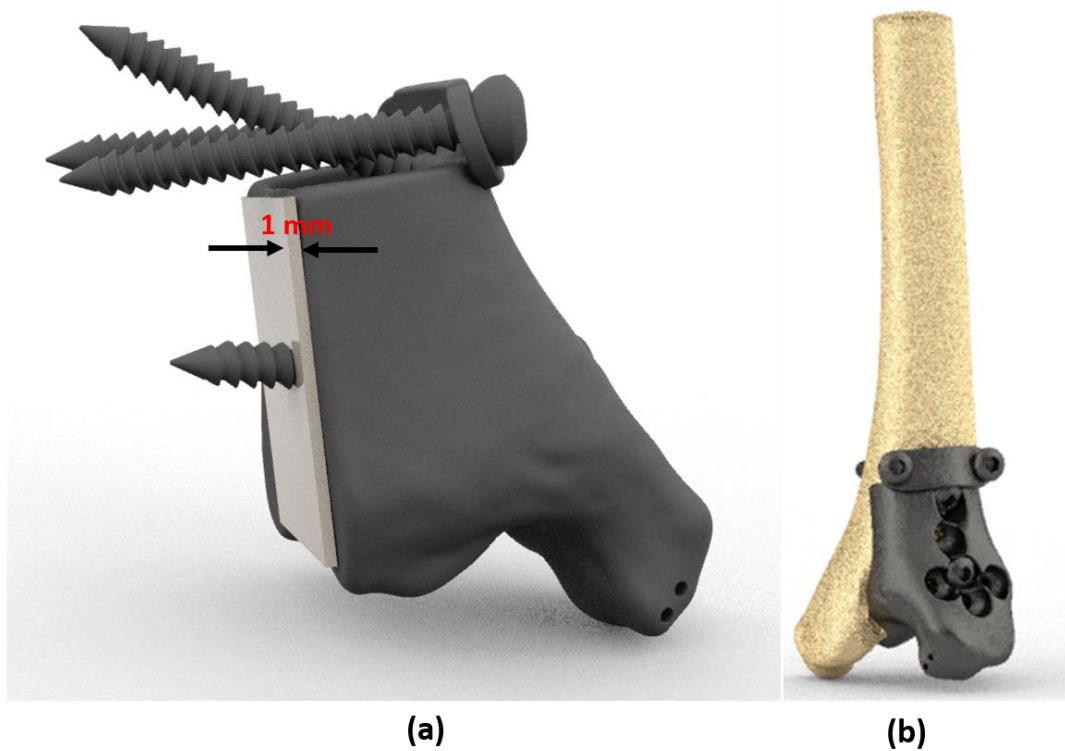


**Fig. 2.9:** 3D CAD model: (a) Implant, (b) Tibia extracted from CT dataset

v15.0 (ANSYS Inc., PA) to generate volumetric meshing comprising 10-noded tetrahedral elements. Mesh convergence analysis was carried out with three different mesh sizes and the final mesh size was predicted to be 1 mm for the implant and coating, and 1.5mm for the bone [Nag and Chanda, 2022]. Thereafter, the volumetric mesh was imported into Ansys Mechanical v15.0 (ANSYS Inc., PA, USA) for FE analysis (Fig. 2.10). The nodes of the proximal part of the tibia were constrained both in the translational and rotational degree of freedoms (DOFs) and the load was applied distally on the tibia [Seireg et al., 1975; Stauffer et al., 1977]. Only axial compressive load was considered for the model which was 3000 N, to simulate dorsiflexion loading condition [Procter et al., 1982; Jyoti and Ghosh, 2023]. The implanted tibia was made vertically upside down for the present analysis to match the experimental protocol for

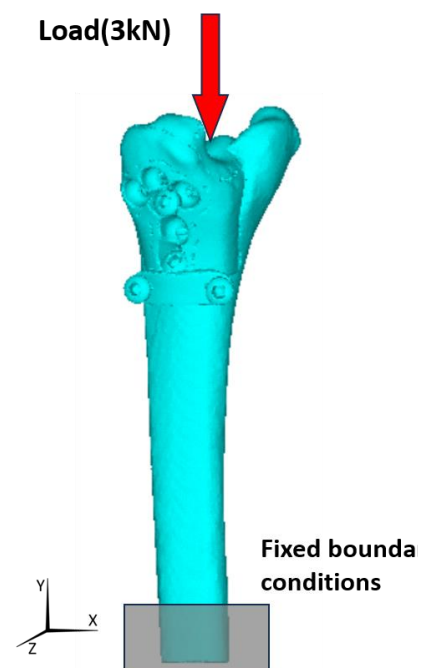


**Fig. 2.10:** 3D FE model of the implanted tibia (vertically upside down) with loading and boundary conditions.

such cases for further future study (Fig. 2.10) [Cristofolini and Viceconti, 2000]. The material for the implant and screw was considered to be Titanium (Ti-6Al-4V) with Young's modulus of 113GPa whereas for the tibia it was 16.7 GPa (cortical bone). Poisson's ratio was set as 0.3 for all materials. All interfaces of the FE models were assumed to be bonded under all conditions.



## Chapter 3

### **Fabrication of nano-hydroxyapatite and chitosan-reinforced polylactic acid bio-composite for bioresorbable internal fixation device**

#### **3.1 Introduction**

The selection of internal fixation devices, like bone plates, screws, pins, and staples, depends on the fracture site. According to the global market scenarios, the market share of fixation devices is set to reach USD 9.5 billion by 2025. The market for trauma fixation devices will experience growth due to the increasing incidence of osteoporosis, rheumatoid arthritis, and sports injuries. Although conventional metallic fixation implants provide good stability, the main disadvantage is the need for revision surgery to remove the metallic implant after healing [Subbiah et al.,2005]. As a result, it leads to a more invasive procedure. The other disadvantages include stress shielding, corrosion, image interference with CT scans, MRIs, and others [Onche et al., 2011; Nag and Chanda, 2021; Nag et al., 2022]. The alternative solution could be replacing conventional fixation devices with bioresorbable polymeric systems, whose properties almost match those of natural bone. Once implanted in the body, the bioresorbable implants break down into harmless by-products that are eventually eliminated from the body and replaced by host tissue [Yetkin et al., 2000]. Thus, the need for revision surgery can be averted, thereby controlling the limitations.

The material of interest for this application includes mainly biodegradable polyesters, which comprise synthetic biopolymers like poly lactic acid (PLA), polyglycolic acid (PGA), polycaprolactone (PCL), and natural polymers such as chitosan, alginate, collagen, and fibrin [Suzuki and Yakada, 2012; Bhasney et al., 2017; Russias et al., 2006; Kontakis et al., 2007]. Parameters like mechano-thermal stability and easy processing capability also play an essential role in selecting materials and subsequent fabrication. Among the polymers mentioned above, PLA is an aliphatic polyester with advantages such as renewability, biocompatibility, and processibility compared to other bioresorbable polymers [Tripathi et al., 2016]. PLA, derived from

renewable natural resources by the fermentation of agricultural feedstock, has garnered much attention in the biomedical field. The degradation products of PLA are not toxic and serve as an excellent material for implants and drug delivery systems [Shan et al., 2020].

An ideal polymeric implant material must not only meet the physical properties of the bone but also be bioactive to promote host-cell adhesion. Various inorganic materials, such as hydroxyapatite, bio-glass, chitosan, silver, copper, and other bioactive fillers, are incorporated into the PLA matrix to enhance its effectiveness [Gross et al., 2013; Binay and Kumar, 2019; Liu et al., 2014]. Work on fabricating composite materials is also carried out by combining biopolymers to enhance their efficacy and feasibility [Buzarovska et al., 2018].

The inorganic phase of bone is mainly hydroxyapatite ( $\text{Ca}_{10}(\text{PO}_4)_6(\text{OH})_2$ ) (HAp), which constitutes 60–70% of the dry weight of the bone [Wendel et al., 1998]. Using nanohydroxyapatite (nHAp) as filler material for bone tissue scaffolds will promote good cell adhesion and enhance the bioactivity process [Shepherd et al., 2012]. Also, nHAp is an excellent bioactive site and imparts mechanical stability due to its high aspect ratio. Hence, it is extensively considered as a filler material for orthopaedic fracture fixation devices [Felfel et al., 2013]. On the other hand, chitosan (CS) is a natural biopolymer resulting from the partial deacetylation of chitin [Singh et al., 2018; Cheung et al., 2015; Kumar et al., 2004]. The use of CS in the biomedical field is due to its good antimicrobial properties, biodegradability, and biocompatibility [Cheung et al., 2015]. Apart from these characteristics, chitosan promotes the bone cells' adhesion and proliferation, along with a low cellular response (non-toxicity). CS can be modified by adopting a graft co-polymerisation procedure to enable its better dispersion in the hydrophobic PLA matrix and thereafter will be referred to as modified chitosan (MCS) in the manuscript. MCS synthesised through the condensation polymerisation procedure resulted in enhanced physical properties and surface characteristics of the composite that are significant for tissue engineering applications [Pal and Katiyar, 2016].

It is evident from the literature that osteogenic capability improves with the use of PLA/nHAp in repairing bone defects. Also, improvement in neovascularisation and newer bone formation was reported by [Tu et al., 2020]. Moreover, the PLA/nHAp combination has the proven ability to improve the osteo-conductivity [Liu et al., 2020].

In addition, PLA/nHAp also supports cell adhesion and proliferation [Sun et al., 2022]. Many researchers reported the ability of PLA/nHAp bio-composite in the application of bone tissue repair and biomedical implants [Jia et al., 2023; Bikiaris et al., 2023; Prasad et al., 2023 (A); Prasad et al., 2023(B)].

Though several studies have reported using PLA and its composites as a biodegradable, non-load-bearing implant material, the strength, morphology, and other physicochemical properties are still a matter of concern [Prasad et al., 2017; Tripathi et al., 2016]. To the author's knowledge, no study has combined PLA, modified chitosan (MCS), and nHAp for biomedical applications as an alternative to the metallic fixation device for non-load-bearing applications. We hypothesize that the present combination of PLA, MCS, and nHAp would have justified mechanical properties and physiochemical characteristics to be used as a non-load-bearing internal fixation device.

### 3.2 Results and Discussion

#### 3.2.1 Mechanical tests

The mechanical tests were carried out with the samples prepared from PLA, PLA + 15% nHAp, PLA + 15% nHAp + 6% MCS and PLA + 15% nHAp + 9% MCS. The Young's modulus (GPa), tensile strength (MPa), and percentage of elongation are shown in Fig. 3.1. Fig. 3.1 (a) shows Young's modulus of the prepared film samples. The addition of nHAp to the PLA has resulted in an increase in Young's modulus by 11.86% compared to the neat PLA. On further addition of MCS (6%), a slight increase in Young's modulus (up to 7.75%) was witnessed. However, when the percentage of MCS

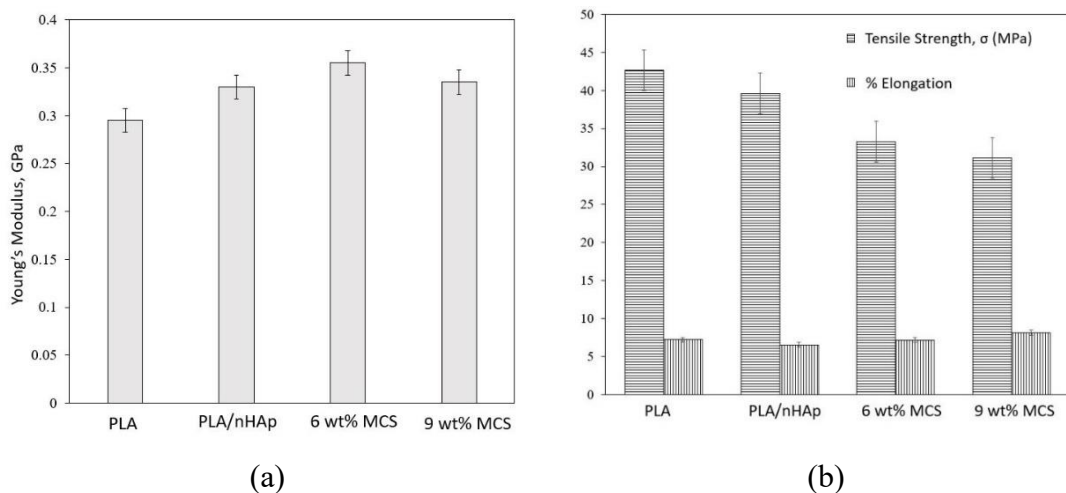


**Fig. 3.1:** Mechanical testing (a) Young's modulus (b) tensile strength and elongation of the prepared samples.

was further increased from 6 to 9%, it resulted in decrease of the Young's modulus by 5.6%. The Young's modulus was found to be higher for PLA+nHAp+6%MCS composite whereas the influence of both 6% and 9% MCS in the PLA+nHAp matrix in the ultimate tensile strength is almost similar (Fig. 3.1). A reduction of 26.91% (from 42.62 MPa to 31.15 MPa) was witnessed with the ultimate tensile strength of PLA+15% nHAp + 9% MCS compared with PLA. The reason might be the presence of low molecular weight MCS in the matrix. With the increase in MCS wt%, the associated number of shorter polymer chains also increased. During the tensile testing of prepared samples, these shorter chains align faster than the longer ones, resulting in lower tensile strength values.

### 3.2.2 Fourier transform infrared analysis

In FTIR analysis, the peaks corresponding to PLA (Fig. 2) depict the asymmetric CH<sub>3</sub> stretching at 2996 cm<sup>-1</sup>, symmetric CH<sub>3</sub> stretching at 2946 cm<sup>-1</sup>, C–H stretching at 2880 cm<sup>-1</sup>, C=O stretching at 1748 cm<sup>-1</sup>, symmetric bending of CH<sub>3</sub> at 1382 cm<sup>-1</sup>, and 1381–1358 cm<sup>-1</sup>, asymmetric bending of CH<sub>3</sub> at 1452 cm<sup>-1</sup>, asymmetric C–O–C asymmetric rocking CH<sub>3</sub> at 1180 cm<sup>-1</sup>, symmetric rocking CH<sub>3</sub> at 1128 cm<sup>-1</sup>, symmetric stretching C–O–C at 1080 cm<sup>-1</sup>, stretching C–CH<sub>3</sub> at 1041 cm<sup>-1</sup>, stretching C–COO at 868 cm<sup>-1</sup>, rocking CH<sub>3</sub> and stretching C–C at 954 cm<sup>-1</sup>, and bending C=O in PLA due to its crystalline phase at 753 cm<sup>-1</sup>. From the FTIR spectra of MCS, it is evident that the strong –N–H bending vibrations of secondary amides and –C=O stretching vibrations of primary amides in the chitosan powder occurred at 1545 and 1640 cm<sup>-1</sup>, respectively. But in the case of MCS, the regular peak (1545 cm<sup>-1</sup>) observed in the OLLA was shifted to a higher wavenumber (1550 cm<sup>-1</sup>) in OLLA-g-CH. Pal et al. (2016) in their study has also reported similar kind of findings. Also, an extra peak was detected at 1539 cm<sup>-1</sup> in the modified chitosan, ensuring the amide ester linkage of chitosan with repeat lactic acid units. This peak (1539 cm<sup>-1</sup>) is evidence of the structural modification in the chitosan backbone. Fig. 3.2 also depicts the polymeric chain growth of OLLA on the chitosan backbone because of grafting. The nHAp spectrum shows the bands corresponding to O–P–O bending at 570 cm<sup>-1</sup>, the bands corresponding to 1097 cm<sup>-1</sup>, 1048 cm<sup>-1</sup>, 603 cm<sup>-1</sup>, and 507 cm<sup>-1</sup> corresponded to various vibration modes of the phosphate group, while the band at 3574 cm<sup>-1</sup> was assigned to the stretching of the hydroxyl group.

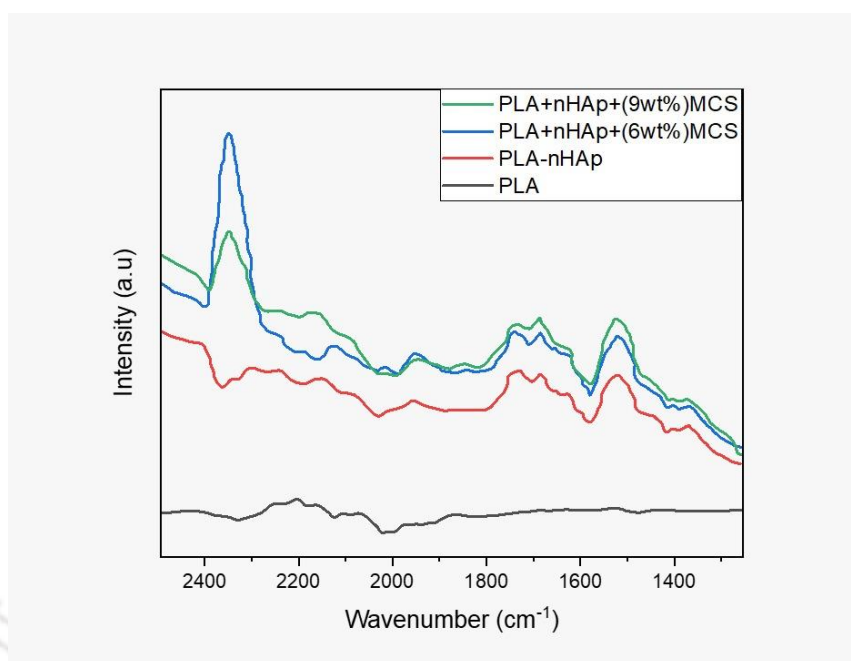


**Fig. 3.2:** FTIR spectra of the neat PLA and the prepared bio-composites.

The FTIR spectra of all the PLA/nHAp/MCS bio-composites show the C=O band at  $1716\text{ cm}^{-1}$  as compared to  $1746\text{ cm}^{-1}$  for PLA. Also, the spectra are observed with a decreased intensity because of the presence of MCS on the PLA surface. Further, it shows the presence of hydrogen bonding interactions between PLA and MCS. The –N–H bending vibration at  $1545\text{ cm}^{-1}$  in the case of MCS was shifted to  $1510\text{ cm}^{-1}$  in all the bio-composites.

### 3.2.3 Thermogravimetric analysis

The temperature variation with a weight loss percentage (TGA) and derivative of weight loss (DTG) of the fabricated melt-extruded strips of neat PLA, PLA/nHAp, and PLA/nHAp/MCS bio-composites is shown in Fig. 3.3. The bulk of the thermal degradation occurred in the  $350\text{--}440\text{ }^{\circ}\text{C}$  range. The onset degradation temperature ( $T_{on}$ ) of purified PLA, PLA/nHAp, bio-composite with 6% MCS, and bio-composite with 9% MCS occurred at 270, 276, 278, and 280  $^{\circ}\text{C}$ , respectively. In contrast, the ending point degradation temperature ( $T_{end}$ ) was observed at 388, 402, 390, and 397  $^{\circ}\text{C}$  for purified PLA, PLA/nHAp, bio-composite with 6% nHAp, and bio-composite with 9% nHAp, respectively. The maximum degradation temperature rate ( $T_{max}$ ) was 378, 389, 381, and 383  $^{\circ}\text{C}$  for PLA, PLA/nHAp, bio-composite with 6% nHAp, and bio-composite with 9% nHAp. The weight loss % at  $T_{max}$  for PLA, PLA/nHAp, bio-composite with 6% MCS, and bio-composite with 9% MCS was around 37%, 35%,

26%, and 25%, respectively. The corresponding residual weight % observed was 0.61%, 3.9%, 6.62%, and 7.2%, respectively. The residual weight is mainly because of the formation of carbonaceous char. Moreover, the primary reason for thermal degradation of PLA and its composite is attributed to the intramolecular transesterification or backbiting reaction of PLA [Backes et al., 2019].

The thermal stability of neat PLA and its bio-composites is increased with nHAp and MCS fillers. On further addition of nanofillers (MCS), the thermal stability decreased due to the increment in the short-chain oligomer, which degraded the composites at lower temperatures [Ambrosio-Martín et al., 2016]. The observed peak

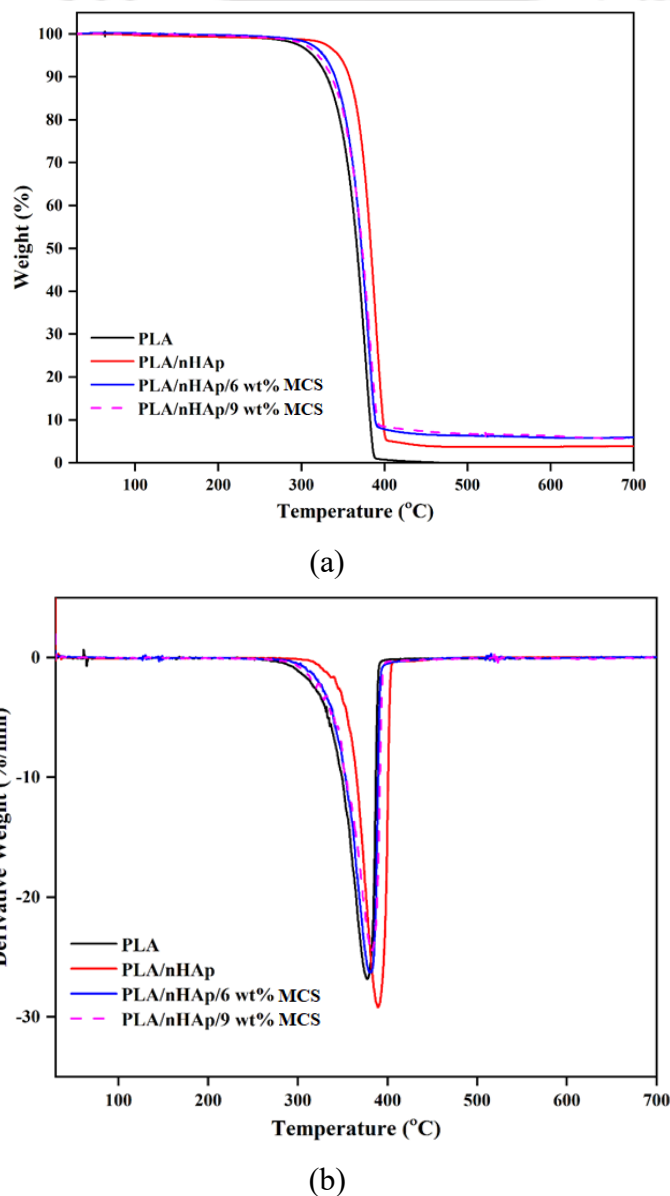


**Fig. 3.3:** Plots of (a) TGA and (b) DTG of the prepared samples.

of maximum degradation of the bio-composites (Fig. 3.3) signifies that the thermal degradation occurred in the single-step process.

The degradation temperature of the PLA/nHAp/MCS composites was higher than the neat PLA and Chitosan. Studies involving PLA composites prepared with neat chitosan and nHAp showed a maximum degradation temperature of  $\sim 357$  °C [Torres-Hernández et al., 2018]. In another study, Mohamad et al. observed the maximum degradation temperature ( $T_{max}$ ) of PLA composites with MCS, synthesised similarly to that of the current study, to be around 290 °C [Mohamad et al., 2021], whereas the  $T_{max}$  of the bio-composite developed in the present investigation was found to be higher. Thus, the interaction of nHAp with MCS and PLA made the synthesised bio-composites superior in terms of thermal stability compared to neat PLA and PLA with chitosan.

### 3.2.4 Differential scanning calorimetry analysis

The DSC analysis of the samples indicated that with addition of nHAp in the PLA, the glass transition temperature ( $T_g$ ) has increased as compared to the neat PLA. The reason for this occurrence can be attributed to the hindering of movements of the PLA chain caused by nHAp [Injorhor et al., 2022]. In contrast, a reduction in  $T_g$  was witnessed on addition of MCS with the PLA/nHAp (Fig. 3.4 and Table 3.1). This might be due to the fact that the oligomer chain present in the MCS leads to the plasticising effect, which in turn increases the PLA chain mobility and subsequently reduces the  $T_g$ . Further addition of MCS has lowered the cold crystallisation temperatures in the bio-composites revealing that the MCS could support the crystallisation of PLA. This observation agrees with the other studies in which the investigators reported that chitosan promotes faster crystallisation by acting as a nucleating agent [Correlo et al., 2005; Răpă et al., 2016]. In the case of melting temperature, no obvious change in trend was witnessed.

**Table 3.1:** DSC thermogram results.

	$T_g$ (°C)	$T_{cc}$ (°C)	$T_m$ (°C)
PLA	59.2	114.1	150.74
PLA-nHAp	61.2	123.2	151.20
6 wt % MCS	59.6	111.3	149.80
9 wt % MCS	56.8	110.4	150.40

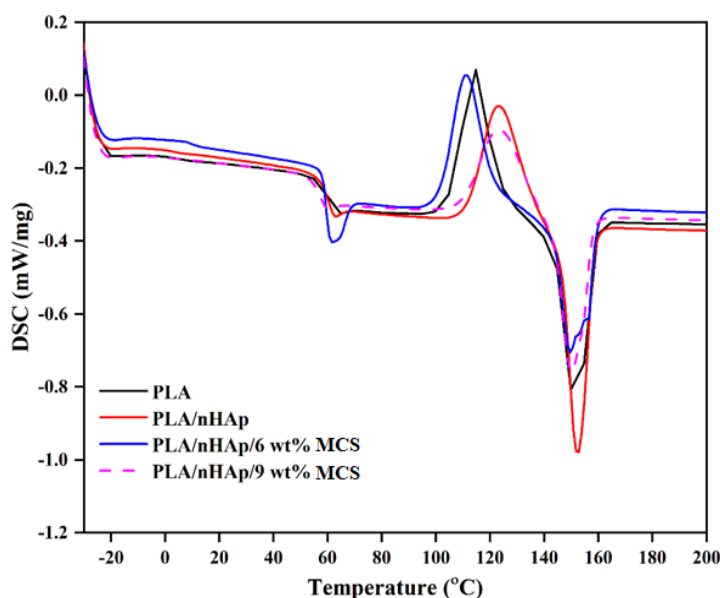


**Fig. 3.4:** DSC plot of PLA, PLA/nHAp, PLA/nHAp/6 wt% MCS, and PLA/nHAp/9 wt% MCS.

### 3.2.5 Contact angle study

The contact angle (Fig. 5) of the neat PLA was observed as  $74.1^\circ$ , which signifies the poor affinity of water on the polymer surface, i.e. its hydrophobic nature [Prasad et al., 2017]. The addition of 15% nHAp into the neat PLA matrix drastically decreased the contact angle to  $72.7^\circ$ , suggesting the composite's hydrophilic behaviour.

The modification of the chitosan through grafting technique provides good dispersion in the PLA matrix; however, it retains the nature of hydrophilicity regardless of the modification. In addition, the grafted oligomer which is the precursor of PLA has a hydrophilic nature. Moreover, the nHAp particles being hydrophilic itself contributed towards the overall hydrophilicity of the PLA composite [Liu et al., 2020]. Thus, the further addition of MCS to the PLA/nHAp composite showed a decrease of contact angle to  $70.1^\circ$ . The decrease in the contact angle, compared to the PLA/nHAp composite, might be due to the presence of modified chitosan in the PLA matrix. However, all the composites showed a less contact angle with respect to neat PLA. Also, the composites exhibited hydrophilic nature. Noteworthy to mention, the enhancement in the surface wettability property suggests that the bio-composites are suitable for cell adhesion.

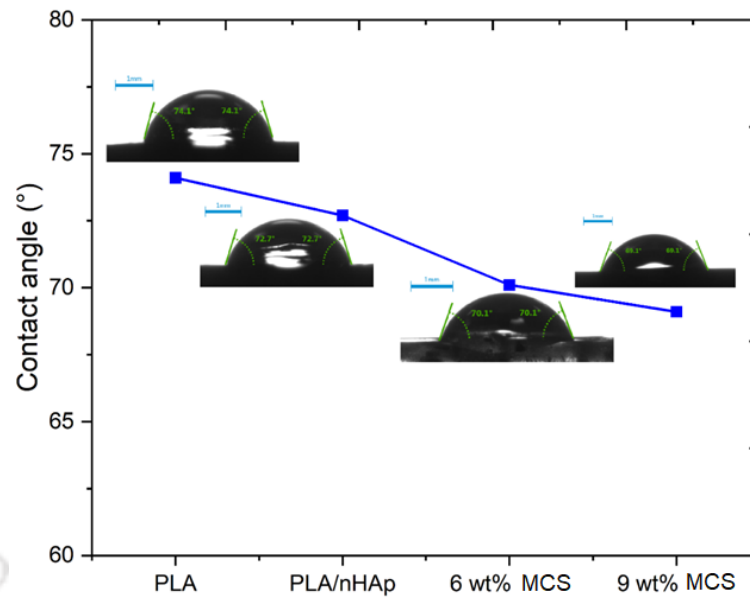


**Fig. 3.5:** Contact angle analysis of the prepared samples.

### 3.2.6 Surface morphology

PLA is a semi-crystalline and hydrophobic polymer with inherent brittleness and low toughness that limits its application [Tripathi et al., 2016]. In contrast, CS is a hydrophilic filler with non-uniform distribution in the polymeric matrix due to amine and hydroxyl groups [Veljović et al., 2011]. However, adding a bio-compatibiliser can help to overcome this hydrophilic nature. Thus, when CS is grafted to lactic acid (oligomer), it results in the formation of chemically modified chitosan. Fig 3.6 depicts the difference in the surface texture of the composites with respect to the neat polymeric ones. Also, it shows how the morphology of PLA scaffolds changes before and after HAp and MCS incorporation. It can be observed that the pores present in the PLA/HAP composite got partially filled with CS [Gupta et al., 2017].

The presence of a filler in the polymer matrix augments the mechanical and resorption characteristics. However, the homogenous dispersion of fillers in the matrix is a more significant criterion [Veljović et al., 2011; Gupta et al., 2017]. Figure 6 also shows the surface morphology through FESEM of the extruded strips of neat PLA and the composites consisting of MCS and nHAp. The difference in the surface texture of the composites with respect to the neat PLA strips was observed. The smooth PLA surface indicates the swelling of PLA chains due to the presence of MCS in the matrix. The microscopy image of the neat PLA was found to be flaky, as shown in Fig. 6c

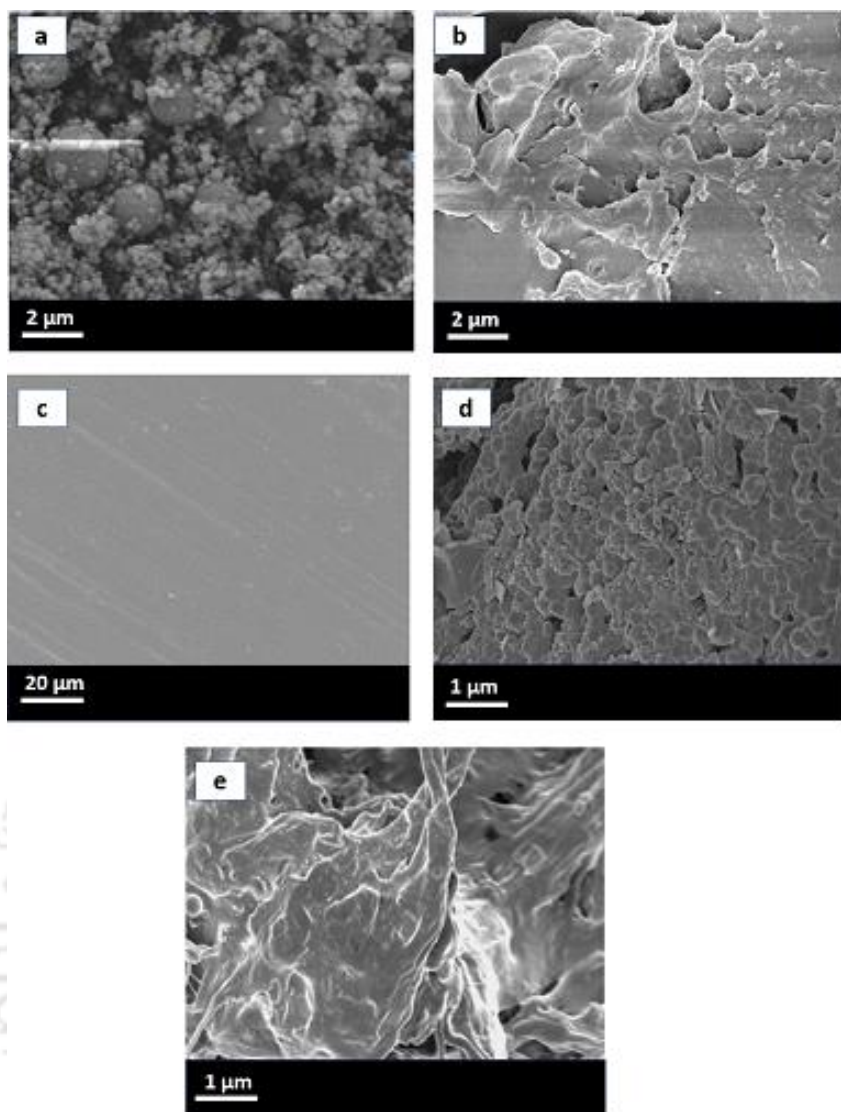


**Fig. 3.6:** FESEM images of (a) nHAp (b) modified chitosan (MCS) (c) neat PLA (d) PLA/nHAp (e) PLA/nHAp/MCS.

which was eventually made smoother surface after the addition of the MCS in the PLA matrix.

This is evident of the plasticizing effect of the filler, which has increased filler loading and changed to a smoother surface. Also, the effect of extrusion is evident from the proper dispersion of MCS without any voids in the PLA matrix. The presence of nHAp on the surface is difficult to be differentiated from that of MCS through SEM. Hence, EDX analysis was also carried out (Fig. 3.7). Fig. 3.7 shows the EDX analysis in which the presence of a specific element was ensured by mapping the X-rays generated from the elements. In the nHAp-containing composites, the calcium (Ca) and phosphorus (P) were confirmed with the X-ray coming from the spectra. The FESEM and EDX analysis confirmed that the non-uniform distribution problem associated with

the chitosan has been overcome with the MCS. Moreover, it also ensures that the nHAp is dispersed properly and present at the nanoscale on the matrix. The results have also demonstrated the uniform distribution and dispersion of nHAp with MCS as a compatibiliser. During the processing of polymers, it is generally observed that a trace amount of contamination may occur and sometimes it gets reflected in the results of few analyses. This explains the presence of a peak of phosphorus for the neat PLA and for the modified chitosan (Fig. 7). This may be considered to bear insignificant relevance to the overall composition of the composite. The biocompatibility and cell viability analysis of the prepared composition needs to be carried out before fabricating

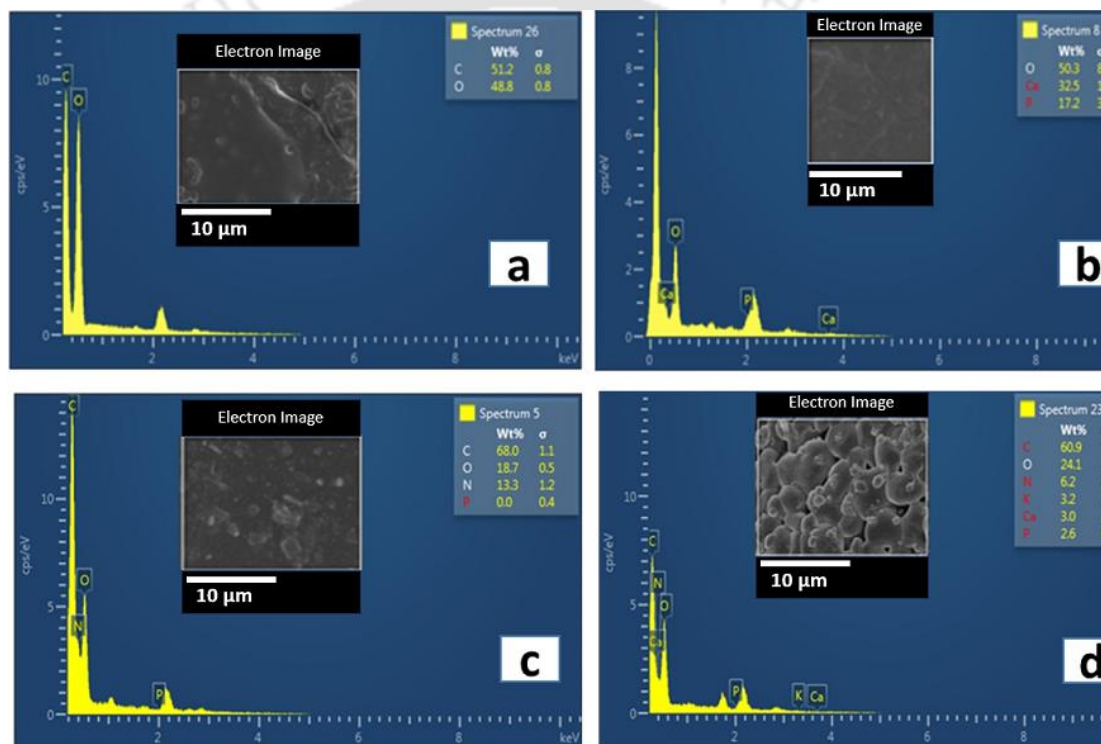


**Fig. 3.7:** EDX analysis of (a) neat PLA (b) nHAp (c) modified chitosan (MCS) (d) PLA/nHAp/MCS.

biomedical implants like bone screws and plates.

### 3.3 Summary of the findings

In the present investigation, an attempt has been made to develop novel bio-composites made of PLA, nHAp, and MCS. Also, the novelty of the work lies in the fact that the bio-composites were made through a solvent-free process through extrusion cum injection moulding. The prepared samples were tested for their morphology, mechanical strength, and thermal stability. CS has the drawback of poor dispersion in the PLA matrix, which has been overcome with the synthesised MCS. The addition of

MCS and nHAp to the pristine PLA has attributed to the improvement of the thermal and mechanical properties of the material for biomedical applications. Uniform dispersion of nHAp was observed in the PLA matrix by FESEM. The TGA analysis of the fabricated sample showed that it has a degradation temperature that is suitable for high-temperature melt-processing techniques. The contact angle of the composites is found to decrease as compared to neat PLA which suggests that the hydrophilic nature of the composite has been increased. From the DSC results, no phase separation was witnessed, which confirms the proper mixing of the bio-fillers in the matrix. Overall, the developed PLA/nHAP/MCS bio-composites have the potential to be an alternative biodegradable implant material suitable for biomedical applications.



## Chapter 4

### **A finite element study to predict the viability of PLA-based composite implants for mandibular joint fracture**

#### **4.1 Introduction**

The growing incidence of facial fractures and deformities resulting from any trauma, falls, personal assaults, oral cancer or motorized vehicle accidents has led to a significant rise in surgical interventions in the mandibular region [Marx, 2013; Ferlay, 2013; Cai, 2016]. The mandibular bone, located in the lower facial region, is responsible for the movement of the lower teeth and jawline, making it prone to fractures when subjected to trauma. The primary goal in such mandibular fracture management is to re-establish pre-morbid anatomy, stabilizing the fracture region to restore functionality at the earliest. Therefore, craniomaxillofacial surgery involves the mandibular reconstruction of segmental defects in the affected condylar region through the implantation of a rigid internal fixation device [Park, 2018; Narra 2014]. Traditional treatment choices in open reduction techniques involve wire osteosynthesis and intramaxillary fixations. Common complications of such techniques include infections (osteomyelitis), broadening of the face, malocclusion, and implant failure. Plating techniques are the preferred treatment choice owing to their rigid fixations in which a metallic plate and a screw are fixed to the fractured bone with the head of the screw being tightly inserted into the plate, eliminating potential nerve damage by avoiding external incisions. Also, mini plates are easy to apply for fixations at all points of the mandible. [Levy, 1991]. Generally, Titanium micro-plates and screws have been widely used for the rigid fixation of mandibular fractures. However, certain disadvantages associated with metallic plates and screws are the dissolution of metallic ions and their accumulation in loco-regional lymph nodes and other organs, stress shielding phenomenon, and the generation of artefacts on computed tomography. Therefore, a secondary re-surgery is required at the earliest to remove the metallic implant often after fracture healing. This results in a more invasive surgical procedure increasing the overall socio-economic burden of the patients. The development of resorbable

polymeric fixation system can be proposed as an effective remedy to the conventional system [Neumann, 2019]. The degraded byproducts from the polymeric system will get naturally eliminated from the body once the fractured bone is healed, thereby avoiding a secondary surgery. Biocompatible and resorbable polymers, particularly polyester is gaining attention in biomedical applications owing to its superior mechanical properties, biodegradability and low immunogenicity. Few noteworthy bioresorbable polyesters include poly glycolic acid (PGA), poly lactic acid (PLA), poly caprolactone (PCL) and their copolymers. PLA is an aliphatic polyester having advantages such as renewability, biocompatibility, and processibility compared to other bioresorbable polymers [Pine, 2012]. Lactic acid, the monomer of PLA is derived from renewable natural resources by fermentation of agricultural feedstock. PLA is produced by either polycondensation of lactic acid or ring-opening polymerization of lactide [Torres-Hernández, 2018] and has garnered much attention in the biomedical field. The degradation products of PLA are neither toxic nor carcinogenic to the human body and serve as an excellent material for implants and drug delivery systems [Peng, 2015]. However, due to the intrinsic brittle nature and very low elongation at the break of PLA, modification to improve the flexibility of the polymer is required by incorporating bio-fillers such as HAp, MCS into the PLA matrix.

Finite Element (FE) -based in-silico methods have emerged as a reliable technique for the pre-clinical assessment of various implantation techniques associated with fractured bones. Lovald et al. used FE analysis in their study to carry out parametric optimization of bone plates for fractures of the mandible. Shape and design variable parameters such as the width of the bars of the bone plate., fillet radii, plate thickness and the spatial location of the screw holes are optimized to provide maximum fracture stability with minimum implanted volume [Lovald, 2006]. Cox et al. investigated the resorbable plastic copolymers of polylactic acid and polyglycolic acid as a plate & screw (implant) material for a typical mandibular angle fracture [Cox, 2003]. Using FE analysis, they concluded that the materials are of adequate strength and stiffness for their successful applications to the rigid fixation of mandibular angle fractures. Various other authors have also previously employed FE analysis to assess the performance of metallic plates for mandibular joint fracture fixation, there is no clear FE study on PLA-based fractured plates in low load-bearing body regions [Peng, 2015; Ilavarasi, 2011; Vajgel, 2013; Tarashi, 2006; Mohamed Haneef, 2019]. Most of the FE analysis work on polymeric implants are based on simplistic assumptions or data

carried from other reported experiments [Vajgel, 2013; Tarashi, 2006; Mohamed Haneef, 2019].

With current improved knowledge of oral biomechanics and advances in biomaterials, FE analysis can be employed to successfully predict load transfer across mandibular fractures, assess the performance of different implant materials, and evaluate the efficacy of various implantation techniques. The specific aims of the study is to check the viability of the formulated bio-composite as an alternative implant material to the metallic fixation device for mandibular fractures using FE analysis. To the author's knowledge, this is hardly any study where the systematic formulation of the PLA-based composite was demonstrated, and subsequently, FE-based pre-clinical assessments were carried out to determine the viability of the material as a probable implant. We hypothesize that tailored bio-composites can be used as a material for implants associated with tiny fractures for low load-bearing regions in place of conventional metallic implants. The objective of the present study has been divided into two parts. The first part consisted of the experimental fabrication of the polymeric composites of PLA/nHAP/MCS by extrusion cum injection molding followed by its mechanical analysis to determine the strength of the composites under universal testing machine (UTM). Two different fracture model were virtually developed and analysed using FE methods: one with hairline fracture in the mandibular joint and the other with varied fracture gap~1mm.

#### 4.2 Results and Discussions

The elastic modulus of the various PLA-based composites was determined using mechanical testing under UTM (Fig. 4.1). The maximum modulus composition among the various formulated composites was chosen as the desired material for the *in silico*

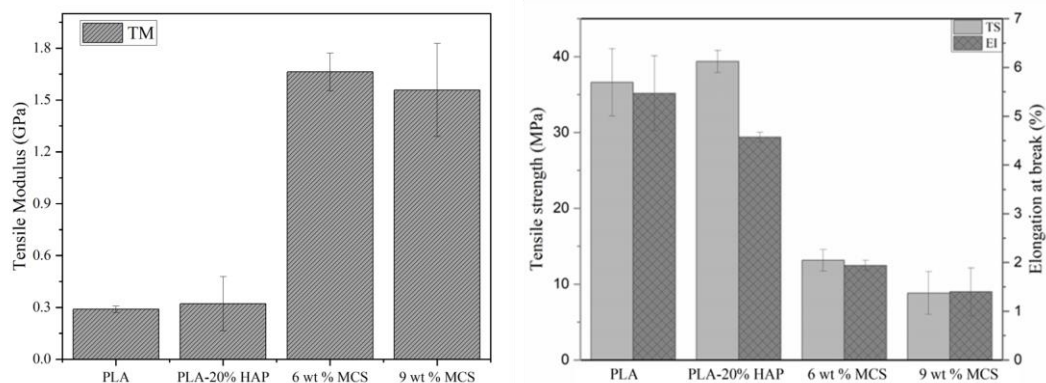


**Fig. 4.1:** Mechanical testing (a) Young's modulus (b) tensile strength and elongation of the prepared samples (MCS containing PLA bio-composites consists 20% HAp).

study. Fig. 4.2 represents the von Mises stress contours associated with PLA composite and Ti alloy implants, used as a fixation for hairline mandibular fracture. The maximum von Mises stress associated with PLA-based composite implanted mandibular construct, under biting force loading conditions, was around 110 MPa in the cortical bone around the fracture region. On the contrary, the Ti alloy implanted construct exhibited maximum von Mises stress around 150 MPa at the distal screw plate interface of the upper plate. The von Mises stress contours of the both implanted construct with a 1mm fracture gap in the mandibular bone, under biting force loading consideration, are shown in Fig. 4.3.

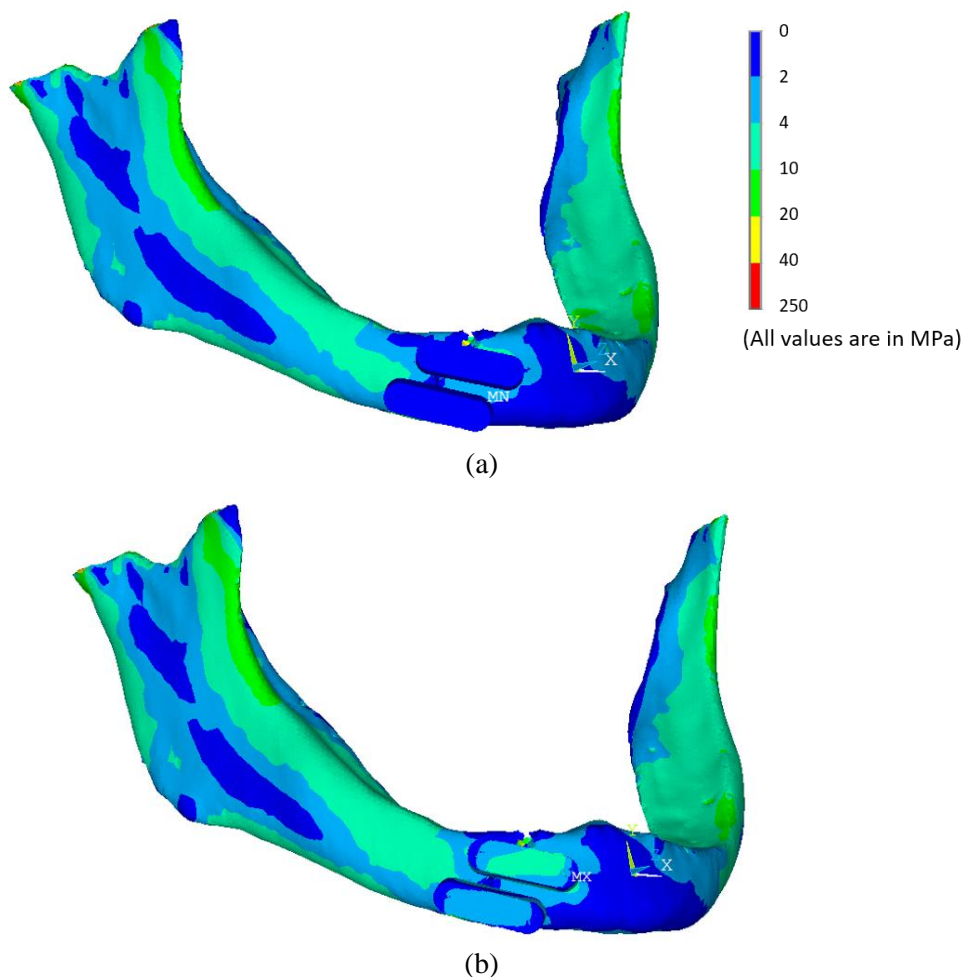


**Fig. 4.2:** Predicted von Mises stress distribution in hairline mandibular fracture considered under biting load condition: (a) PLA+HAp+MCS composite plate, (b) Ti alloy plate.

In contrast, Fig. 4.4 depicts the von Mises stress contours of the 1mm fracture gap mandibular joints under both biting and occlusal load consideration. The maximum displacement associated to implanted hairline mandibular fracture was observed at the lower edge of the mandibular joint. This may be attributed to the fact that total load

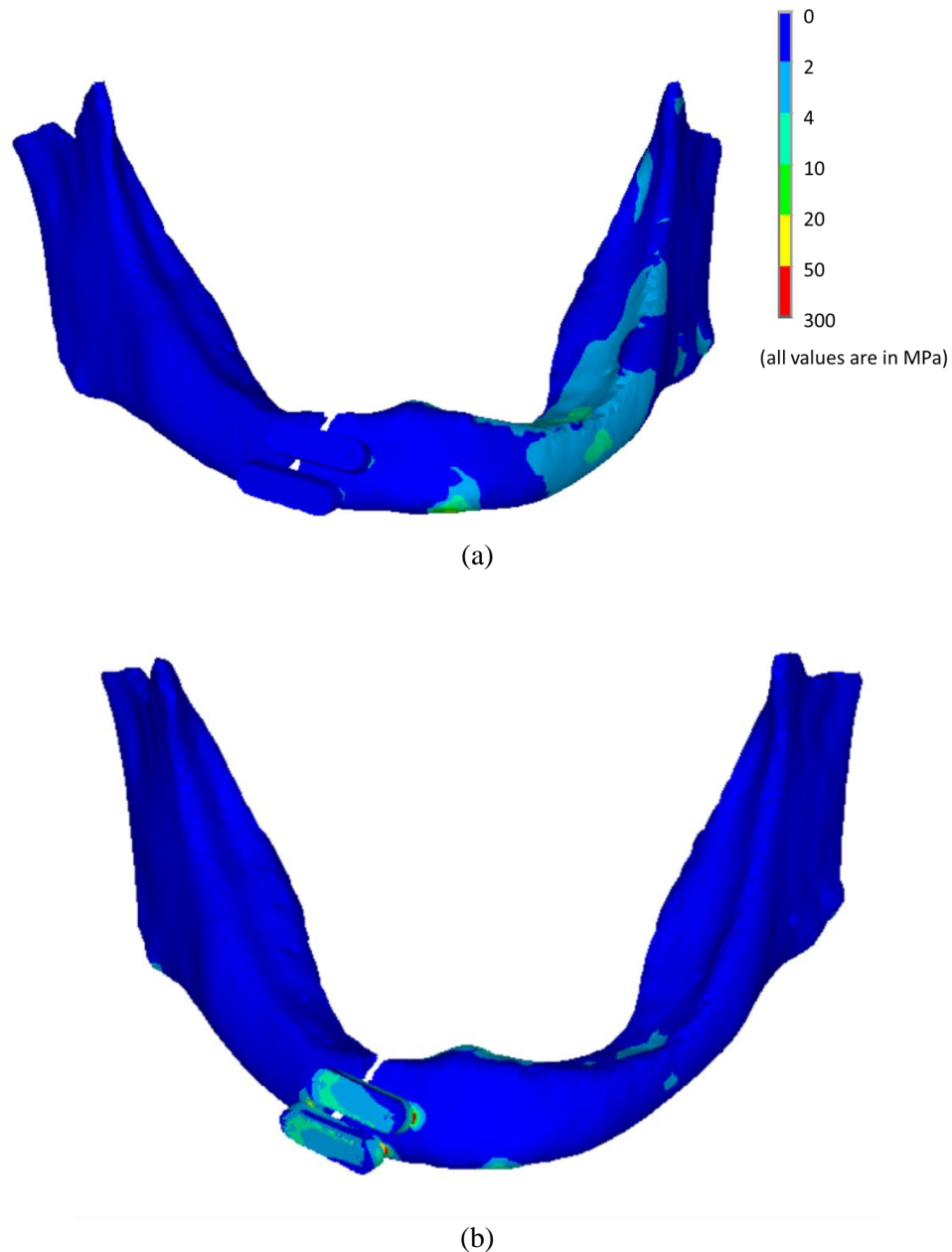


**Fig. 4.3:** Predicted von Mises stress distribution in mandibular fracture having gap ~1mm considered under the biting load condition: (a) PLA+HAp+MCS composite plate, (b) Ti alloy plate.

transfer was possible across the fracture region and the combining fractured parts showed the maximum displacement around biting the load applying area. Whereas, in case of 1 mm fracture gap, the maximum displacement for both the implanted construct was observed in the fracture end region of the left mandibular part (Fig. 4.5). It can be noted here that the biting force is acting on the left mandibular bone part and hence the maximum displacement. As the mandibular bone is totally disassociated in the fracture region, the displacement was noted at the free fracture end more. However, when the occlusal load was applied in the same fracture gap (1mm) of both the implanted

mandibular bone construct, the right part of the broken mandibular bone was found to be associated with maximum displacement (Fig. 4.6). The reason behind this could be the short distance between the point of application of left occlusal load and the fracture region as compared to the left occlusal loading point.

For both the loading conditions, the displacement of the PLA composite construct was found higher as compared to the Ti alloy implanted construct. Ti being implant of

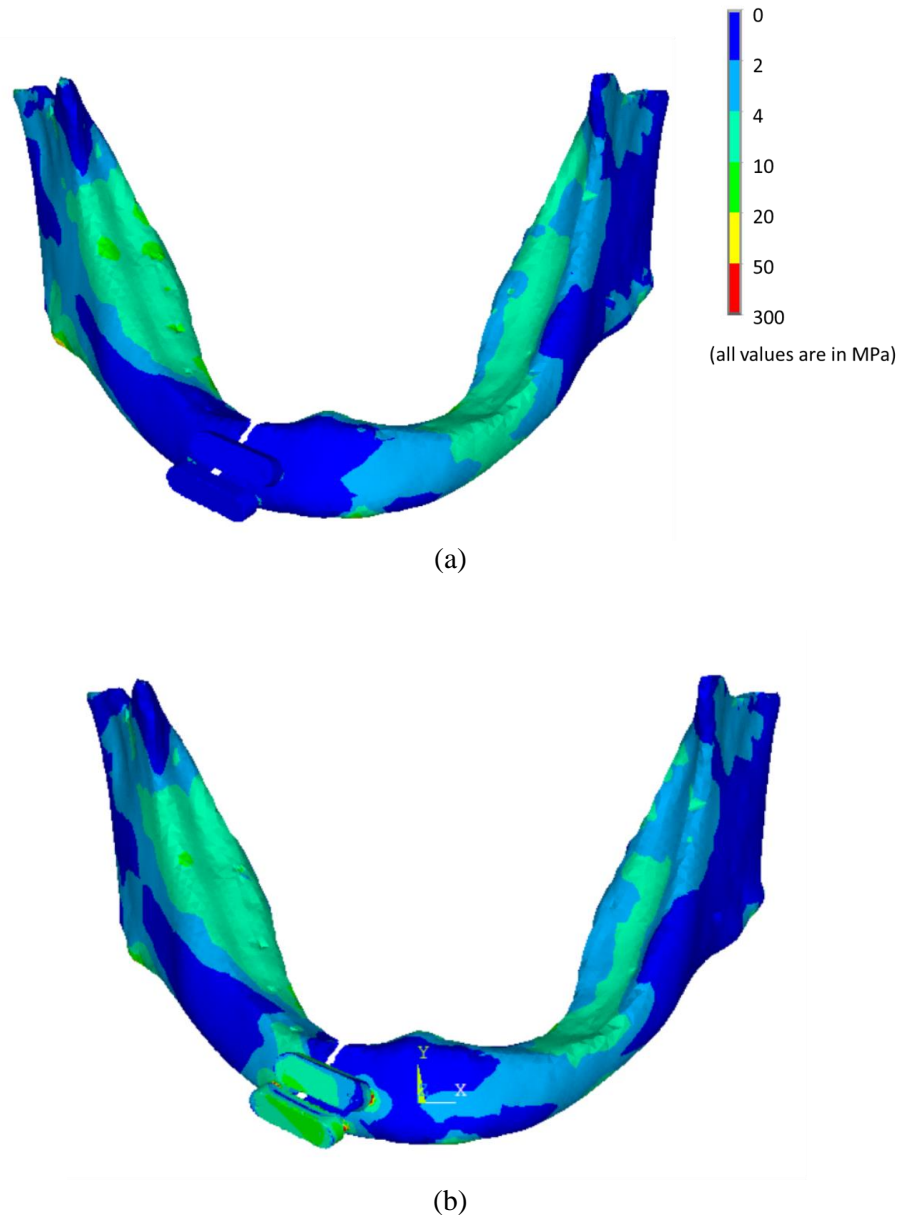
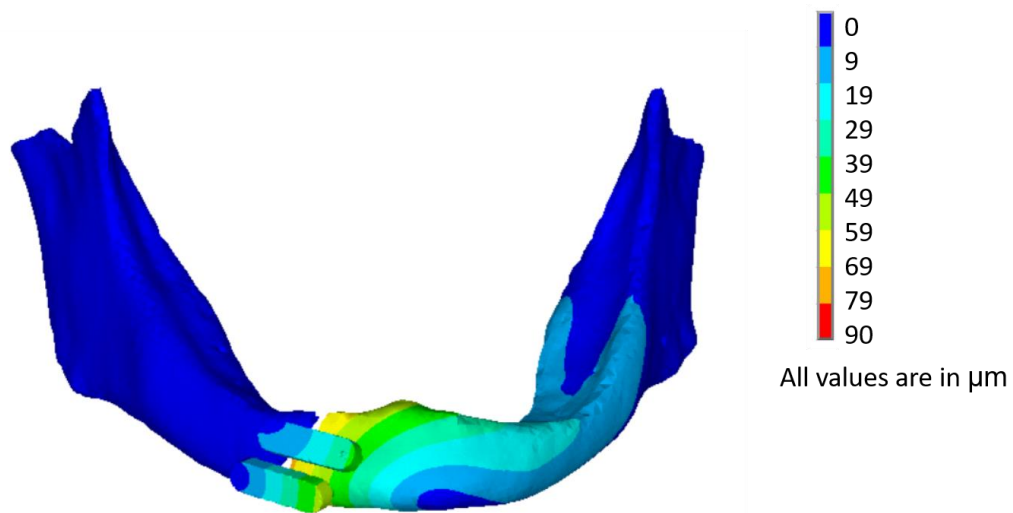


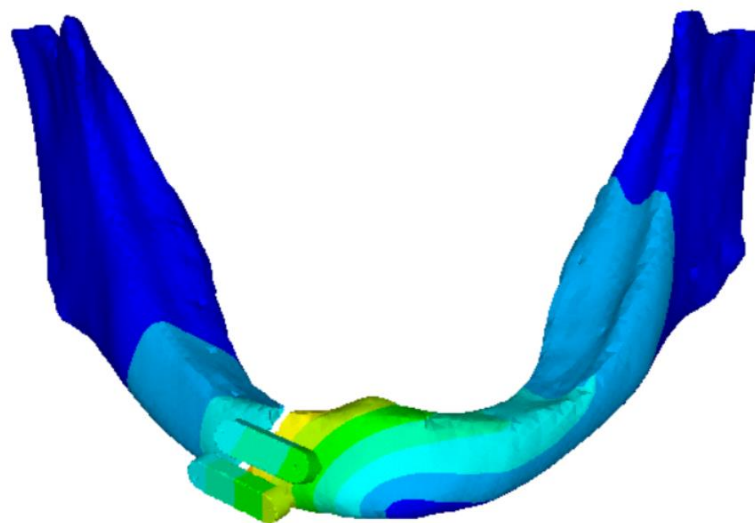
**Fig. 4.4:** Predicted von Mises stress distribution in mandibular fracture having gap ~1mm considered under the biting load and occlusal loading condition: (a) PLA+HAp+MCS composite plate, (b) Ti alloy plate.

higher modulus has the ability to impart greater rigidity and stability to the fractured parts. In case of 1 mm fracture gap under biting load considerations, the PLA based

implant showed almost twice the displacement as compared to Ti implanted construct. Further two more variations were tried out to understand whether plate or screw material plays crucial role in stability. With PLA based composite plate and Ti screw, the displacement of the implanted construct was observed as 0.069mm as compared to the 0.085 mm associated with Ti plate and PLA screw construct. This suggests that the screw material plays a vital role as per the stability is concerned (Fig. 4.7). This can be attributed to the fact that screws connect to the bone and can enhance the bone-implant anchorage and overall compressive strength of the construct. Similar trends were also



(a)



(b)

**Fig. 4.5:** Predicted displacement plots in mandibular fracture having gap ~1mm considered under the biting load condition: (a) PLA+Hap+MCS composite plate, (b) Ti alloy plate.

observed on addition of occlusal forces to the biting forces in the mandibular joint. PLA based composite mandibular construct showed max displacement of 0.114 mm as compared to the 0.074mm associated to Ti alloy implant. However, the PLA based implanted construct in the present study, exhibited displacement below 150  $\mu\text{m}$  under

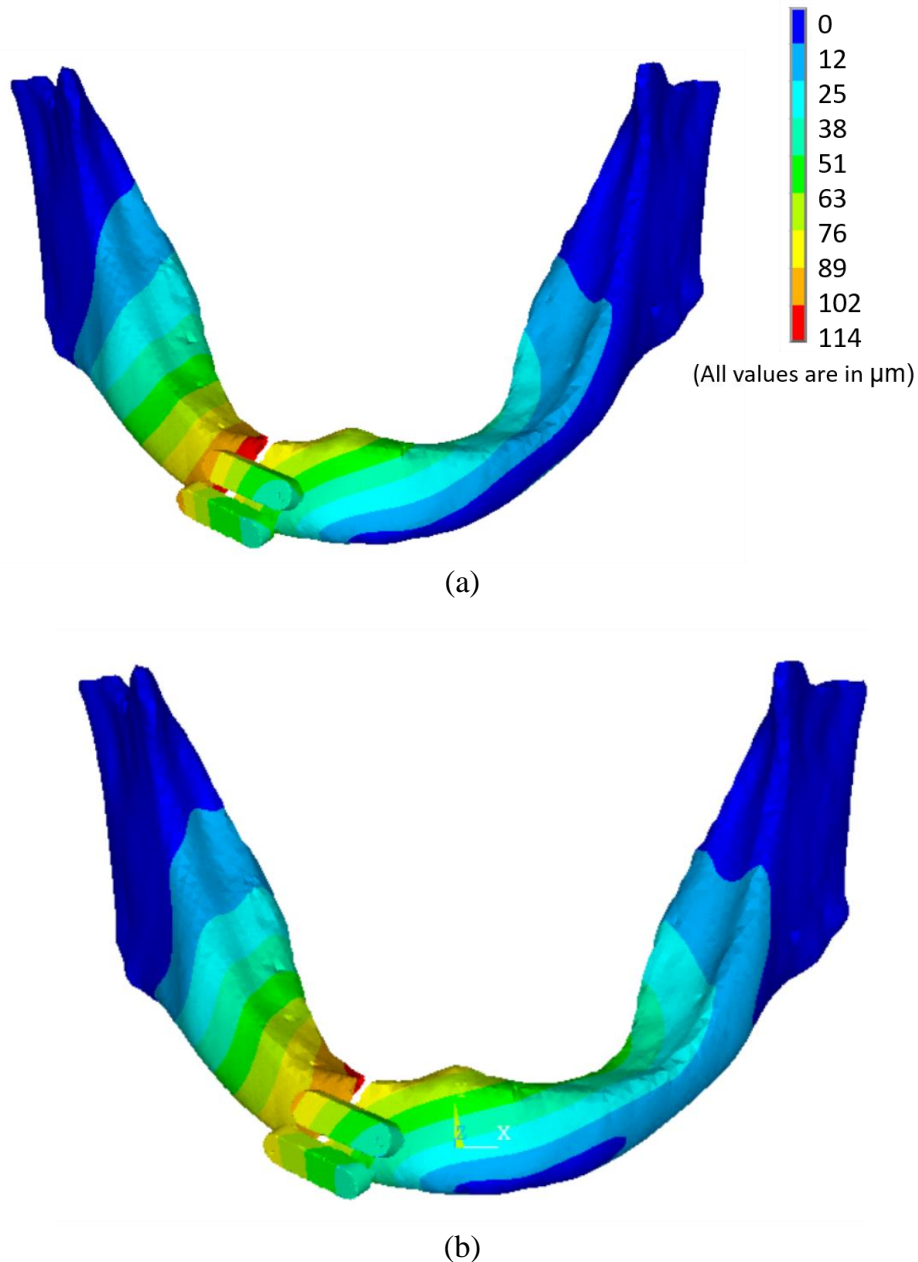


**Fig. 4.6:** Predicted displacement plots in mandibular fracture having gap  $\sim 1\text{mm}$  considered under the biting load and occlusal loading condition: (a) PLA+Hap+MCS composite plate, (b) Ti alloy plate.

any kind of loading consideration, which is essential for bone healing [Soballe et al., 1992; Bragdon et al., 1996]. The Ti alloy implant being associated with higher modulus, bears a major proportion of the physiological load. The conventional metallic implants deprive the mandibular bone of the much essential stress, which otherwise available

sufficiently in an intact bone. Stress shielding is the phenomenon in which the implanted bone gets devoid of the essential stress required for its growth and consequently initiates cortical thinning [Nag and Chanda, 2021]. Cortical thinning makes the bone-implant construct loose and eventually it fails. Therefore, it is essential for the patient with metal implants to have frequent post-operative clinical check-ups to assess the healing and undergo implant removal surgery. In the present study, PLA based composite implants exhibited very minimal stress shielding owing to their low modulus property. Further, there is no requirement for re-surgery as the implant is made of a biodegradable polymer. Thus, the present study finds the PLA-based composite implant as a viable alternative to the conventional metallic implantation technique for low load-bearing mandibular joint fractures.

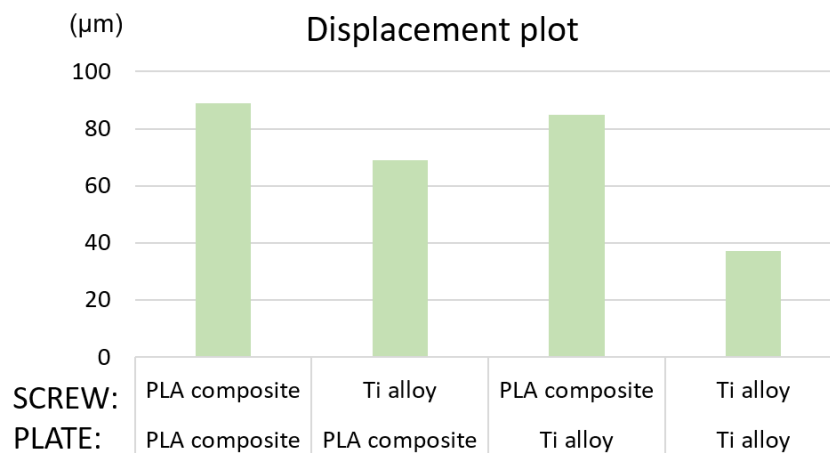


**Fig. 4.7:** Displacement plot of PLA composite and Ti alloy based mandibular construct: comparison under biting force with different combination of plate and screw material.

### 4.3 Summary of the findings

The PLA based bio-composite implant was found to be a viable alternative to the conventional metallic implant for mandibular fracture. In this study, PLA-based composite implants exhibited minimal stress shielding due to their lower modulus properties. Overall, the developed bio-composites have the potential for an alternative biodegradable implant material suitable for biomedical applications in cases of fracture in low load-bearing sites. The PLA based implant comes with an added advantage of avoiding re-surgery once bone union happens. Further, when combinations between metallic plates and PLA based bio-composite screw and vice versa was considered, it was observed that the material of screw has dominant effect on the overall stability of

the implant. In such scenarios, PLA based bio-composite plates and Ti alloy screws can be an interesting solution to mid-level load bearing regions of human body.



## Chapter 5

### ***in vitro* cytotoxicity study and *in silico* analysis of the PLA/nHAp/MCS bio-composite as a coating material for high load-bearing implants**

#### **5.1 Introduction**

The risk of aseptic loosening in metallic implants can be avoided by improving osseointegration with osteoconductive coating. Such coating favours long-term implant stability. The primary cause that leads to failure of the implant bone association is the aseptic loosening i.e., the macroscopic instability of the metallic implant with respect to the host bone [Katz et al., 2007; Kenny et al., 2079]. Generally, the initial micromotion at the bone implant interface may develop fibrous and non-mineralised tissue that are weak to stabilize the implant. Thus, a viscous feedback loop gets created where increased micromotion further prevents bone growth and delays the union [Albrektsson et al., 2001]. As a result, the patient suffers significant pain under load and often requires revision surgery. Thus long term stability is essential for successful bone union, and that can be achieved by osseointegration where bone tissue grows and forms a direct bond with implants [Araújo-Gomes et al., 2018; Lewallen et al., 2015]. A bio compatible osteo inductive layer between bone and implant can be effective strategy to prevent aseptic loosening. The PLA\nHAp\MCS bio-composite being resorbable will facilitate new mineralized tissue growth towards the implant filling some gaps between the implant and the bone. In previous studies, *in vivo* experiments were used to evaluate how the osteoconductive coating layers affect the tissue response to induce micromotion.

PLA is an ecofriendly bio-polymer which doesn't produce any carcinogenic effect in local tissue and is bio-compatible in nature. PLA products were approved by the US FDA for direct contact with biological fluids. It has better thermal processability and saves 25-55% energy from production compared to other bio-polymers [Rasal and Douglas, 2010]. Chitosan is a naturally occurring biopolymer resulting from the partial deacetylation of chitin. The conversion of chitosan from chitin depends on the degree of deacetylation (DD%). Higher DD% is linked to higher conversion of chitin to chitosan and vice versa. Chitosan has four major important properties, which include

solubility, flexibility and polymer conformation. It is a hydrophilic polymer which is soluble in weakly acidic solutions. It is insoluble in chlorinated and organic solvents. The amines in chitosan are deprotonated and reactive at higher pH (>6.5), making it insoluble. In contrast, it is protonated and converts into  $\text{NH}_3^+$  at low pH (<6), thus making it soluble [Pal et al., 2017]. The use of chitosan in the biomedical field is due to its good antimicrobial properties, biodegradability, and biocompatibility [Bose et al., 2023]. Apart from these characteristics, chitosan promotes bone cells' adhesion and proliferation, has a low cellular response and has non-toxicity. On the other hand, an existing limitation is it exhibits poor mechanical properties because of its hydrophilicity. This can be improved by modification of CS by adopting a graft copolymerisation procedure.

Surgical bone restoration using implantation devices affects the mechanical environment within the bone by modifying the load transmission mechanism. As a result, the implant begins to share the joint strain that was previously carried solely by the bone in the pre-operative periods. This causes a significant post-operative complication known as stress shielding. Bones require constant stress to grow. Stress shielding happens when two or more components with different moduli are used in the same mechanical system. The component with the greater modulus bears the majority of the stress and protects the other component [Ferguson, 1996]. Similar situations happen with stiff fixation devices. In the early phase, hard fixation devices assist in the restoration or healing of the fractured sections of the fractured bone by sharing most of the load itself. However, in the later stages of healing, it may lead to osteoporosis with decreased bone strength [Tonino et al., 1984]. Stress shielding, as reported by several in vivo studies, occurs due to the use of rigid internal fixation plates. Conversely, using flexible plates with insufficient strength may lead to nonunion of the fracture, resulting in pain. Therefore, a balance must be struck between strength and stiffness. Ideally, as the fracture heals, the stiffness of the fixation device should decrease while the bone strength increases.

Uhtoff et al. (1981) studied fracture healing using stainless steel plates and less rigid titanium alloy plates. They found that the titanium plates were as strong as the steel plates but had half the stiffness. This reduction in stiffness resulted in less stress shielding and, consequently, less bone loss in femurs treated with titanium plates. Stress concentration occurs at the edges of screw holes after the removal of a plate and can result in refracture of the bone. Additionally, the presence of isolated bone screws can

lead to bone resorption around the screw holes. When the screws are removed, the stress concentration at the sides of the holes affects the already weakened bone—due to the remodelling process—thereby increasing the likelihood of fracture.

In the present study, we focused on formulating a bio-composite PLA, MCS, and nHAp. This combination of PLA/nHAp is a well-known biomaterial that has received approval from the Food and Drug Administration (FDA). Research indicates that PLA/nHAp exhibits biocompatibility. Studies have shown that PLA/Chitosan enhances the osteogenic capability for repairing large bone defects [Zhang et al., 2016]. Additionally, newer bone formation and improved neovascularisation have been observed with PLA/nHAp [Tu et al., 2020]. The viability and proliferation of MG63 osteoblast-like cells seeded on PLA–chitosan–keratin samples are comparable to the control, with only slight variations that may be influenced by the material composition [Tanase et al., 2014]. Furthermore, researchers have reported that PLA/nHAp enhances both osteoinductivity and osteoconductivity [Liu et al., 2020]. In vitro studies with PLA/nHAp have demonstrated that the bio-composite supports cell adhesion and proliferation, confirming its biocompatible nature [Gupta et al., 2017]. Therefore, based on the literature, it is evident that the PLA/nHAp combination proposed in this study is biocompatible. The surface properties of modified scaffolds were enhanced in terms of hydrophilicity and bioactivity through the incorporation of CS and HAp. This modification resulted in improved attachment and proliferation of human osteosarcoma cells compared to unmodified poly(lactic acid) (PLA) scaffolds [Nazeer et al., 2020]. These scaffolds can be customised to fit the size and shape of bone defects and can be used as implants to regenerate damaged bone. It is hypothesized that PLA-bio-composite coated implants will facilitate higher stress to the bone as compared to the uncoated implant, without compromising any structural rigidity.

## 5.2 Results and Discussions

In the present study, the structural rigidity of metallic implant with bio-composite coating was compared to that of only metallic implants. The tibia bone extracted from the CT data was of a carcinoma patient. After the infection has been removed from the tibia, a metallic implant in shape of the tibia is designed so that the rest of the bone can continue to be in use. The developed implanted bone is shown in Fig.5.1. Appropriate mesh was generated for the implant-bone construct based on the mesh convergence analysis. FE analysis was conducted on the coated and uncoated implants to predict the influence of the coating over the bone,

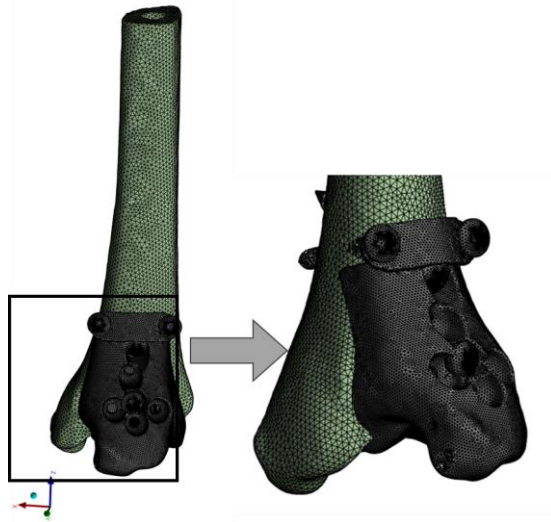


**Fig.5.1:** FE model of the tibia and implant.

Fig. 5.2 showcases the von Mises stress distribution of the coated and un-coated implant. The maximum stress was similar for both the implants  $\sim 120$  MPa. The location of the maximum stress was near the end of the proximal screw (screw projecting

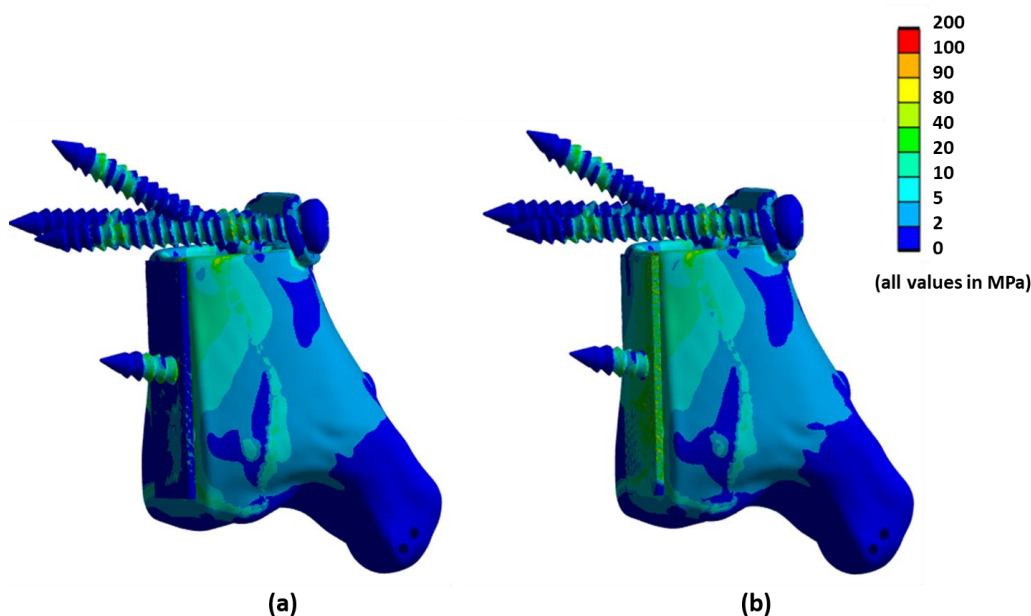


**Fig. 5.2:** von Mises stress distribution of the implant: (a) PLA+HAp+MCS coated Ti alloy implant; (b) Ti alloy implant.

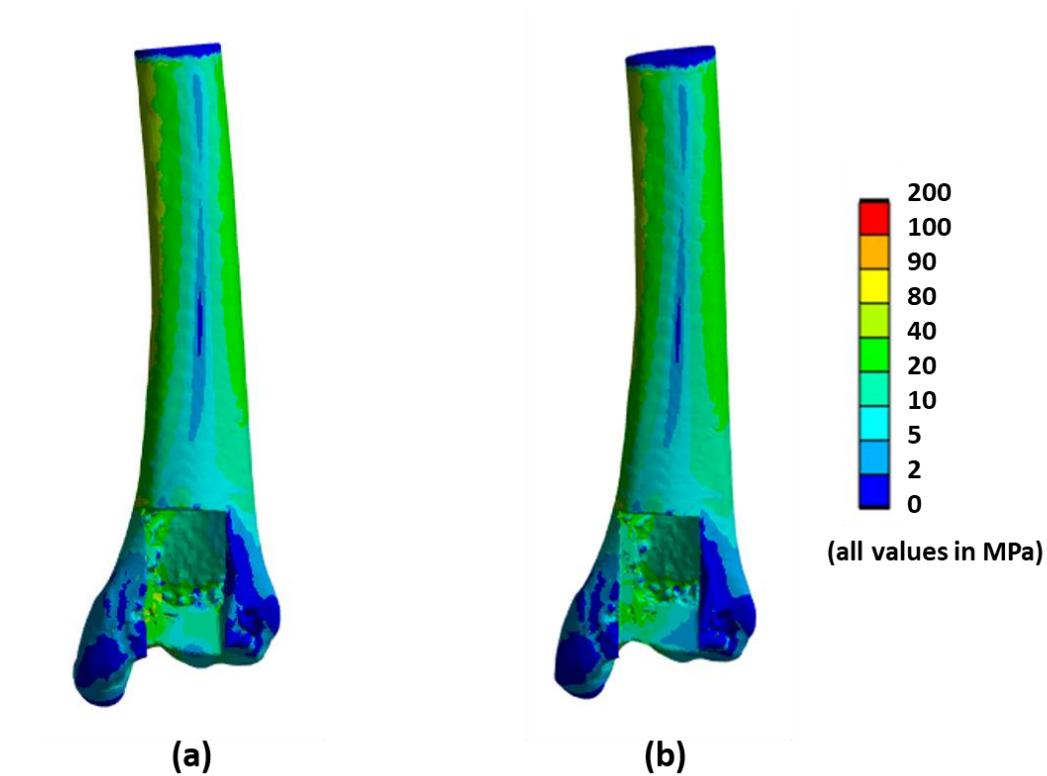


**Fig. 5.3:** von Mises stress distribution of the tibia: (a) PLA+HAp+MCS coated Ti alloy implant; (b) Ti alloy implant.

upward). The blue region of the coating indicates lower stress intensity as compared to the green in the uncoated. The average stress in the coating area was around 1 MPa as compared to 12 MPa in the uncoated one. Fig. 5.3 depicts the von Mises stress distribution of the tibia. The infected region of the tibia, which is also our region of interest for the present analysis, was observed to have 11.05 MPa average stress in the coated implant as compared to 9.6 MPa associated with the uncoated implant. Thus this 15 % increase of stress in bone with the coated implant signifies less stress shielding in the area. Contrary to the overall uniform load distribution in the intact bone region, the load flow pattern in a laterally plated bone is predominantly mediolateral (Fig. 5.4). The load that applies on the bone, distal to the fracture site is passed from bone to the implant. Proximally above the fracture site, the load flow pattern, however, is reverse since the same is transferred from on from the plate to screw and then finally to the bone. As a result, the maximum stress in the implant was found to be at the proximal screw. Displacement contours –FE predicted – in the fabricated bio-composite coated implant and only metallic implant constructs under an axial compressive load of 3kN are shown in Fig. 5.5. The maximum displacements at peak load of 3kN for coated and

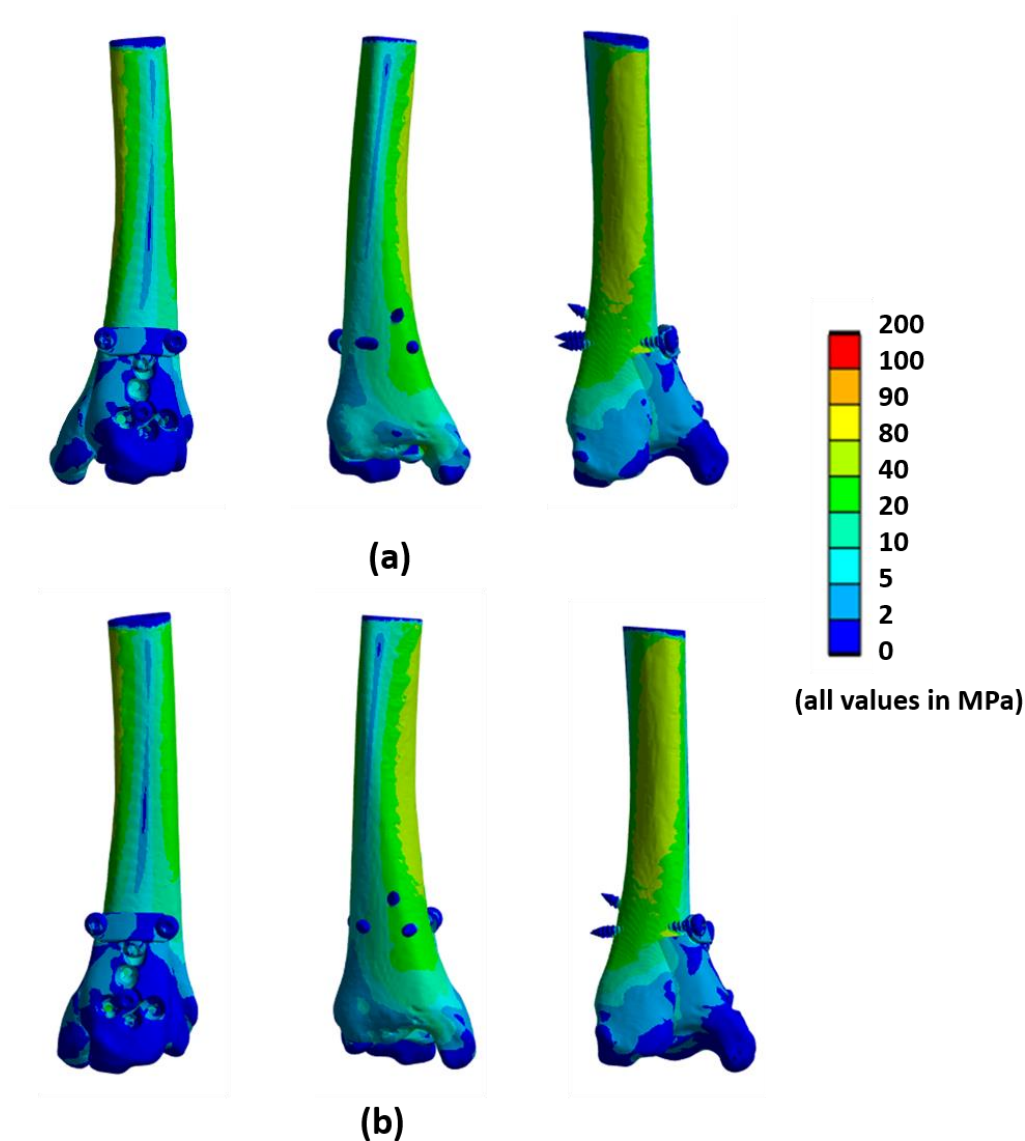


**Fig. 5.4:** von Mises stress distribution of the implanted tibia: (a) PLA+HAp+MCS coated Ti alloy implant; (b) Ti alloy implant.

uncoated implanted constructs were found out to be almost identical to similar  $\sim 0.450$  mm.

The bio-composite coating with modulus of rigidity closer to bone can initiate bone implant binding at a faster rate. The non-union of bone and implant is a major cause of failure. Mostly in the high load-bearing regions of our body, the non-union can arise due to the loosening of the implant's grip on the bone. This happens due to the phenomenon of stress shielding by which implants take away the bulk amount of the load and devoid bone of the necessary stress that is required for its growth. As a result, bone starts to shrink and the union between bone and implant fails. On the other hand, a thick coating of bio-compatible layer between bone and implant can help the bone

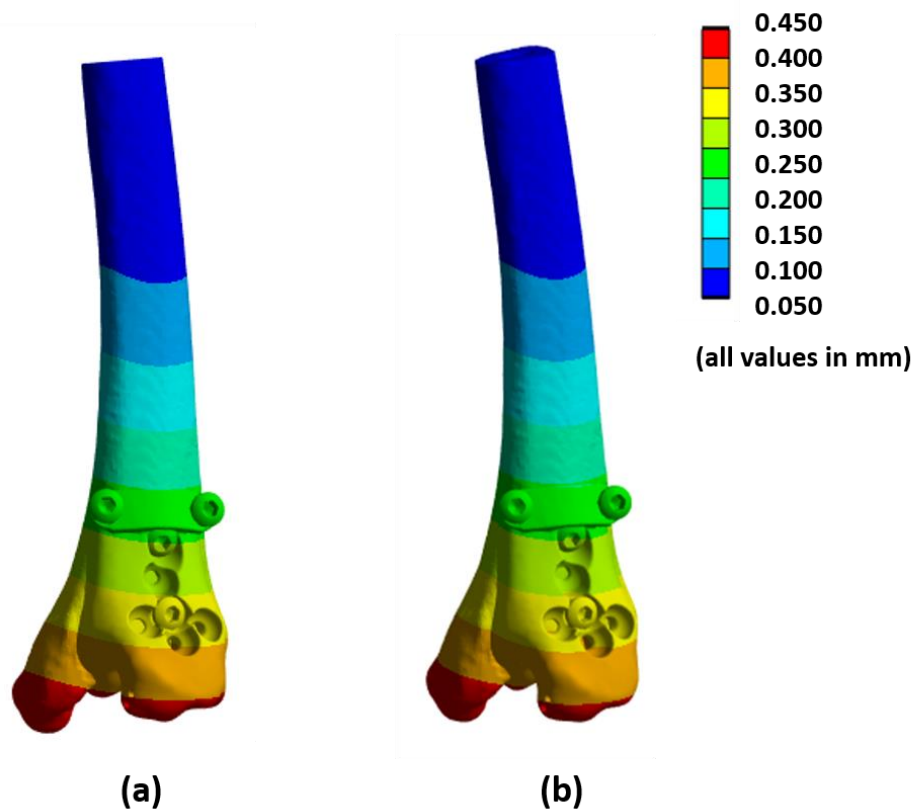


**Fig. 5.5:** displacement plot of the implanted tibia: (a) PLA+HAp+MCS coated Ti alloy implant; (b) Ti alloy implant.

interface to have more load and continue growing. Moreover, if that coating surface is bio-resorbable like in the present study after certain time the coating layer will start

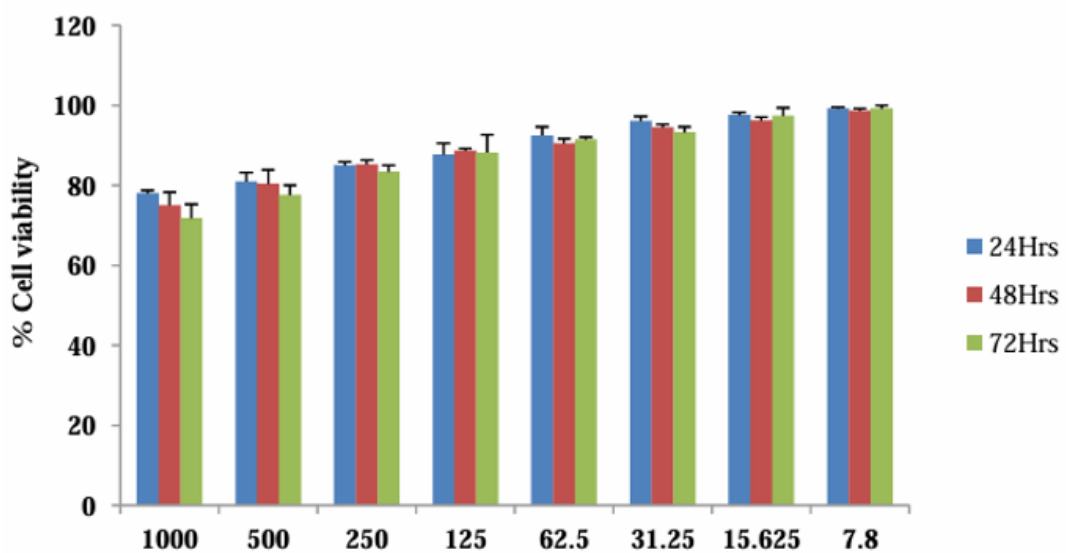


**Fig. 5.6:** *in vitro*– 24 hrs, 48 hrs, and 72 hrs cytotoxicity of test product in terms of percentage cell viability against Mouse fibroblast (L929) cell line by MTT assay.

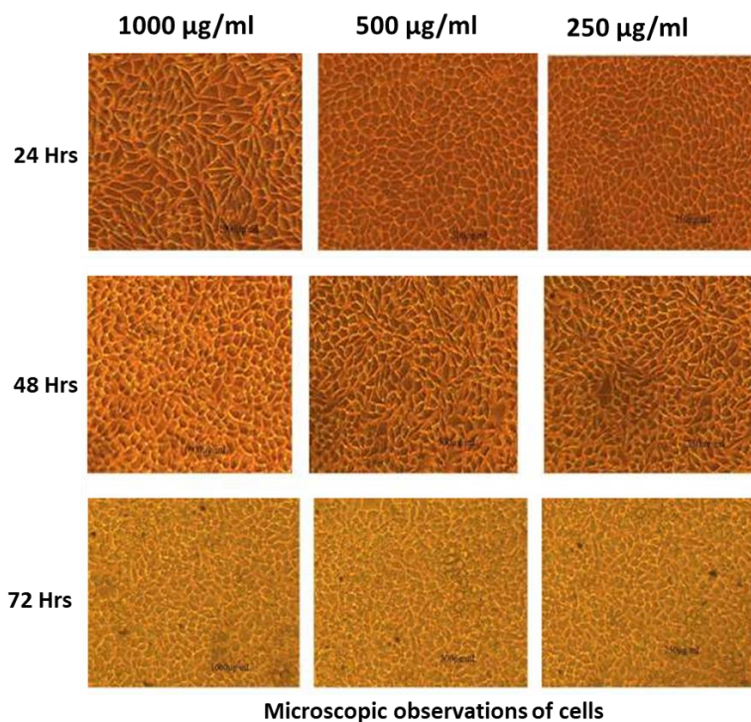


**Fig. 5.7:** Microscopic observations of cells after 72 hrs treatment with test product.

getting degraded and a porous structure formation will be initiated. Bone will have the chance to grow into that structure and have a proper grip with the implant eventually. The thick coating of implants which almost acts as a bio insert between the implant and the bone can also help get rid of the detrimental avascular necrosis [Lu-Yao et al., 1994; Perren et al., 1988].

Gel - PHM was assayed for In vitro cytotoxicity study against Mouse fibroblast (L929) cells by exposing the cells to different concentrations ranging from 1000µg/mL to 7.8µg/mL at different time intervals (24h,48h & 72h). MTT assay was employed to test the cytotoxic effect of selected concentrations by measuring the metabolic activity through a colorimetric determination. The MTT assay is usually carried out to detect the cells with constant mitochondrial activity, thereby an increase or decrease in the number of viable cells is linearly related to mitochondrial activity. In the present study, the cytotoxicity of Gel - PHM was determined in terms of percentage cell viability and it was found to be  $77.99 \pm 0.80\%$ ,  $75.09 \pm 3.28$  and  $71.87 \pm 3.43$  at 24h,48h and 72hr respectively with CTC50 of  $>1000\mu\text{g/mL}$  at higher concentration (1000µg/mL) on Mouse fibroblast (L929) cell line.

### **5.3 Summary of the findings**

The PLA based bio-composite coating can was found to have better stress/load transfer to the bone as compared to uncoated implant. Implants with thick coating act as bio-inserts between the implant and the bone and helps in avoiding avascular necrosis, osteopenia, osteo necrosis rising from stress shielding effect. Furerther, the Gel-PHM was found to be nontoxic on mouse fibroblast (L929) cell lines at higher concentrations. In the future, the fabricated PLA-based bio-composite coated over metallic implants can also be used as a drug delivery technique with target specific treatment strategies.





## Chapter 6

### Conclusions

#### 6.1 Introduction

In the present study, an attempt has been made to develop bio-composites made of PLA, nHAp, and MCS for the first time as an implant material. Bio-composites made of PLA/nHAp and PLA/nHAp/MCS were fabricated through extrusion cum injection molding. The prepared samples were tested for their morphology, mechanical strength, and thermal stability. The drawbacks of metallic implants, such as stress shielding and revision surgery, can be avoided using bioabsorbable implants. Hence, in this work, bio-composites made of different compositions of PLA, nHAp, and MCS were prepared. The prepared bio-composite was subjected surface morphology, differential scanning calorimetry, contact angle analysis, thermogravimetric, Fourier transform infrared spectroscopy, and mechanical characterisation.

The field emission scanning electron microscopy with energy-dispersive X-ray spectroscopy analysis demonstrated that the drawback of non-uniform distribution associated with CS had been overcome with the MCS. The maximum degradation temperature obtained with the bio-composite developed in the present investigation was higher (389 °C) than with neat PLA and PLA with chitosan. Thus, the interaction of nHAp with MCS and PLA made the fabricated bio-composites superior in terms of thermal stability. The contact angle study enhanced the surface wettability property, suggesting that the prepared bio-composites are suitable for cell adhesion.

The study found PLA/nHAp/MCS composite to have better modulus and elongation than PLA and PLA/nHAp. Also, the characterisation of the materials showcased better physiochemical properties with PLA/nHAp/MCS bio-composite. Moreover, the DSC results confirmed that no phase separation has occurred in the formed bio-composites. Thus, the developed bio-composites have the potential to be an alternative biodegradable implant material, especially for fabricating bone screws and

plates to be used as non-load-bearing internal fixation devices. Fig. 8.1 is the schematic illustration of the work done in the present thesis, segmented chapter-wise.

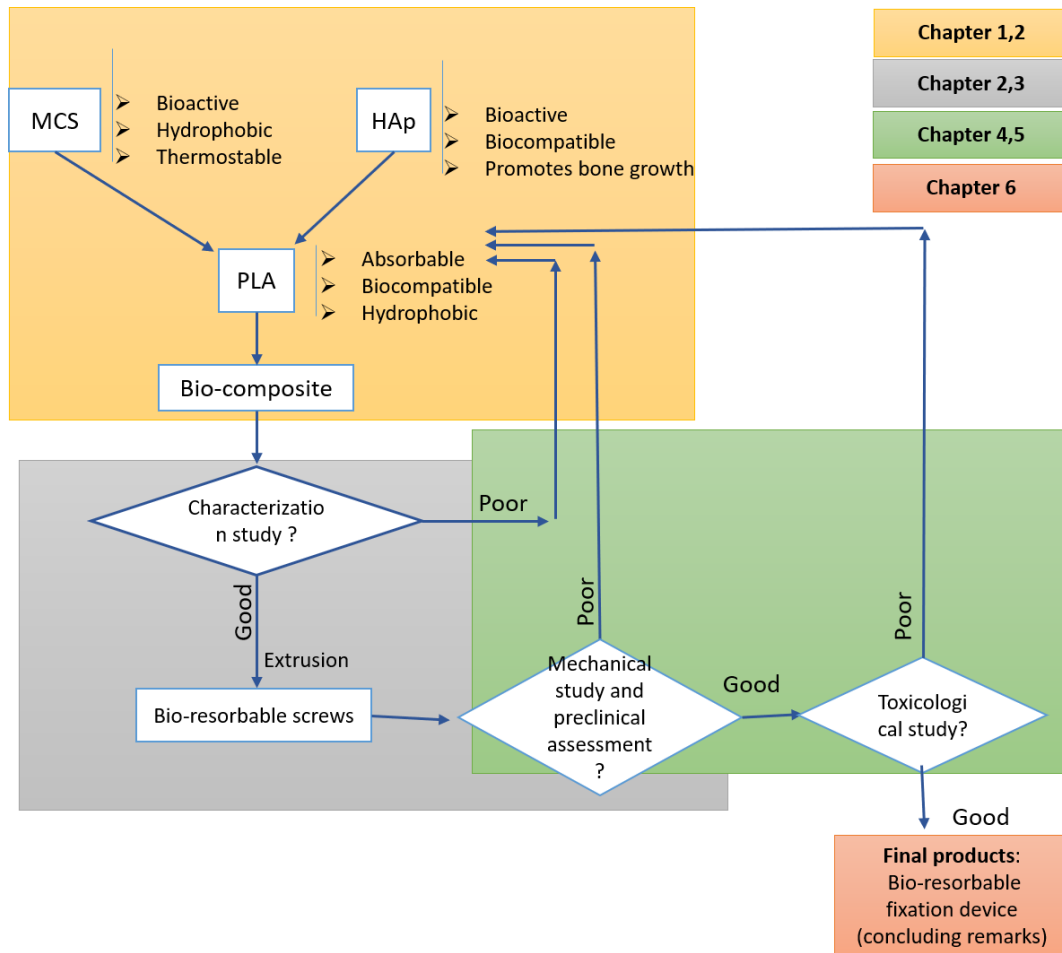


**Fig. 6.1:** Schematic illustration of the work done in the present thesis.

Chitosan has the drawback of poor dispersion in the PLA matrix, which has been overcome with the synthesized modified chitosan. Uniform dispersion of nHAp was observed in the PLA matrix by FESEM. Based on the investigation, it was identified that the bio-composite materials proposed in the study possess superior strength and thermal stability compared to conventional PLA and HAp-based composites. From the DSC results, no phase separation was witnessed, which confirms the proper mixing of the bio-fillers in the matrix. This research aims to develop a bioresorbable orthopaedic construct for low and non-load-bearing applications. It incorporates nano-hydroxyapatite (nHAp) and modified chitosan (MCS) as filler materials to enhance the strength of a polylactic acid (PLA)-based composite. Importantly, this can negate the question of secondary removal surgery, which will help reduce overall surgery costs and make the procedure less invasive. The study includes both computational validation

and experimental fabrication methods. Additionally, it seeks to develop a bioabsorbable internal fixation device intended for craniofacial and maxillofacial surgical applications. This investigation marks the first attempt to create biocomposites made of PLA, nHAp, and modified chitosan.



**Fig. 6.2:** Fabricated screw from PLA-based bio-composite as per ASTM standards by extrusion cum injection molding.

Purification of PLA for Use as Base Material in fabricating the biocomposites. Optimization of Twin-Screw Extruder and Injection Molding Parameters for fabricating PLA/nHAp/MCS bioabsorbable composites as per ASTM standards per ISO527-1BA. The test was carried out by a load cell of 5kN in a controlled environment (25 °C and 78% RH) and at a cross-head speed of 1 mm/min. accordance with ASTM D638

The bio-composites, PLA/nHAp and PLA/nHAp/MCS were produced through melt-extrusion cum injection molding. The prepared samples were evaluated for morphology, mechanical strength, and thermal stability. While chitosan typically has poor dispersion in the PLA matrix, this issue has been addressed with the use of synthesized modified chitosan. Field Emission Scanning Electron Microscopy (FESEM) revealed uniform dispersion of nHAp within the PLA matrix.

The findings indicate that the bio-composite materials proposed in this study demonstrate superior strength and thermal stability compared to conventional PLA and HAp-based composites. Differential Scanning Calorimetry (DSC) results showed no phase separation, confirming the proper mixing of the bio-fillers within the matrix.

Overall, the developed biocomposites have the potential to serve as alternative biodegradable implant materials suitable for biomedical applications.

The PLA based bio-composites were further evaluated *in silico* as an implant material of bone plates for mandibular joint fracture using FE analysis. The biomechanical parameters, such as maximum displacements and von Mises stress distribution of the PLA bio-composites, were compared to conventional metallic implants. To further investigate the impact of plate or screw material on stability, two additional variations were tested. When a PLA-based composite plate was paired with a Ti screw, the observed displacement of the implanted construct was 0.069 mm. In contrast, the construct with a Ti plate and a PLA screw exhibited a displacement of 0.085 mm. This indicates that the screw material significantly influences stability. The importance of the screw material can be attributed to its role in connecting to the bone, thereby enhancing bone-implant anchorage and the overall compressive strength of the construct. Similar patterns were noted when considering the addition of occlusal forces in the mandibular joint. The PLA-based composite mandibular construct showed a maximum displacement of 0.114 mm, whereas the Ti alloy implant recorded a 0.074 mm displacement. Notably, the PLA-based implant in this study exhibited displacement below 150  $\mu\text{m}$  under various loading conditions, which is crucial for bone healing. PLA based bio-composite plates and Ti alloy screws can be an interesting solution to mid-level load bearing regions of human body. In this study, PLA-based composite implants exhibited minimal stress shielding due to their lower modulus properties. Overall, the developed bio-composites have the potential for an alternative biodegradable implant material suitable for biomedical applications in cases of fracture in low load-bearing sites.

Further, the PLA-based bio-composites were coated over metallic implants for high load-bearing fracture site- distal tibia. The coated implant facilitated in having 15% higher stress to the tibia bone as compared to the uncoated implants. The thick coating of implants which almost acts as a bio insert between the implant and the bone can also help get rid of the detrimental avascular necrosis. Also, this will further help to reduce stress shielding. In the present study, the cytotoxicity of Gel - PHM was determined in terms of percentage cell viability and it was found to be  $77.99 \pm 0.80\%$ ,  $75.09 \pm 3.28$ , and  $71.87 \pm 3.43$  at 24h, 48h, and 72h respectively with CTC50 of  $>1000\mu\text{g/mL}$  at higher concentration ( $1000\mu\text{g/mL}$ ) on mouse fibroblast (L929) cell line. The Gel-PHM was found to be nontoxic on mouse fibroblast (L929) cell lines at

higher concentrations. In the future, the fabricated PLA-based bio-composite coated over metallic implants can also be used as a drug delivery technique with target specific treatment strategies.

## 6.2 Future Scope

The following studies can be conducted to explore this area of research further:

1. Conduct *in vitro* bioactivity studies in simulated body fluid of the fabricated composites, following ASTM F1635-11. These studies should be performed in simulated body fluid (SBF) at 37.5°C, maintained at a pH of 7.4.
2. Perform *in vivo* studies on the developed internal fixation devices to observe their behavioural changes when exposed to living organisms.
3. Conduct a detailed *in vitro* bioactivity study of the fabricated internal fixation devices.
4. Incorporate functional nanofillers into the existing matrix and reinforcement to enhance the properties of internal fixation devices.



## References

- “Global Market Study on Bioabsorbable Implants: Incorporation of 3D Printing Technology to Create Multiple Potential Opportunities - GII.”  
<https://www.giiresearch.com/report/pmrs833195-global-market-study-on-bioabsorbable-implants.html> (accessed Jun. 26, 2020).
- “Global Medical Devices Packaging Market: Growth, Trends and Forecast (2020- 2025) - ResearchAndMarkets.com | Business Wire.”  
<https://www.businesswire.com/news/home/20200519005812/en/Global-Medical-Devices-Packaging-Market-Growth-Trends> (accessed Jun. 26, 2020).
- “MediPoint: Trauma Fixation - Global Analysis and Market Forecasts.”  
<https://www.prnewswire.com/news-releases/medipoint-trauma-fixation---global-analysis-and-market-forecasts-235037151.html> (accessed Jun. 26, 2020).
- “Orthopedic Devices Market – At a Turning Point - Sathguru News.”  
<https://www.sathguru.com/news/2017/06/23/orthopedic-devices-market-at-a-turning-point/> (accessed Jun. 26, 2020).
- “Trauma Fixation Devices Market Global Industry Analysis,Growth,Trends andForecast 2019.” <https://www.transparencymarketresearch.com/trauma-fixation-devices-market.html> (accessed Jun. 26, 2020).
- “Trauma Fixation Devices Market to Hit USD 9.5 Billion by 2025: Global Market Insights Inc.” <https://www.prnewswire.com/news-releases/trauma-fixation-devices-market-to-hit-usd-9-5-billion-by-2025-global-market-insights-inc-300880635.html> (accessed Jun. 26, 2020).
- Albrektsson, T., and Johansson. C. (2001). Osteoinduction, osteoconduction and osseointegration. *Eur. Spine J.* 10:S96–S101, 2001.
- Ambrosio-Martín, J., Fabra, M.J., López-Rubio, A., Gorrasi, G., Sorrentino, A., Lagaron, J.M. (2016). Assessment of ball milling as a compounding technique to develop

nanocomposites of poly(3-hydroxybutyrate-co-3-hydroxyvalerate) and bacterial cellulose nano whiskers. *J Polym Environ* (24): 241–254.

Andreopoulos, A., Korakis, T., Duonis, E., Anastasiadis, A., Tzivelekis, P. & Kanellakopoulou, K. (1996). In vitro release of new quinolones from biodegradable systems: A comparative study. *J Biomat Appl* 10: 338-347.

Araújo-Gomes, N., F. Romero-Gavilán, I. García-Arnáez, et al. (2018). Osseointegration mechanisms: a proteomic approach. *J. Biol. Inorg. Chem.* 23:459–470, 2018.

Arbag, H., Korkmaz, H., Ozturk, K. and Uyar, Y. (2008). Comparative evaluation of different miniplates for internal fixation of Mandible fractures using finite element analysis. *Journal of Oral Maxillofacial Surgery*, Vol. 66 No. 6, pp. 1225-1232

Ashammakhi N. and Rokkanen, P. (1997). Absorbable polyglycolide devices in trauma and bone surgery. *Biomaterials*, vol. 18, no. 1. Elsevier Science Ltd, pp. 3–9.

Ashammakhi, N. (2005). Reactions to Biomaterials: the Good, the Bad, and Ideas for Developing New Therapeutic Approaches. *Journal of Craniofacial Surgery* 16(2): p 195-196.

Ashammakhi, N., Veiranto, M., Niemelä, S.M., Tiainen, J., Leinonen, S., Suokas, E. & Törmälä, P. (2005a), Development of Multifunctional Materials (MFM): Bioabsorbable Drug Releasing Hard Tissue Fixation Screws. *Mat Sci Forum* 492-493: 195-200.

Atali, O., Gocmen, G., aktop, S., Ak, E., Basa, S. and Cetinel, S. (2016). Bone healing after biodegradable mini-plate fixation. *Acta Cirúrgica Brasileira*, Vol. 31 No. 6, pp. 364-370.

- Backes, E.H., Pires, L.D.N., Costa, L.C., Passador, F.R., Pessan, L.A. (2019). Analysis of the degradation during melt processing of PLA/Biosilicate® composites. *Journal of Composites Science* 3 (2): 52.
- Bernakiewicz, M., Viceconti, M. (2002). The role of parameter identification in finite element contact analysis w.r.t orthopaedic biomechanics applications. *Journal of Biomechanics* 35: 61-67.
- Bhasney, S.M., Patwa, R., Kumar, A., Katiyar, V. (2017). Plasticizing effect of coconut oil on morphological, mechanical, thermal, rheological, barrier, and optical properties of poly (lactic acid): A promising candidate for food packaging. *Journal of Applied Polymer Science* 134(41): 1–12.
- Bikiaris, N. D., Koumentakou, I., Samiotaki, C., Meimaroglou, D., Varytimidou, D., Karatza, A., ... & Papageorgiou, G. Z. (2023). Recent advances in the investigation of poly (lactic acid) (PLA) nanocomposites: incorporation of various nanofillers and their properties and applications. *Polymers*, 15(5), 1196.
- Binay, B. and Kumar, R. (2019). Plasma treated and untreated thermoplastic biopolymers/biocomposites in tissue engineering and biodegradable implants. *Materials for Biomedical Engineering*: 339-369.
- Bose, D., Prasannavenkadesan, V. & Katiyar, V. (2024). Tailored material for bioresorbable internal fixation devices: a novel approach using nanohydroxyapatite and chitosan in polylactic acid. *J Mater Sci* 59, 215–227.
- Böstman, O., and Pihlajamäki, H. (2000). Clinical biocompatibility of biodegradable orthopaedic implants for internal fixation: a review. *Biomaterials*, 21(24), 2615-2621.
- Bragdon, C.R., Burke, D., Lowenstein, J.D., O'Connor, D.O., Ramamurti, B., Jasty, M., Harris, W.H. (1996). Differences in stiffness of the interface between a cementless

porous implant and cancellous bone in vivo in dogs due to varying amounts of implant motion. *Journal of Arthroplasty* 11, 945–951.

Brandwood, A., K. R. Noble, and Schindhelm, K. (1992). Phagocytosis of carbon particles by macrophages In vitro,” *Biomaterials*, vol. 13, no. 9, pp. 646–648.

Brown, M., & Farrar, D. (2008). Development of bioresorbable polymers in orthopaedics. *Plastics, rubber and composites*, 37(2-4), 46-49.

Buzarovska, A., Sorina, D., Leona, C., Marieta, C. (2018). Porous poly (L-lactic acid) nanocomposite scaffolds with functionalized TiO<sub>2</sub> nanoparticles: Properties, cytocompatibility and drug release capability. *Journal of Materials Science* 53(16): 11151-11166.

Cansiz, E., Dogru, S. and Arslan, Y. (2015). Comparative evaluation of the mechanical properties of resorbable and titanium miniplates used for fixation of Mandibular condyle fractures. *Journal of Mechanics in Medicine and Biology*, Vol. 15 No. 2, pp. 1540032-1540040.

Chen, Y., Frith, J. E., Dehghan-Manshadi, A., Attar, H., Kent, D., Soro, N. D. M., and Dargusch, M. S. (2017). Mechanical properties and biocompatibility of porous titanium scaffolds for bone tissue engineering. *Journal of the mechanical behavior of biomedical materials*, 75, 169-174.

Cheung, R.C.F., Ng, T.B., Wong, J.H., Chan, W.Y. (2015). Chitosan: an update on potential biomedical and pharmaceutical applications. *Marine drugs* 13(8):5156-5186.

Correlo V.M., L.F. Boesel, Bhattacharya M., Mano J.F., Neves N.M., Reis R.L. (2005). Properties of melt processed chitosan and aliphatic polyester blends. *Mat Sci Eng A-Struct* 403: 57-68

- Cox, T., Kohn, M.W., Impelluso, T. (2003). Computerized analysis of resorbable polymer plates and screws for the rigid fixation of mandibular angle fractures. *J Oral Maxillofac Surg.* ;61(4):481-7; discussion 487-8.
- Cristofolini, L., Viceconti, M. (2000). Mechanical validation of whole bone composite tibia models. *J Biomech.*;33(3):279-288.
- Daniels, A.U., Chang, M.K.O., Andriano, K.P. and Heller, J. (1990), Mechanical properties of biodegradable polymers and composites proposed for internal fixation of bone. *J. App. Biomater.*, 1: 57-78.
- Disegi JA. (2000). Titanium alloys for fracture fixation implants. *Injury. Suppl* 4:14-7
- Durucan, C., and Brown, P. W. (2001). Biodegradable hydroxyapatite–polymer composites. *Advanced Engineering Materials*, 3(4), 227-231.
- Enislidis, G., Pichorner, S., Lambert, F., Wagner, A., Kainberger, F., Kautzky, M., & Ewers, R. (1998). Fixation of zygomatic fractures with a new biodegradable copolymer osteosynthesis system: Preliminary results. *International journal of oral and maxillofacial surgery*, 27(5), 352-355.
- F. Sun, T. Wang, Y. Yang, *Rapid Prototyp. J.* 2022; 28, 585.
- Felfel, R. M., Ahmed, I., Parsons, A. J., and Rudd, C. D. (2013). Bioresorbable screws reinforced with phosphate glass fibre: manufacturing and mechanical property characterisation. *Journal of the mechanical behavior of biomedical materials*, 17, 76-88.
- Felfel, R. M., Parsons, A. J., Chen, M., Stuart, B. W., Wadge, M. D., & Grant, D. M. (2021). Water resistant fibre/matrix interface in a degradable composite: Synergistic effects of heat treatment and polydopamine coating. *Composites Part A: Applied Science and Manufacturing*, 146, 106415.
- Ferguson, S. J., Wyss, U. P., & Pichora, D. R. (1996). Finite element stress analysis of a hybrid fracture fixation plate. *Medical engineering & physics*, 18(3), 241-250.

- Ferlay, J., Shin, H. R., Bray, F., Forman, D., Mathers, C., & Parkin, D. M. (2012). Cancer Incidence and Mortality Worldwide: IARC CancerBase No. 10. GLOBOCAN 2008 v1. 2, Lyon, France: International Agency for Research on Cancer; 2010. *Lancet Oncol*, 13(6), 607-15.
- Fortune business insight: Report ID: FBI102586, Orthopaedic device market (2020-2027) (<https://www.fortunebusinessinsights.com/orthopedic-devices-market>)
- Ghosh, R. (2023). The role of the depth of resection of the distal tibia on biomechanical performance of the tibial component for TAR: a finite element analysis with three implant designs. *Medical Engineering & Physics*, 119, 104034.
- Gibson, L. (1985). The mechanical behaviour of cancellous bone. *J Biomech* 18(5):317–328.
- Gross, K.A., Komarowska, L., and Viksna, A. (2013). Efficient zinc incorporation in hydroxyapatite through crystallization of an amorphous phase could extend the properties of zinc apatites. *J. Aust. Ceram. Soc* 49 (2): 129–135.
- Gu, X., Zheng, Y., Zhong, S., Xi, T., Wang, J., & Wang, W. (2010). Corrosion of, and cellular responses to Mg–Zn–Ca bulk metallic glasses. *Biomaterials*, 31(6), 1093-1103.
- Gupta, A., Prasad, A., Mulchandani, N., Shah, M., Mamilla, R.S., Kumar, S., Katiyar, V. (2017) Multifunctional nanohydroxyapatite-promoted toughened high-molecular-weight stereocomplex poly (lactic acid)-based bio nanocomposite for both 3D-printed orthopedic implants and high-temperature engineering applications. *ACS omega* 2 (7): 4039-4052.
- Harada, K., Watanabe, M., Ohkura, K., & Enomoto, S. (2000). Measure of bite force and occlusal contact area before and after bilateral sagittal split ramus osteotomy of the

mandible using a new pressure-sensitive device: a preliminary report. *Journal of oral and maxillofacial surgery*, 58(4), 370-373.

Hefzy, M.S., Singh S.P. (1997). Comparison between two techniques for mode I/II interface condition in a porous coated hip endoprosthesis. *Medical Engineering & Physics* 19, 50-62.

Heikkilä, J.T. et al. (1995). Bone formation in rabbit cancellous bone defects filled with bioactive glass granules. *Acta Orthopaedica*. 66, 5 (Jan. 1995), 463–467.

Henkel, J., Woodruff, M. A., Epari, D. R., Steck, R., Glatt, V., Dickinson, I. C. and Hutmacher, D. W. (2013). Bone regeneration based on tissue engineering conceptions—a 21st century perspective. *Bone research*, 1, 216.

Holland, S. J., Jolly, A. M., Yasin, M., & Tighe, B. J. (1987). Polymers for biodegradable medical devices: II. Hydroxybutyrate-hydroxyvalerate copolymers: Hydrolytic degradation studies. *Biomaterials*, 8(4), 289-295.

Huang G, Du Z, Yuan Z, Gu L, Cai Q, Yang X. (2018). Poly(L-lactide) nanocomposites containing poly(D-lactide) grafted nanohydroxyapatite with improved interfacial adhesion via stereo complexation. *J Mech Behav Biomed Mater*; 78:10-19.

Huang, J., Xiong, J., Liu, J., Zhu, W., & Wang, D. (2013). Investigation of the in vitro degradation of a novel polylactide/nanohydroxyapatite composite for artificial bone. *Journal of Nanomaterials*, 2013(1), 515741.

Ilavarasi, P.U. and Anburajan, M. (2011). Design and finite element analysis of Mandibular prosthesis. 3rd International Conference on Electronics Computer Technology, pp. 325-329.

Ilavarasi, P.U. and Anburajan, M. (2011). Design and finite element analysis of Mandibular prosthesis”, 3rd International Conference on Electronics Computer Technology, pp. 325-329.

- Injorhor, P., Trongsatitkul, T., Wittayakun, J., Ruksakulpiwat, C., Ruksakulpiwat, Y. (2022). Nano-Hydroxyapatite from White Seabass Scales as a Bio-Filler in Polylactic Acid Bio composite: Preparation and Characterization. *Polymers (Basel)*14(19):4158
- Inzana, J.A., Schwarz, E.M., Kates, S.L., Awad, H.A. Biomaterials approaches to treating implant-associated osteomyelitis. *Biomaterials*. 2016 Mar; 81:58-71.
- Jain, R. A. (2000). The manufacturing techniques of various drug loaded biodegradable poly (lactide-co-glycolide) (PLGA) devices. *Biomaterials*, 21(23), 2475-2490.
- Jaiswal, S., Kumar, R. M., Gupta, P., Kumaraswamy, M., Roy, P., and Lahiri, D. (2018). Mechanical, corrosion and biocompatibility behaviour of Mg -3Zn-HA biodegradable composites for orthopaedic fixture accessories. *Journal of the mechanical behavior of biomedical materials*, 78, 442-454.
- Jia, Z., Ma, H., Liu, J., Yan, X., Liu, T., Cheng, Y. Y., Li, X., Wu, S., Zhang, J., & Song, K. (2023). Preparation and Characterization of Polylactic Acid/Nano Hydroxyapatite/Nano Hydroxyapatite/Human Acellular Amniotic Membrane (PLA/nHAp/HAAM) Hybrid Scaffold for Bone Tissue Defect Repair. *Materials*, 16(5), 1937.
- Katz, J. N., Wright, J. O. H. N., Wright, E. A., & Losina, E. L. E. N. A. (2007). Failures of total hip replacement: a population-based perspective. *Orthop. J. Harvard Med. Sch*, 9, 101-106.
- Kenney, C., Dick, S., Lea, J., Liu, J., & Ebraheim, N. A. (2019). A systematic review of the causes of failure of Revision Total Hip Arthroplasty. *Journal of orthopaedics*, 16(5), 393-395.
- Klee, D., and Höcker, H. (2000). Polymers for biomedical applications: improvement of the interface compatibility. In *Biomedical Applications Polymer Blends* (pp. 1-57). Springer, Berlin, Heidelberg.

- Kontakis GM, Pagkalos JE, Tosounidis TI, Melissas J, Katonis P. (2007). Bioabsorbable materials in orthopaedics. *Acta orthopaedica belgica* 73(2): 159-169.
- Koort, J. K., Mäkinen, T. J., Suokas, E., Veiranto, M., Jalava, J., Knuuti, J., ... & Aro, H. T. (2005). Efficacy of ciprofloxacin-releasing bioabsorbable osteoconductive bone defect filler for treatment of experimental osteomyelitis due to *Staphylococcus aureus*. *Antimicrobial agents and chemotherapy*, 49(4), 1502-1508.
- Kulkarni, R. K., Moore, E. G., Hegyeli, A. F., & Leonard, F. (1971). Biodegradable poly (lactic acid) polymers. *Journal of biomedical materials research*, 5(3), 169-181.
- Kulkova, J., Moritz, N., Huhtinen, H., Mattila, R., Donati, I., Marsich, E., and Vallittu, P. K. (2017). Hydroxyapatite and bioactive glass surfaces for fiber reinforced composite implants via surface ablation by Excimer laser. *Journal of the mechanical behavior of biomedical materials*, 75, 89-96.
- Kumar, M. R., Muzzarelli, R., Muzzarelli, C., Sashiwa, H., & Domb, A. J. (2004). Chitosan chemistry and pharmaceutical perspectives. *Chemical reviews*, 104(12), 6017-6084.
- Langer, R., Vacanti, J. P. (2003). *Tissue Engineering Science*, 260, 920-926.
- Lebre, F., Sridharan, R., Sawkins, M. J., Kelly, D. J., O'Brien, F. J., and Lavelle, E. C. (2017). The shape and size of hydroxyapatite particles dictate inflammatory responses following implantation. *Scientific Reports*, 7(1), 1–13.
- Levy, F.E., Smith, R.W., Odland, R.M., Marentette, L.J. (1991). Monocortical miniplate fixation of mandibular angle fractures. *Archives of Otolaryngology Head and Neck Surgery* 117, 149–154.
- Lewallen, E. A., Riester, S. M., Bonin, C. A., Kremers, H. M., Dudakovic, A., Kakar, S., ... & Van Wijnen, A. J. (2015). Biological strategies for improved osseointegration and osteoinduction of porous metal orthopedic implants. *Tissue Engineering Part B: Reviews*, 21(2), 218-230.

- Liang J, Lu X, Zheng X, Li YR, Geng X, Sun K, Cai H, Jia Q, Jiang HB, Liu K. (2023) Modification of titanium orthopedic implants with bioactive glass: a systematic review of in vivo and in vitro studies. *Front Bioeng Biotechnol.*; 11:1269223.
- Lin S, File I, Shah A, Pizzutillo P & Tuan R. (1992). A bioresorbable drug delivery system for the treatment of chronic osteomyelitis. Fourth World Biomaterials Congress, April 24-28, Berlin, Federal Republic of Germany.
- Liu S, Zheng Y, Liu R, Tian C. (2020). Preparation and characterization of a novel polylactic acid/hydroxyapatite composite scaffold with biomimetic micro-nanofibrous porous structure. *J. Mater. Sci. Mater. Med.*; 31:74.
- Liu, S., Qin, S., He, M., Zhou, D., Qin, Q., & Wang, H. (2020). Current applications of poly (lactic acid) composites in tissue engineering and drug delivery. *Composites Part B: Engineering*, 199, 108238.
- Liu, S., Yan, H., Fang, Z., & Wang, H. (2014). Effect of graphene nanosheets on morphology, thermal stability and flame retardancy of epoxy resin. *Composites Science and Technology*, 90, 40-47.
- Lovald ST, Khraishi T, Wagner J, Baack B, Kelly J, Wood J. 2006. Comparison of plate-screw systems used in mandibular fracture reduction: finite element analysis. *J Biomech Eng.* ;128(5):654-62.
- Lucke, M., Wildemann, B., Sadoni, S., Surke, C., Schiller R, Stemberger, A., Raschke, M., Haas, N, & Schmidmaier, G. (2005). Systemic versus local application of gentamicin in prophylaxis of implant-related osteomyelitis in a rat model. *Bone* 36(5): 770-778.
- Lu-Yao GL, Keller RB, Littenberg B, Wennberg JE. (1994). Outcomes after displaced fractures of the femoral neck. A meta-analysis of one hundred and six published reports. *J Bone Joint Surg Am*; 76: 15-25
- Ma J., M. Thompson, N. Zhao, and Zhu D. (2014). Similarities and differences in coatings for magnesium-based stents and orthopaedic implants,” *Journal of Orthopaedic*

Translation, vol. 2, no. 3. Elsevier (Singapore) Pte Ltd, pp. 118–130, Jul. 01, 2014,doi: 10.1016/j.jot.2014.03.004.

Mäkinen T, Veiranto M, Knuuti J, Jalava J, Törmälä P & Aro H. (2005). Efficacy of bioabsorbable antibiotic containing bone screw in the prevention of biomaterialrelated infection due to *Staphylococcus aureus*. *Bone* 36: 292-299.

Marx, R. E. (2003). Pamidronate (Aredia) and zoledronate (Zometa) induced avascular necrosis of the jaws: a growing epidemic. *Journal of oral and maxillofacial surgery*, 61(9), 1115-1117.

Middleton, J. C., & Tipton, A. J. (2000). Synthetic biodegradable polymers as orthopedic devices. *Biomaterials*, 21(23), 2335-2346.

Mohamad, S. N. K., Ramli, I., Abdullah, L. C., Mohamed, N. H., Islam, M. S., Ibrahim, N. A., & Ishak, N. S. (2021). Evaluation on structural properties and performances of graphene oxide incorporated into chitosan/poly-lactic acid composites: Cs/pla versus cs/pla-go. *Polymers*, 13(11), 1839.

Mohamed Haneef, I. N. H., Shaffiar, N., Buys, Y. F., & Abd. Hamid, A. M. (2019). Finite element analysis (FEA) of polylactic acid/polypropylene carbonate (PLA/PPC) blends fixation plate for craniomaxillofacial surgery. *International Journal of Structural Integrity*, 10(5), 678-691.

Monika, Pal, A. K., Bhasney, S. M., Bhagabati, P., & Katiyar, V. (2018). Effect of dicumyl peroxide on a poly (lactic acid)(PLA)/poly (butylene succinate)(PBS)/functionalized chitosan-based nanobiocomposite for packaging: A reactive extrusion study. *Acs Omega*, 3(10), 13298-13312.

Nag, P. and Chanda, S. (2021). Biomechanical Design Prognosis of Two Extramedullary Fixation Devices for Subtrochanteric Femur Fracture: A Finite Element Study. *Medical & Biological Engineering & Computing*, Springer 59: 271–285.

- Nag, P., Borgohain, B., Ahmed, K. A., Phukan, P., Kumar, N., Borjali, A., ... & Chanda, S. (2022). The influence of static load and sideways impact fall on extramedullary bone plates used to treat intertrochanteric femoral fracture: a preclinical strength assessment. *Annals of biomedical engineering*, 50(12), 1923-1940.
- Narra N, Valášek J, Hannula M, Marcián P, Sándor GK, Hyttinen J, Wolff J. (2014). Finite element analysis of customized reconstruction plates for mandibular continuity defect therapy. *J Biomech.*;47(1):264-8.
- Narra, N., Valášek, J., Hannula, M., Marcián, P., Sándor, G., Hyttinen, J. and Wolff, J. (2014). Finite element analysis of customized reconstruction plates for Mandibular continuity defect therapy”, *Biomechanics*, Vol. 47 No. 1, pp. 264-268.
- Nazeer, M. A., Onder, O. C., Sevgili, I., Yilgor, E., Kavakli, I. H., & Yilgor, I. (2020). 3D printed poly (lactic acid) scaffolds modified with chitosan and hydroxyapatite for bone repair applications. *Materials Today Communications*, 25, 101515.
- Neumann, A. and Kevenhoerster, K. (2009). Biomaterials for craniofacial reconstruction. *GMS Current Topic in Otorhinolaryngology-Head and Neck Surgery*, Vol. 8 No. 8, pp. 1-17.
- Nie, L., Nicolau, D., Tessier, P., Kourea, H., Browner, B. & Nightingale, C. (1998). Use of bioabsorbable polymer for the delivery of ofloxacin during experimental osteomyelitis treatment. *J Orthop Res* 16(1): 76-79.
- Niemelä, S.M., Ikäheimo, I, Koskela, M., Veiranto, M., Suokas, E., Törmälä, P., Waris, T., Ashammakhi, N. & Syrjälä, H. (2006). Ciprofloxacin-releasing bioabsorbable polymer is superior to titanium in preventing *Staphylococcus epidermidis* attachment and biofilm formation in vitro. *J Biomed Mater Res[B] Appl Biomater* 76(1): 8-14.
- Nomura, N. (2010). Artificial organs: recent progress in metals and ceramics. *Journal of Artificial Organs*, 13(1), 10-12.

- Onche, I. I., Osagie, O. E., & INuhu, S. (2011). Removal of orthopaedic implants: indications, outcome and economic implications. *Journal of the West African College of Surgeons*, 1(1), 101.
- Overbeck J, Winckler S, Meffert R, Törmälä P, Spiegel H & Brug E. (1995). Penetration of ciprofloxacin into bone: a new Bioabsorbable Implant. *J Investigat Surg* 8: 155-162.
- Ozan, S., Lin, J., Li, Y., and Wen, C. (2017). New Ti-Ta-Zr-Nb alloys with ultrahigh strength for potential orthopedic implant applications. *Journal of the mechanical behavior of biomedical materials*, 75, 119-127.
- Özbek, I., Konduk, B. A., Bindal, C., & Ucisik, A. H. (2002). Characterization of borided AISI 316L stainless steel implant. *Vacuum*, 65(3-4), 521-525.
- Pal, A. K., & Katiyar, V. (2017). Theoretical and analyzed data related to thermal degradation kinetics of poly (L-lactic acid)/chitosan-grafted-oligo L-lactic acid (PLA/CH-g-OLLA) bio nanocomposite films. *Data in brief*, 10, 304-311.
- Pal, A. K., Bhattacharjee, S. K., Gaur, S. S., Pal, A., & Katiyar, V. (2018). Chemomechanical, morphological, and rheological studies of chitosan-graft-lactic acid oligomer reinforced poly (lactic acid) bionanocomposite films. *Journal of Applied Polymer Science*, 135(3), 45546.
- Pal, A.K., Katiyar, V. (2016). Nanoamphiphilic chitosan dispersed poly (lactic acid) bionanocomposite films with improved thermal, mechanical, and gas barrier properties. *Biomacromolecules* 17(8): 2603-2618.
- Park, S. M., Lee, J. W., & Noh, G. (2018). Which plate results in better stability after segmental mandibular resection and fibula free flap reconstruction? *Biomechanical analysis. Oral surgery, oral medicine, oral pathology and oral radiology*, 126(5), 380-389.

- Peng, W., Zheng, W., Shi, K., Wang, W., Shao, Y. and Zhang, D. (2015). An in Vivo evaluation of PLLA/ PLLA-gHA Nano-composite for internal fixation of mandibular bone fractures. *Biomedical Materials*, Vol. 10 No. 6, pp. 1-10
- Perren, S. M., CORDEY, J., RAHN, B. A., GAUTIER, E., & SCHNEIDER, E. (1988). Early temporary porosis of bone induced by internal fixation implants a reaction to necrosis, not to stress protection?. *Clinical Orthopaedics and Related Research®*, 232, 139-151.
- Pietrzak, W. S., Caminear, D. S., and Perns, S. V. (2002). Mechanical characteristics of an absorbable copolymer internal fixation pin. *The Journal of foot and ankle surgery*, 41(6), 379-388.
- Pina, S. and Ferreira, J. (2012). Bioresorbable plates and screws for clinical applications: a review. *Journal of Healthcare Engineering*, Vol. 3 No. 2, pp. 243-260.
- Prasad A, Bhasney SM, Sankar MR, Katiyar V. (2017). Fish scale derived hydroxyapatite reinforced poly (lactic acid) polymeric bio-films: possibilities for sealing/locking the internal fixation devices. *Materials Today* 4(2) :1340-1349.
- Prasad, A., Bhasney, S. M., Prasannavenkadesan, V., Sankar, M. R., & Katiyar, V. (2023). Nano-hydroxyapatite reinforced polylactic acid bioabsorbable cancellous screws for bone fracture fixations. *Journal of Applied Polymer Science*, 140(43), e54577.
- Prasad, A., Bhasney, S. M., Prasannavenkadesan, V., Sankar, M. R., & Katiyar, V. (2023). Polylactic acid reinforced with nano-hydroxyapatite bioabsorbable cortical screws for bone fracture treatment. *Journal of Polymer Research*, 30(5), 177.
- Prati, J. L., Kim, D. H., and Matthewson, M. J. (2017). Application of static fatigue testing to the behavior of absorbable sutures. *Journal of the Mechanical Behavior of Biomedical Materials*, 74, 232–235

- Procter, P., & Paul, J. P. (1982). Ankle joint biomechanics. *Journal of biomechanics*, 15(9), 627-634.
- Râpă M, Miteluț AC, Tănase EE, Grosu E, Popescu P, Popa ME, Rosnes JT, Sivertsvik M, Darie-Niță RN, Vasile, C. (2016). Influence of chitosan on mechanical, thermal, barrier and antimicrobial properties of PLA-bio composites for food packaging. *Compos Part B: Eng* 102:112–121
- Rasal, Rahul M., Hirt, Douglas E. (2010). Poly(lactic acid) Toughening with a Better Balance of Properties, *Macromolecular Materials and Engineering* 295(204-209).
- Ratner, B. D., Hoffman, A. S., Schoen, F. J., and Lemons, J. E. (2004). *Biomaterials science: an introduction to materials in medicine*. Elsevier.
- Rezwan, K., Chen, Q. Z., Blaker, J. J., and Boccaccini, A. R. (2006). Biodegradable and bioactive porous polymer/inorganic composite scaffolds for bone tissue engineering. *Biomaterials*, 27(18), 3413-3431.
- Ricci, W. M., Tornetta III, P., Petteys, T., Gerlach, D., Cartner, J., Walker, Z., and Russell, T. A. (2010). A comparison of screw insertion torque and pullout strength. *Journal of orthopaedic trauma*, 24(6), 374-378.
- Rokkanen, P., Hirvensalo, E., Böstman, O., Vainionpää, S., & Törmälä, P. (1990). Absorbable rods in internal fracture fixation. In *Abstracts, SICOT 90, XVIII World Congress, Montreal, September 9-14, 1990* (pp. s. 317)
- Russias J, Saiz E, Nalla RK, Gryn K, Ritchie RO, Tomsia A.P. (2006). Fabrication and mechanical properties of PLA/HA composites: a study of in vitro degradation. *Materials Science and Engineering C* 26(8):1289-1295.
- Ruuttila, P., Niiranen, H., Kellomäki, M., Törmälä, P., Konttinen, Y.T. and Hukkanen, M. (2006). Characterization of human primary osteoblast response on bioactive glass (BaG 13–93)- coated poly-L,DL-lactide (SR-PLA70) surface in vitro. *J. Biomed. Mater. Res.*, 78B: 97-104.

- Seireg, A., & Arvikar, R. J. (1975). The prediction of muscular load sharing and joint forces in the lower extremities during walking. *Journal of biomechanics*, 8(2), 89-102.
- Serlo, W., Ashammakhi, N., Törmälä, P., & Waris, T. (2002). A new technique for cranial bone osteofixation: use of bioabsorbable tacks and plates to fix parietal bone split grafts used for reconstruction of a posttraumatic frontal bone defect. *Journal of Craniofacial Surgery*, 13(2), 331-336.
- Shan, L., Shuhao, Q., He, M., Zhou, d., Qin, Q., Wang, H. (2020). Current applications of poly (lactic acid) composites in tissue engineering and drug delivery. *Composites Part B: Engineering* 199: 108238.
- Shepherd, J.H., Shepherd, D.V., Best, S.M. (2012). Substituted hydroxyapatites for bone repair. *Journal of Materials Science: Materials in Medicine* 23(10): 2335-2347.
- Shi, C., Pu, X., Zheng, G., Feng, X., Yang, X., Zhang, B., ... & Xia, H. (2016). An antibacterial and absorbable silk-based fixation material with impressive mechanical properties and biocompatibility. *Scientific Reports*, 6(1), 37418.
- Soballe, K., Brockstedt-Rasmussen, H., Hansen, E.S., Bunger, C. (1992a). Hydroxyapatite coating modifies implant membrane formation. Controlled micromotion studied in dogs. *Acta Orthopaedica Scandinavica* 63, 128–140.
- Son, S. H., Kang, Y. N., & Ryu, M. R. (2012). The effect of metallic implants on radiation therapy in spinal tumor patients with metallic spinal implants. *Medical Dosimetry*, 37(1), 98-107.
- Stauffer, R. N., Chao, E. Y., & Brewster, R. C. (1977). Force and motion analysis of the normal, diseased, and prosthetic ankle joint. *Clinical Orthopaedics and Related Research (1976-2007)*, 127, 189-196.
- Suuronen, R., Haers, P. E., Lindqvist, C., & Sailer, H. F. (1999). Update on bioresorbable plates in maxillofacial surgery. *Facial Plastic Surgery*, 15(01), 61-72.
- Suuronen, R., Kallela, I., & Lindqvist, C. (2000). Bioabsorbable plates and screws: Current state of the art in facial fracture repair. *The Journal of cranio-maxillofacial trauma*, 6(1), 19-27.
- Suzuki, S., Ikada, Y. (2012). Bioabsorbable Polymers. *Biomaterials for Surgical Operation*: 19-38.

- T. Nakano. (2019). Physical and Mechanical Properties of Metallic Bio-materials. *Metals for Biomedical Devices*, 97–129.
- Tajbakhsh, S., and Hajiali, F. (2017). A comprehensive study on the fabrication and properties of biocomposites of poly(lactic acid)/ceramics for bone tissue engineering. *Materials Science and Engineering C*, 70, 897–912.
- Tanase, C. E., & Spiridon, I. (2014). PLA/chitosan/keratin composites for biomedical applications. *Materials Science and Engineering: C*, 40, 242-247.
- Tappa, K., Jammalamadaka, U., Weisman, J. A., Ballard, D. H., Wolford, D. D., Pascual-Garrido, C., ... & Mills, D. K. (2019). 3D printing custom bioactive and absorbable surgical screws, pins, and bone plates for localized drug delivery. *Journal of functional biomaterials*, 10(2), 17.
- Tarashi, V. (2016). Patient- specific 3D finite element modelling, analysis, and verification of dental implant navigation and insertion system”, doctoral dissertation, University of Technology, Sydney.
- Tonino, A.J., Davidson, C.L., Klopper, P.J., Linclau, L.A. (1984). Protection from stress in bone and its effects: experiments with stainless steel and plastic plates in dogs. *J.Bone joint surg.*; 58-B: 107-113.
- Torres, J., Cotelo, J., Karl, J. and Gordon, A.P. (2015). Mechanical property optimization of FDM PLA in shear with multiple objectives. *The Minerals, Metals & Materials Society*, Vol. 67 No. 5, pp. 1183-1193
- Torres-Hernández, Y. G., Ortega-Díaz, G. M., Téllez-Jurado, L., Castrejón-Jiménez, N. S., Altamirano-Torres, A., García-Pérez, B. E., & Balmori-Ramírez, H. (2018). Biological compatibility of a polylactic acid composite reinforced with natural chitosan obtained from shrimp waste. *Materials*, 11(8), 1465.
- Tripathi, N. and Katiyar, V. (2016). PLA/functionalized-gum arabic based bio nanocomposite films for high gas barrier applications. *Journal of Applied Polymer Science* 133(21) :1–8.
- Tu, C., Chen, J., Huang, C., Xiao, Y., Tang, X., Li, H., ... & Liu, C. (2020). Effects of electromagnetic fields treatment on rat critical-sized calvarial defects with a 3D-printed composite scaffold. *Stem cell research & therapy*, 11(1), 433.

- Tu, C., Chen, J., Huang, C., Xiao, Y., Tang, X., Li, H., ... & Liu, C. (2020). Effects of electromagnetic fields treatment on rat critical-sized calvarial defects with a 3D-printed composite scaffold. *Stem cell research & therapy*, 11(1), 433.
- Turunen, O., Wahlström, T., & Vaheri, A. (1994). Ezrin has a COOH-terminal actin-binding site that is conserved in the ezrin protein family. *The Journal of cell biology*, 126(6), 1445-1453.
- Uthoff HK, Bardos DI, Liskova-Kiar M. (1981). The advantages of titanium alloys over stainless steel plates for the internal fixation of fractures. *J. Bone joint surg.*; 63-B: 427-34.
- Vajgel, A., Camargo, I.B., Willmersdorf, R.B., Melo, T.M., Filho, J.R.L. and Vasconcellos, R.J.H. (2013). Comparative finite element analysis of the biomechanical stability of 2.0 fixation plates in atrophic mandibular fractures. *Biomechanical Stability in Mandibular Fractures*, Vol. 71 No. 2, pp. 335-342.
- Veiranto, M. & Törmälä, P. (2002). In vitro mechanical and drug release properties of bioabsorbable ciprofloxacin containing and neat self-reinforced P(L/DL)LA 70/30 fixation screws. *J Mater Sci Mater Med* 13: 1259-1263.
- Veljović, D., Jančić-Hajneman, R., Balać, I., Jokić, B., Putić, S., Petrović, R., Janačković, D. (2011). The effect of the shape and size of the pores on the mechanical properties of porous HAP-based bioceramics. *Ceramics International* 37(2): 471-479.
- Villette, C. C., & Phillips, A. T. M. (2018). Rate and age-dependent damage elasticity formulation for efficient hip fracture simulations. *Medical Engineering & physics*, 61, 1-12.
- Vojtěch, D., Kubásek, J., Šerák, J., & Novák, P. (2011). Mechanical and corrosion properties of newly developed biodegradable Zn-based alloys for bone fixation. *Acta biomaterialia*, 7(9), 3515-3522..
- Wallner, J., & Egger, J. (2018). Mandibular CT dataset collection. Figshare.(doi: 10.6084/m9.figshare.6167726.v5).
- Wang G., Liu S., Ueng S & Chan, E.C. (2004). The release of cefazolin and gentamicin from biodegradable PLA/PGA beads. *Int J Pharmac* 273(1-2): 203-212.

- Wang, P., Zhao, L., Liu, J., Weir, M. D., Zhou, X., and Xu, H. H. (2014). Bone tissue engineering via nanostructured calcium phosphate biomaterials and stem cells. *Bone research*, 2, 1-13.
- Wang, R., Liu, Y., Wang, J. and Baur, D. (2016). Effect of infragap on mechanical behavior of Mandibular angle fracture with three fixation designs – a finite element analysis”, *Journal of Plastic, Reconstructive and Aesthetic Surgery*, Vol. 70 No. 3, pp. 360-369.
- Weiler, A., Hoffmann, R. F., Stähelin, A. C., Helling, H. J., & Südkamp, N. P. (2000). Biodegradable implants in sports medicine: the biological base. *Arthroscopy: The Journal of Arthroscopic & Related Surgery*, 16(3), 305-321.
- Wen, C. E., Mabuchi, M., Yamada, Y., Shimojima, K., Chino, Y., and Asahina, T. (2001). Processing of biocompatible porous Ti and Mg. *Scripta Materialia*, 45(10), 1147-1153.
- Wen, C. E., Xiong, J. Y., Li, Y. C., & Hodgson, P. D. (2010). Porous shape memory alloy scaffolds for biomedical applications: a review. *Physica scripta*, 2010(T139), 014070.
- Wendel, M., Sommarin, Y., Heine Gard D. (1998). Bone matrix proteins: isolation and characterization of a novel cell-binding keratan sulfate proteoglycan (osteoaderin) from bovine bone. *The Journal of cell biology*, 141(3): 839-47.
- Yang, H., Xia, K., Wang, T., Niu, J., Song, Y., Xiong, Z., and Lu, W. (2016). Growth, in vitro biodegradation and cytocompatibility properties of nano-hydroxyapatite coatings on biodegradable magnesium alloys. *Journal of Alloys and Compounds*, 672, 366-373.
- Yetkin H, Senköylü A, Cila E (2000) Biodegradable Implants in Orthopaedics and Traumatology. *Turk J Med Sci* 30 (2000), 297–301.
- Z. Cai, C. Zhu, L. Wang, L. Zhu, Z. Zhang, H. Zhu, Wang. Y. (2016). A retrospective study of six patients with mandibular metastatic carcinoma, *Oncol. Lett.* 11 (6) 3650–3654, <https://doi.org/10.3892/ol.2016.4484>.
- Zhang H, Mao X, Du Z, et al. (2016). Three-dimensional printed macroporous polylactic acid/hydroxyapatite composite scaffolds for promoting bone formation in a critical-size rat calvarial defect model. *Science and Technology of Advanced Materials*;17(1):136-148.
- Zhang, H., Mao, X., Du, Z., Jiang, W., Han, X., Zhao, D., ... & Li, Q. (2016). Three dimensional printed macroporous polylactic acid/hydroxyapatite composite scaffolds

for promoting bone formation in a critical-size rat calvarial defect model. *Science and Technology of Advanced materials*, 17(1), 136-148.

Zysset P. K., Edward Guo. X., Edward Hoffer. C., Moore. K. E., and Goldstein S. A. (1999). Elastic modulus and hardness of cortical and trabecular bone lamellae measured by nanoindentation in the human femur," *J. Biomech.*, vol. 32, no. 10, pp. 1005–1012.



## About the Author

Devleena Bose was born in Tripura, India. In the year 2012, she passed the Higher Secondary (10+2) Examination with the first division under the Tripura Board of Secondary Education. From 2012 until 2016, she studied her Bachelor's course in Chemical Engineering at the National Institute of Technology Agartala, India and passed out with a first-class. From 2016 to 2017, she was associated with an industry. In 2018, she joined the Indian Institute of Technology Guwahati, India, to pursue PhD research in the field of Polymer science and applications at the Department of Chemical Engineering under Prof. Vimal Katiyar. In February 2020, she was awarded the prestigious Prime Minister Industrial Research Fellowship under the SERB-FICCI Govt. of India. Her doctoral research study is on the topic of 'Studies on Polylactic acid/Chitosan based composite for orthopaedic application'.

### List of publications from the present thesis

#### Journal

1. **Bose D.**, Prasanna V., Katiyar V. Tailored material for bioresorbable internal fixation devices: a novel approach using nanohydroxyapatite and chitosan in polylactic acid. *J Mater Sci* 59, 215–227 (2024). <https://doi.org/10.1007/s10853-023-09110-1>
2. **Bose D.**, Nag P., Dall M., Katiyar V., A finite element study to predict the viability of PLA based composite implants for mandibular joint fractures (Under revision)
3. **Bose D.**, Nag P., Katiyar V., The influence of PLA based coating over Ti implant for high load-bearing distal tibia region: A finite element study (to be submitted)

#### Conferences

1. **Bose D.**, Katiyar V., - Development of PLA-based bioresorbable formulation for Orthopaedic applications. (**Taiwan-India 2022 Exchange Workshop and Symposium on Intensifying the Connection of Sustainable Technology, Sept. 2022**) (Poster).
2. **Bose D.**, Katiyar V., -Thermostable drug-coated PLA-HAp Biocomposites for Orthopaedic application-an experimental study. (**North-East Research Conclave-IITG, May,2022**) (Poster)
3. **Bose D.**, Katiyar V., - A study on Bioresorbable Orthopaedic Fixation Devices. (**International Conference on Smart materials for Sustainable Technology, Goa, Feb.2020**) (Poster)
4. **Bose D.**, Katiyar V., - Studies on Biopolymer based composites for bone healing applications. (**Internation Symposium on Sustainable Polymers, IITG, Aug.2019**) (Poster)

